



HAL
open science

Structure, Rheological Properties and Connectivity of Gels Formed by Carrageenan Extracted from Different Red Algae Species

Tran Nu Thanh Viet Bui

► **To cite this version:**

Tran Nu Thanh Viet Bui. Structure, Rheological Properties and Connectivity of Gels Formed by Carrageenan Extracted from Different Red Algae Species. Organic chemistry. Le Mans Université, 2019. English. NNT : 2019LEMA1007 . tel-02077051

HAL Id: tel-02077051

<https://theses.hal.science/tel-02077051>

Submitted on 22 Mar 2019

HAL is a multi-disciplinary open access archive for the deposit and dissemination of scientific research documents, whether they are published or not. The documents may come from teaching and research institutions in France or abroad, or from public or private research centers.

L'archive ouverte pluridisciplinaire **HAL**, est destinée au dépôt et à la diffusion de documents scientifiques de niveau recherche, publiés ou non, émanant des établissements d'enseignement et de recherche français ou étrangers, des laboratoires publics ou privés.

THESE DE DOCTORAT DE

LE MANS UNIVERSITE
COMUE UNIVERSITE BRETAGNE LOIRE

ECOLE DOCTORALE N° 596
Matière Molécules et Matériaux
Spécialité : « *Chimie et Physicochimie des Polymères* »

Par

« Tran Nu Thanh Viet BUI »

**« Structure, Rheological Properties and Connectivity of Gels Formed
by Carrageenan Extracted from Different Red Algae Species »**

Thèse présentée et soutenue à « Le Mans Université », le « Jeudi 28 Février, 2019 »

Unité de recherche : Le Mans Université, Institut des molécules et matériaux du Mans UMR CNRS 6283

Thèse N° : 2019LEMA1007

Composition du Jury :

M. **Jacques DESBRIERES**, Professeur, Université de Pau et des Pays de l'Adour (Rapporteur)

M. **Luc PICTON**, Professeur, Université Rouen Normandie (Rapporteur)

Mme **Isabelle CAPRON**, Directrice de Recherche, INRA- BIA (Examineur)

M. **Taco NICOLAI**, Directeur de Recherche CNRS, Le Mans Université (Directeur de thèse)

M. **Frédéric RENO**, Maître de conférences, Le Mans Université (Co-encadrant de thèse)

M. **Trong Bach NGUYEN**, Docteur, Nha Trang Université, Vietnam (Co-encadrant de thèse)

ACKNOWLEDGEMENTS

First I would like to acknowledge my supervisors: Dr. Taco Nicolai, Dr. Frédéric Renou and Dr. Nguyen Trong Bach for their support and advice throughout my thesis. Sincere gratitude I would like to express to Bach for his help with the experimental material and other works related to my position at Nha Trang University. I appreciate the help from Frédéric not only for his research ideas but also on the technique and documents. I am especially grateful to Taco for his advice and his joy and enthusiasm for scientific research that is contagious and motivation me to finish successfully my thesis and continue doing research in the future as well.

I also gratefully acknowledge to the Ministry of Education and Training of Vietnam for financial support during my study in France.

My sincere thanks are expressed to Prof. Jacques Desbrieres , Prof. Luc Picton and Dr. Isabelle Capron as members in my academic committee for their time, and interest and helpful comments.

I have had the pleasure to work with the staffs from PCI. I would like to thank to Prof. Christophe Chassenieux and Prof. Lazhar Benyahia for their useful discussions. Many thanks also go to Erwan Nicol, Olivier Colombani, Cyrille Dechancé, Frederick Niepceron, Boris Jacqueline for their technical help on NMR, rheology, confocal microscopy and SEC.

I would like to thank my friends and Vietnamese families living in Le Mans who made my time here more pleasurable.

A special thanks to my parents, my sisters, my brothers and my parents in law for all their love and encouragement. The kindest words I would like to send to my two daughters Dang Viet Han and Dang Viet Linh. Although my absence was hard for them, they encouraged me by showing their happiness every day. Words are not enough to reveal how grateful I am to my husband Dang Thanh Pha who has helped me organize smoothly everything from family to work. Thank you.

TABLE OF CONTENTS

Introduction.....	1
Chapter 1 Background	4
1.1. Marine polysaccharides	4
1.2. Carrageenan	6
1.2.1. Source of carrageenan.....	6
1.2.2. Chemical structure of carrageenan.....	7
1.2.3. Carrageenan extraction	10
1.2.4. Properties of carrageenan in aqueous solution.....	12
1.2.5. Mixtures of different types of carrageenan	19
1.2.6. Microstructure of carrageenan gels.....	20
1.2.7. Applications	22
References	24
Chapter 2 Materials and Methods	33
2.1. Materials	33
2.1.1. Raw carrageenan extracted from red algae	33
2.1.2. Purification of raw carrageenan	34
2.1.3. Fluorescent labelling of carrageenan	35
2.1.4. Preparation of solutions	35
2.2. Methods	36
2.2.1. Light Scattering.....	36
2.2.2. NMR spectroscopy.....	39
2.2.3. Yield, moisture and mineral content determination.....	39
2.2.4. Rheology	40
2.2.5. Turbidity	40
2.2.6. Confocal Laser Scanning Microscopy (CLSM)	40
2.2.7. Release of unbound carrageenan from gels	44
References	46

Chapter 3 Characterization and Rheological Properties of Carrageenan Extracted from Different Red Algae Species.....	48
3.1. Introduction.....	48
3.2. Results.....	49
3.3. Conclusions.....	59
<i>References</i>	60
Chapter 4 Mixtures of Iota and Kappa-Carrageenan.....	63
4.1. Introduction.....	63
4.2. Results and discussion	64
4.2.1. Mixtures of iota and kappa carrageenan in presence of calcium ions	64
4.2.2. Mixtures of iota and kappa carrageenan in presence of potassium ions.....	73
4.3. Conclusions.....	77
<i>References</i>	78
Chapter 5 Mobility of Carrageenan Chains In Iota and Kappa Carrageenan Gels.....	80
5.1. Introduction.....	80
5.2. Results.....	81
5.2.1. Mobility of carrageenan in salt free aqueous solution.....	81
5.2.2. Mobility of carrageen in gels.....	83
5.2.3. Release of carrageenan from the gels	89
5.3. Conclusion	93
<i>References</i>	94
General Conclusion and Outlook.....	96

List of abbreviations

Car: carrageenan

Ka: *Kappaphycus alvarezii*

Ks: *Kappaphycus striatum*

Km: *Kappaphycus malesianus*

Ed: *Euchuma denticulatum*

ι-car: iota carrageenan

κ-car: kappa carrageenan

FAO: Food and Agriculture Organization of the United Nations

R_h: Hydrodynamic radius

R_g: Radius of gyration

M_w: molecular weight

M_a: apparent molar mass

R_{ha}: apparent hydrodynamic radius

T: temperature

T_c: coil –helix temperature

T_g: gelling temperature

T_m: melting temperature

NMR: Nuclear Magnetic Resonance

LS: Light Scattering

FRAP: Fluorescence Recovery After Photobleaching

CLSM: Confocal Laser Scanning Microscopy

G': storage modulus

G'': loss modulus

Introduction

Carrageenan (Car) is a linear sulfated polysaccharide extracted from various species of edible red algae and it is widely used as thickener, stabilizer and gelling agent in food products, pharmaceutical applications and cosmetics. Their demand is expected to increase due to the fact that it is not toxic, cheap and biocompatible^{1,2}. The molecular structure of Car is based on a disaccharide repeat of alternating units of D-galactose and 3,6-anhydro-galactose (3,6-AG) joined by α -1,4 and β -1,3-glycosidic linkage. It is classified into various types such as λ (lambda), κ (kappa), ι (iota), ν (nu), μ (mu) and θ (theta) based on the difference in their content of 3,6-anhydro-D-galactose and the number and position of sulfate groups within the disaccharide repeat structure. Higher levels of sulfate mean lower solubility temperatures and lower gel strength³⁻⁶.

The most common types of Car used in the industry are κ - and ι -car due to their good gelling properties. κ -Car is mainly extracted from *Kappaphycus alvarezii* and ι -car is mainly obtained from *Eucheuma denticulatum*. Southeast Asia is the principal area of production of carrageenan derived from these species^{7,8}. Many species of red marine algae are found to grow well in Vietnam's maritime surroundings such as *Kappaphycus alvarezii*, *Kappaphycus striatum*, *Kappaphycus cottonii*, *Kappaphycus malesianus*, *Kappaphycus ennerme*, *Kappaphycus galatinum* and *Euchuma denticulatum*^{9,10}. *Kappaphycus striatum*, *Kappaphycus alvarezii* and *Euchuma denticulatum* have been selected for expansion of the cultivation areas along coastal provinces. The annual yield of *Kappaphycus alvarezii* is around 4.000 dry tons and it is mainly exported in the form of dried seaweed or raw Car.

Car forms a thermal-reversible gel in aqueous solution via the transition from a random coil to a helical conformation followed by the aggregation of helices to form a space-spanning network^{11,12}. The coil-helix transition is induced by cooling in the presence of cations. The differences in structure of κ - and ι -car result in differences in their gelling properties. κ -Car can form a strong gel in presence of specific monovalent cations, whereas the conformation transition of ι -car is particularly sensitive to divalent ions¹³ and forms a weak gel. Another difference is that ι -car gels show no thermal hysteresis and less syneresis¹⁴⁻¹⁶.

A large number of reports on the gelling properties of individual Car have been published, but there are few investigations on mixtures of κ - and ι -car. Some studies have

shown that the coil-helix transitions of κ - and ι -car are independent^{15,17,18}. It has been suggested that there is a microphase separated network in the mixed system^{16,17,19,20}, which could explain the synergistic effect found for the rheological properties^{20,21}. However, there is lack of microscopic evidence to support this hypothesis. Therefore the gel structure in mixed systems is still an open question.

The mobility of Car within the network can yield information about the extent to which chains are bound to the network and is important with respect to the release of Car from the gel. Very little attention has been paid so far to this issue, probably because it has generally been considered that all Car chains are strongly connected in the gel and their release from the gels has attracted little attention so far.

Objectives

The aim of this research was first to characterize native Car extracted from selected seaweeds cultured in Cam Ranh Bay, Khanh Hoa province of Vietnam in order to select the best types of species for culture in this area. The second objective was to elucidate the gelation process of κ - and ι -car in mixed system. Finally, we investigated the mobility of Car chains within gels.

Outline of the thesis

The thesis consists of five chapters and a general conclusion:

Chapter 1 gives an overview of the literature on carrageenan: source, structure, extraction, properties and application.

Chapter 2 describes the materials and methods used in this research

Chapter 3 presents the characterization and rheological properties of Car extracted from different red algae species. These results have been published: *Viet T. N. T. Bui, Bach T. Nguyen, Frédéric Renou & Taco Nicolai. Structure and rheological properties of carrageenans extracted from different red algae species cultivated in Cam Ranh Bay, Vietnam. Journal of Applied Phycology (2018) <https://doi.org/10.1007/s10811-018-1665-1>.*

Chapter 4 shows results on the microstructure and rheological properties of mixed Car gels. These results have been published: *Viet T. N. T. Bui, Bach T. Nguyen, Frédéric Renou & Taco Nicolai. Rheology and microstructure of mixtures of iota and kappa-carrageenan. Food Hydrocolloids 89 (2019) 180–187.*

Chapter 5 shows results on the mobility of Car chains in Car gels. These results have been published: *Viet T. N. T. Bui, Bach T. Nguyen, Frédéric Renou & Taco Nicolai. Mobility of carrageenan chains in iota- and kappa carrageenan gels. Colloids and Surfaces A 562 (2019), 113-118*

Chapter 1

Background

1.1. Marine polysaccharides

Marine polysaccharides are biopolymers extracted from sea organisms. Seaweeds are the main sources of these carbohydrates, mostly red and brown algae. Widely used seaweed carbohydrates are alginate, agar and carrageenan, which are extracted from selected genera and species of brown (Phaeophyceae) and red (Rhodophyceae) seaweeds. The global value of marine hydrocolloids is estimated at 1.1 billion US\$ and it is expected to increase ²². These products are increasingly preferred for applications in various industries due to the fact that they are cheap, natural, environmentally friendly, biocompatible, not toxic and versatile in properties. According to FAO statistics ^{23,24}, major seaweed producers are in Asia such as China, Indonesia, Philippines and Japan followed by countries elsewhere such as Chile, Tanzania, Spain, France and Madagascar.

Of the three mentioned hydrocolloids, the use of agar was discovered first in Japan in the 17th century ²⁵. Agar is a hydrophilic galactan consisting of β -D-galactopyranose and 3,6-anhydro- α -L-galactopyranose linked via alternating α -(1 \rightarrow 3) and β -(1 \rightarrow 4) glycosidic linkages. Agar is naturally comprised of two polysaccharides fractions, namely agarose and agaropectin ²⁶. Agarose is neutral and responsible for gelling, whereas agaropectin is charged, heterogeneous and highly-substituted, and is responsible for thickening properties. Agar is produced from the agarophytes red seaweed genera *Gelidium*, *Gracilaria*, and *Gelidiella*. The cultivation of these algae is taking place in many places around the globe but mainly in China, Indonesia and Philippines (see table 1.1). It is easy to obtain agar by extraction in hot water, however native agar shows poor gelling properties, hence alkaline treatment is usually applied to reduce the number of sulfate groups in the agaropectin fraction to improve the gel strength. Agar is mainly used in food applications (approximately 80%) and the remaining 20% is used in pharmaceutical and biotechnology industries ²⁷⁻²⁹.

Table 1.1. Commercial marine polysaccharides, their sources and production in 2016 .

Products	Species	Location	Yield* (thousands ton)
Agar	Rhodophyta: <i>Gracilaria</i> <i>Gelidium</i> <i>Gelidiella</i>	China, Indonesia, Philippines, Chile, Tanzania, Spain, France	4150
Alginate	Phaeophyceae <i>Laminaria spp</i> <i>Sargassum spp</i>	Japan, Indonesia, China, Philippines, Madagascar	8000
Carrageenan	Rhodophyta: <i>Kappaphycus</i> <i>Euchuma</i>	Indonesia, Philippines, China, Madagascar, Vietnam	12046

Sources^{23,24,30}; * fresh seaweed

Alginate is a marine hydrocolloid extracted from the outer layer of cell walls of the brown algae genera Phaeophyceae. Alginate is a linear polymer composed of β -D-mannuronic acid (M) and α -L-guluronic acid (G). These two uronic acids are arranged alternately in various proportions of MM, MG and GG blocks, depending on the source of seaweed and extraction methods³¹⁻³³. The M/G ratio and block structure influence the physico-chemical properties of alginate. Typically, with increasing guluronic acid content stronger alginate gels are formed. Inversely, more flexible gels are formed with a higher fraction of alginate-M blocks³³. The most interesting property of alginates is their ability to react with polyvalent metal cations, specifically calcium ions. The ions establish a cooperative association between M and G blocks, resulting in a tridimensional network. Alginate is used as a stabilizer and thickener in food products such as drinks, jelly, ice-cream, desserts, etc. Alginate is also widely used for pharmaceutical applications due to their biodegradability, biocompatibility, non-antigenicity and chelating properties.

Carrageenan has the highest total value of the three main marine polysaccharides²⁴ widely used in food products, pharmaceuticals and cosmetics. In the following we will discuss the properties of Car in more detail.

1.2. Carrageenan

1.2.1. Source of carrageenan

Car can be extracted from several species of Rhodophyta including *Gigartina*, *Chondrus*, *Kappaphycus*, *Eucheuma* and *Hypnea*^{6,34–36}. However, commercial κ -, ι - and λ -car are predominantly obtained from *Kappaphycus alvarezii* known in trade as *Eucheuma cottonii* (or simply cottonii), *Eucheuma denticulatum* (trade name *Eucheuma spinosum* or simply spinosum) and *Chondrus spp*, respectively. Originally, these seaweeds grew naturally in Indonesia and the Philippines, but from the 1970s, cultivation was started in both countries and expanded to other places such as Tanzania, Vietnam and some of the Pacific Islands³⁰. The *Gigartina* and *Chondrus* species are sources of mixtures of λ - and κ -car^{30,37,38}. *Chondrus* is mostly harvested in Canada, Chile and France. The demand for each type of Car is determined by their properties (see table 1.2).

Table 1.2. Main carrageenan, their sources and application

Carrageenan	Seaweed source	Location	Application	References
<i>Kappa</i>	<i>Kappaphycus alvarezii</i>	Indonesia, Philippines Tanzania	Gelling agent (strong and brittle gel)	30,39
<i>Iota</i>	<i>Euheuma denticulatum</i>	Indonesia, Philippine, Tanzania	Gelling agent (weak and elastic gel)	30,39
<i>Lamda</i>	<i>Chondrus crispus</i> , <i>Gigartina</i>	Canada, France, Chile	Thickener	30,40
<i>Mu</i>	<i>Kappaphycus alvarezii</i>		κ -car precursor	41–43
<i>Nu</i>	<i>Euheuma denticulatum</i>		ι -car precursor	41–43

Many studies have shown that the *Kappaphycus* species contains predominantly κ -car with a small amount of ι -car and μ -precursor residues, while *Eucheuma denticulatum* contains mainly ι -car and a small amount of ν -precursor residues^{21,41–43}. Interestingly, the biological precursors μ - and ν -car can be converted into κ - and ι -car by alkaline treatment of raw seaweed which reduces the number of sulfate groups.

1.2.2. Chemical structure of carrageenan

The linear structure of Car is composed of alternating 3-linked- β -D-galactopyranose and 4-linked- α -D-galactopyranose units (Figure 1.1). Different types of Car can be distinguished by the amount and position of the sulfate groups as well as the content of 3,6-AG. Figure 1.2 shows that κ -car and ι -car only differ by the presence of an additional sulfate group at the second carbon of the 1,4 linked galactose unit for the latter. λ -Car has the highest sulfate content and no 3,6-AG^{4,5,44,45}. Higher levels of sulfate lead to lower solubility temperature and lower gel strength^{42,46}.

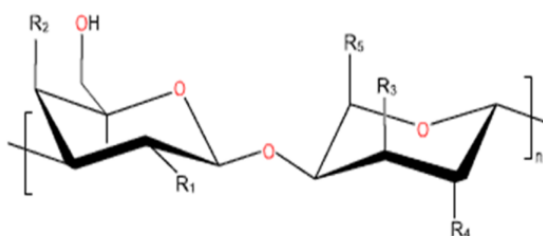


Figure 1.1. Basic repeat structure of carrageenan

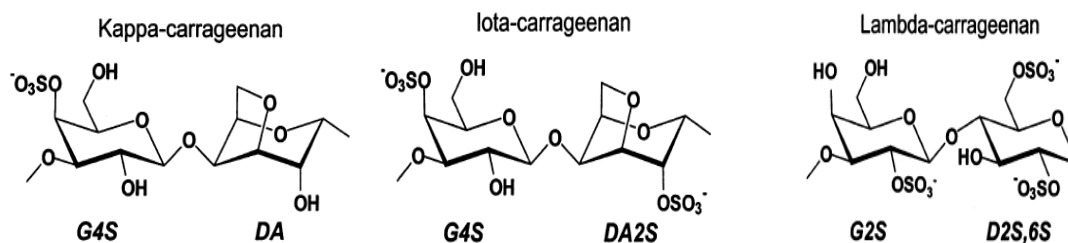


Figure 1.2. Structure of kappa, iota and lambda carrageenan (Knutsen et al³)

μ - and ν -car contain kinking units and are biochemical precursors of κ - and ι -car, respectively. They can be converted into κ - and ι -car by adding OH⁻ as a catalyst, see Figure 1.3. The presence of μ - and ν -car in Car powder has undesirable effects on the gelling properties.

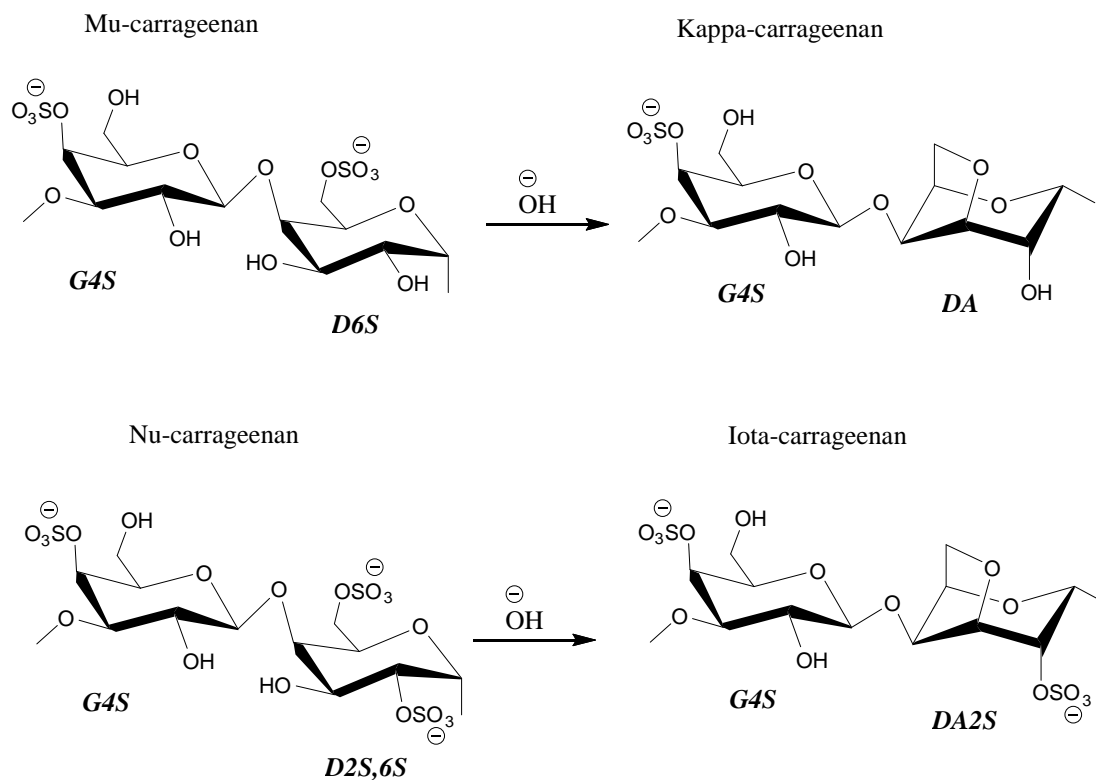


Figure 1.3. Conversion of the precursors μ - and ν -car into κ - and ι -car (Knutsen et al ³)

The Car chain contains not only galactose and sulfate, but also other carbohydrate residues such as xylose, glucose and uronic acids ⁶. Minerals such as ammonium, calcium, magnesium, potassium, and sodium are also present ^{47,48}.

Since Car is naturally contaminated by other carbohydrate residues and is quite polydisperse ⁴⁹⁻⁵², it is difficult to characterize quantitatively. Currently, NMR and light scattering (LS) techniques are utilized to determine the size distribution and structure. Investigations of the molar mass and size of Car using LS have been reported by many authors ⁵²⁻⁵⁶. Car has an average molecular weight (M_w) ranging between 10^5 and 10^6 g/mol ^{34,49,50,57,58}. The average radius of gyration (R_g) of Car chains in the coil conformation is proportional to the molar mass and varies between different types of Car. The hydrodynamic radius (R_h) is systematically smaller than R_g . Table 1.3 shows the molecular characteristics of Car in 0.1 M NaCl evaluated from static and dynamic light scattering at temperature 20-25°C.

Table 1.3. The average molar mass (M_w), the z-average radius of gyration (R_g) and hydrodynamic radius (R_h) of Car

<i>Carrageenan</i>	M_w (g/mol)	R_g (nm)	R_h (nm)	<i>References</i>
κ -car	$3.7 \cdot 10^5$	67	-	Wittgren et al ⁵⁹
κ -car	$6.75 \cdot 10^5$	69	33	Viebke et al ⁶⁰
κ -car	$4.21 \cdot 10^5$	72	32.9	Meunier et al ⁵⁸
κ -car	$3.71 \cdot 10^5$	66.8	29.7	Thanh et al ⁶¹
ι -car	$5.43 \cdot 10^5$	73.3	32.7	Thanh et al ⁶¹
λ -car	$2.3 \cdot 10^6$	109	118	Thanh et al ⁶¹

Table 1.4. Chemical shifts (ppm) of the α -anomeric protons of Car with respect to DSS as an internal standard at 0 ppm, recorded at 65°C (van De Velde et al ⁵)

<i>Car</i>	<i>Monosaccharide</i> *	<i>Chemical shift (ppm)</i>
β (beta)	DA	5.074
ι (iota)	DA2S	5.292
κ (kappa)	DA	5.093
λ (lambda)	D2S, 6S	5.548
ν (nu)	D2S, 6S	5.501
μ (mu)	D6S	5.238

*Codes refer to the nomenclature developed by Knutsen et al ⁶

NMR spectroscopy (both ^1H and ^{13}C NMR) can be used to analyze the sulfate content and monosaccharide composition. Samples for ^{13}C NMR are prepared at relatively high concentrations (5–10% w/w) compared to ^1H NMR samples (0.5–1.0 % w/w) ⁶ and in order to reduce the viscosity of Car in the commonly used solvents D_2O or DMSO, concentrated solutions are sonicated. Table 1.4 shows an example of the ^1H NMR chemical shift of Car

recorded at 65°C obtained at $C = 30$ g/L in D₂O with 20 mM Na₂HPO₄ and with DSS as a reference standard. The results show that different types of Car can be identified by chemical shifts (ppm) between 5.07 and 5.5 ppm. Other studies present similar results^{6,36,42}. The chemical shifts of the α -anomeric protons of the same type of Car depend on the recorded temperature⁶².

1.2.3. Carrageenan extraction

There are mainly two methods to extract Car namely extraction in aqueous and alkaline environments^{30,63–65} (summarized in Figure 1.4). From the early 1970s to the 1980s, extraction of Car with hot water was widely applied, the insoluble part was removed by filtration and Car was recovered from the solution. The native structure of Car could be maintained by this extraction method, but it had disadvantages: difficulty to filter due to the high viscosity of solutions, the presence residual solids in the extract and high costs.

Therefore extraction in an alkaline solution during several hours was preferred, which also led to an increase of the gel strength. In this manner all compounds that dissolve in alkaline solution are washed out. The product obtained in this manner is called semi-refined Car. Refined Car is obtained by heating semi-refined Car in aqueous solution followed by filtration³⁰. The main purpose of the treatment of seaweed with alkaline is that the penetration of OH⁻ groups into seaweed tissues leads to a nucleophilic displacement of some sulfate groups at the C6 position by alkoxy groups (-RO⁻) produced from the hydroxyl groups at the C3 positions to create 3,6-anhydro rings see Figure 1.3. However, exposure to high pH for an extended time leads hydrolysis and thus a decrease of the molar mass of the Car chains⁴³.

Car can be recovered from solution by precipitation or by freezing – thawing cycles and drying. Ethanol is commonly used for precipitation and the use of other solvents like methanol and isopropanol is restricted. Removing water from Car solutions by freezing-thawing has become a favored technique, because it is environmentally friendly. However, this process takes more time than precipitation and it can only be applied to strong gels such as κ -car. The residual water content of Car is removed by various drying techniques such as drying in the sun, hot air drying, vacuum drying and freeze drying. Drying in the sun is generally utilized by pilot manufacturers, while the hot air drying is the common method for producing commercial Car³⁰.

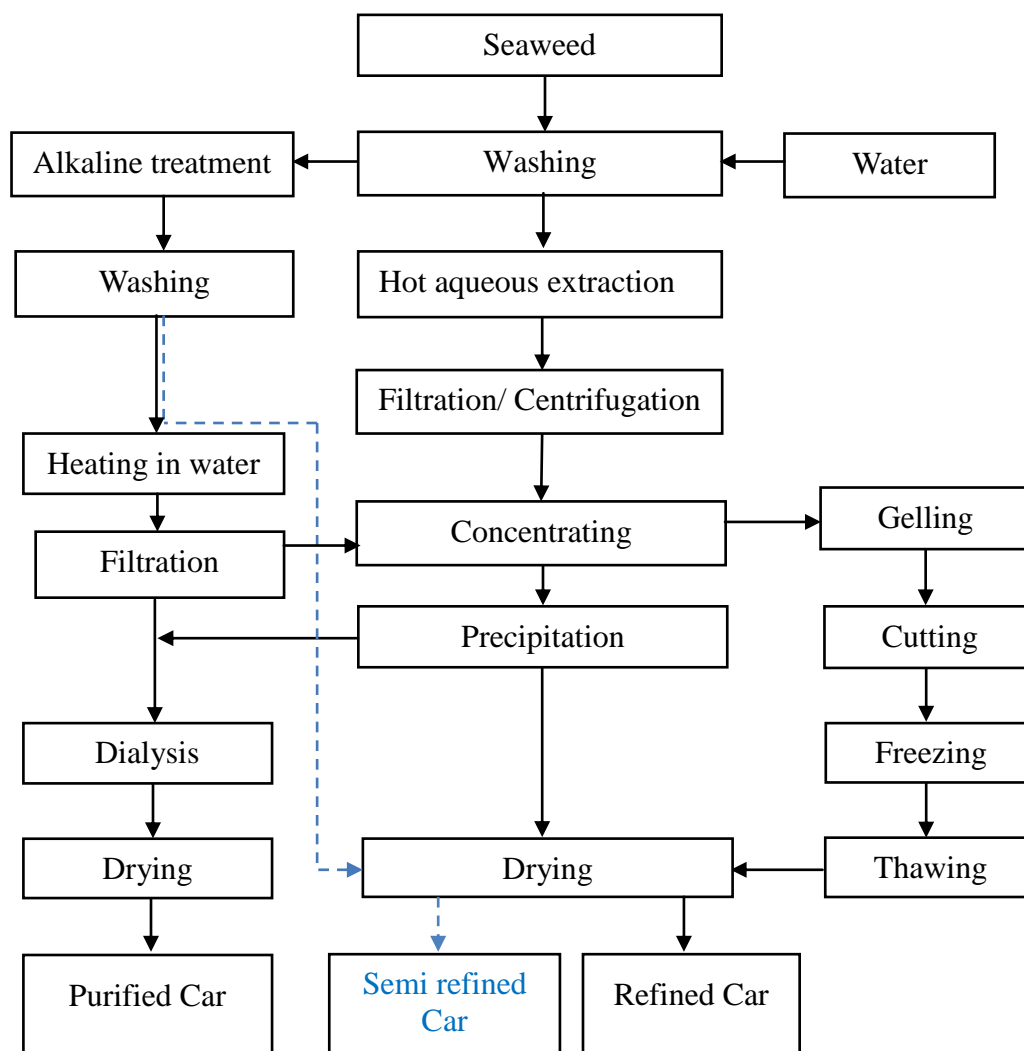


Figure 1.4. Flow chart of carrageenan extraction

Car naturally contains potassium, sodium, magnesium, and calcium sulfate. The relative proportion of ions in Car can be changed by processing methods. Pure sodium Car can be obtained by dialysis first against a NaCl solution and then against deionized water.

Several new extraction methods are being developed as eco-friendly alternatives to the alkaline treatment such as using enzymes to convert bioprecursors (μ - and ν -carrabiose) to the kappa and iota type ^{66,67}, microwave-assisted ⁶⁸ or ultrasound-assisted extraction ⁶⁹. However, the extraction using these methods is currently not commercially viable.

Parameters that influence the yield and quality of Car are not only the processing method^{47,65,70,71}, but also the location and conditions of seaweed cultivation^{10,72} and the storage conditions either⁷³. Increasing the duration of cultivation can increase the Car quality and the highest yields have been obtained from seaweed cultured between 45 and 60 days^{9,72}.

Only κ - and ι -car are used widely in industry due to their gelling properties. In general, seaweed does not produce pure κ - or ι -car with good gelling properties, because they are contaminated with bioprecursors that influence their functional properties. Hence, the manufacturers almost use the alkaline extraction to modify the Car structure to some extent.

1.2.4. Properties of carrageenan in aqueous solution

1.2.4.1. Solubility and stability

All Car are hydrophilic and insoluble in organic solvents such as alcohol, ether, and oil. The solubility depends on the type of Car, temperature and their associated cations. κ -Car is less soluble than others, because contains more hydrophobic 3,6-anhydro-D-galactose residues as part of the repeating unit and less sulfate groups, whereas λ -car that contains more sulfates and is devoid 3,6-anhydro-D-galactose residues is easily soluble at most conditions.

As will be discussed in the following section κ - and ι -car associate in aqueous solutions below a critical temperature that depends on the type and concentration of ions that are present. Therefore these types need to be solubilized at higher temperatures. Car is stable in aqueous solution in the pH range 7-10, but at lower pH and high temperatures hydrolysis may occur leading to loss of viscosity and gelling properties.

1.2.4.2. Gelation

The conformation of κ - and ι -car chains in aqueous solution changes from a random coil to a helix below a critical temperature (T_c)^{74,75}. The helices have a tendency to associate causing aggregation and gelation of the Car below T_c . Figure 1.5 shows example of the

dependence of the oscillatory storage (G') and loss (G'') moduli during cooling and heating.

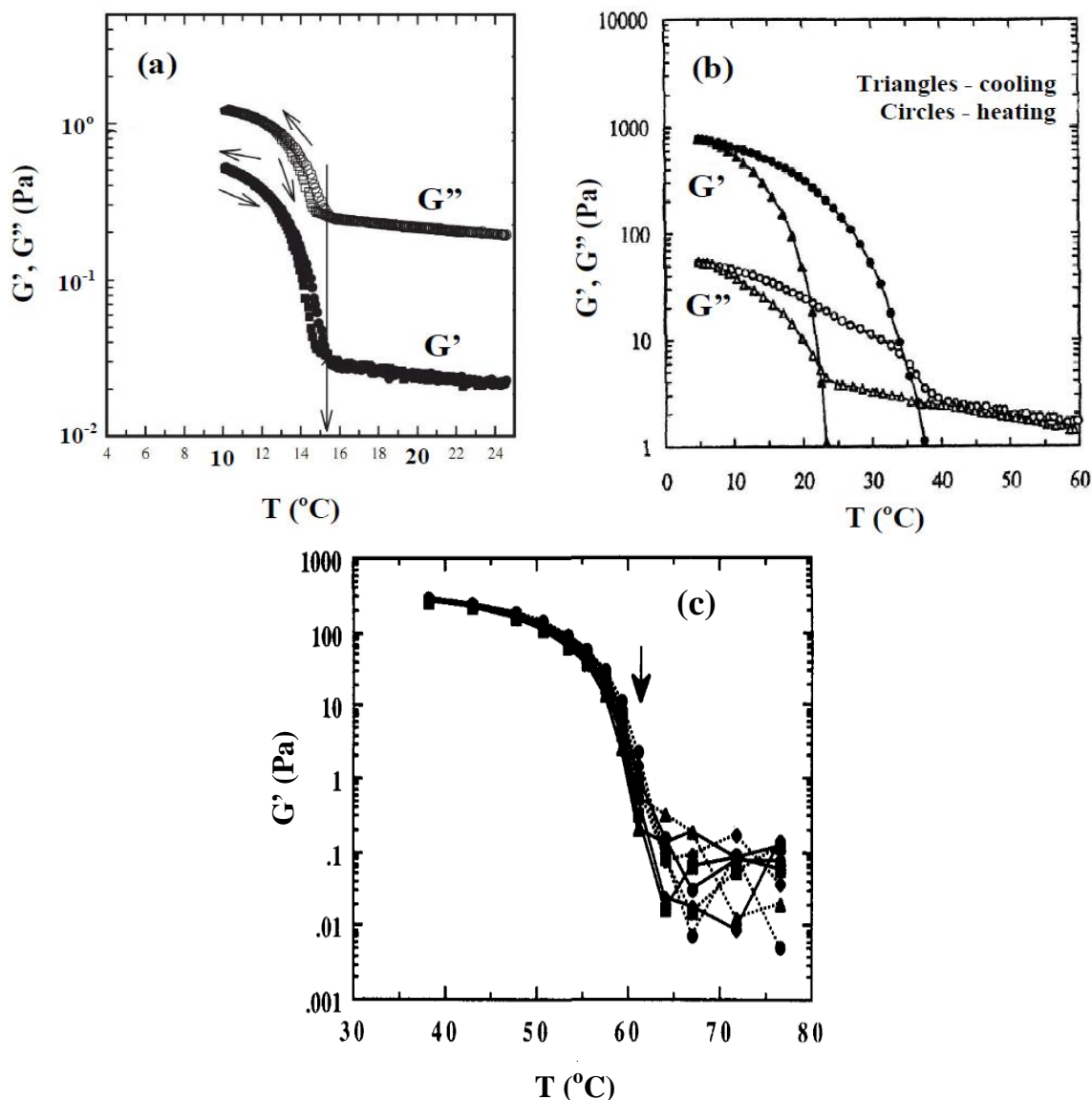


Figure 1.5a. Evolution of G' (closed symbols) and G'' (open symbols) as a function of temperature of κ -car at 0.4 g/L without KCl added, on cooling (circles) and heating (squares) (Núñez-Santiago et al ⁷⁶). Arrow indicates T_c

Figure 1.5b. Changes in G' (closed symbols) and G'' (open symbols) on cooling (triangles) and heating (circles) at $1^{\circ}\text{C}/\text{min}$ for 10 g/L κ -car with 5 mM added KCl. (Doyle et al ⁷⁷).

Figure 1.5c. Temperature dependence of G' of 2.5% purified sodium ι -car in 0.25M NaCl obtained on cooling (solid lines) and heating (dotted lines) at an oscillating frequency of 0.2 (▲), 0.5 (■), 1 (◆) or 2 (●) Hz. The arrow indicates T_c .

The effect of aggregation or gelation when $T < T_c$ causes a sharp increase of the moduli. If the Car concentration is sufficiently high and/or in presence of specific cations gels are formed and G' becomes larger than G'' . T_c and the gel stiffness strongly depend on the type and concentration of Car and the type and concentration of ions that are present^{13,21,78–82}. Rochas *et al*¹³ determined T_c for κ -car as a function of the salt concentration for a range of different cations (see Figure 1.6), ι -car is less sensitive to the presence of monovalent cations, but is more sensitive to divalent ions^{13,15,16}.

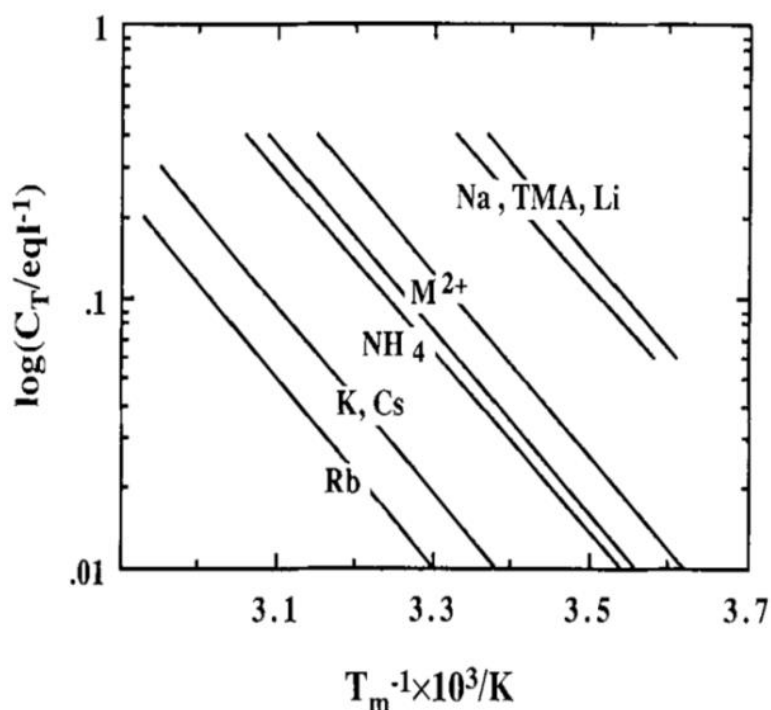


Figure 1.6. Dependence of the critical temperature of κ -car solutions on the total concentration (C_T) of various cations (Rochas *et al*¹³).

There is still controversy about whether double or single helices are formed^{14,51,56,83–87}, see Figure 1.7. In either case gels are formed by association of helices into a system spanning network.

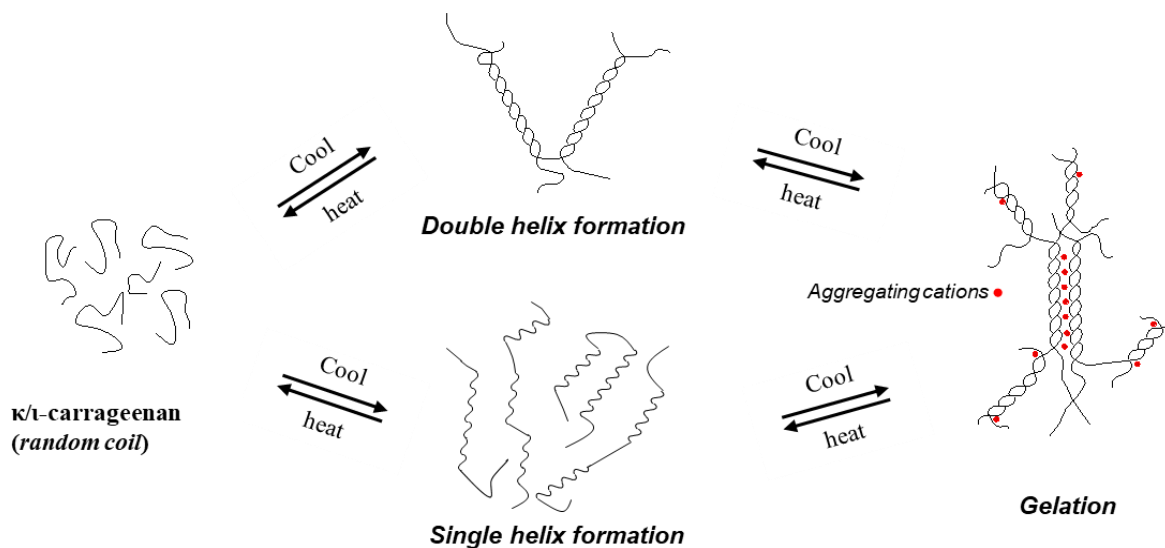


Figure 1.7. Gelation model of Car (Rochas et al⁶⁵ and Smidsrød et al⁸⁰)

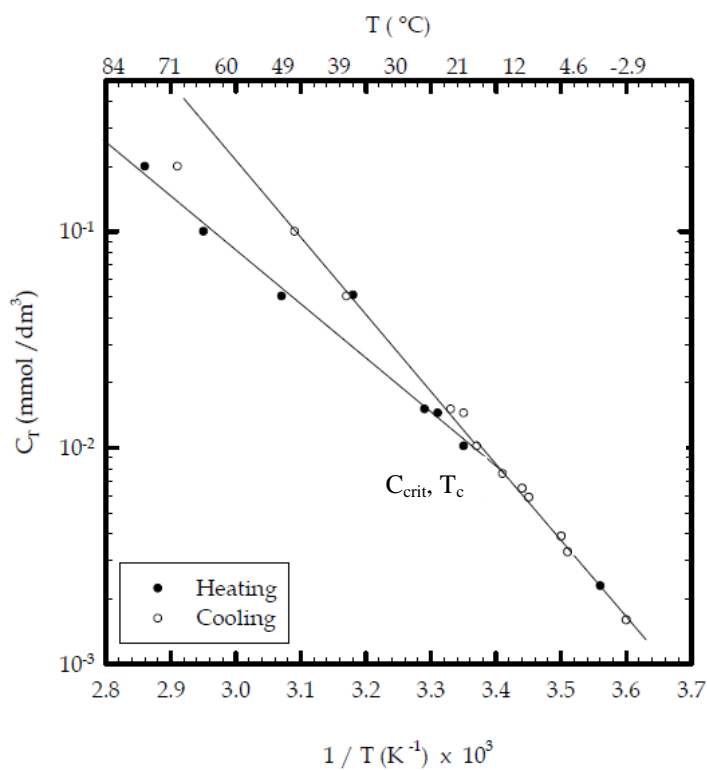


Figure 1.8. Variation of gelling temperature (T_g) and melting temperature (T_m) of κ -car in the presence of KCl for cooling (○) and heating (●) curves (Rochas et al¹³).

The coil-helix transition is thermo-reversible, which means that the gel can be formed by cooling hot solutions and melted by heating. For κ -car gels, the melting temperature (T_m) is often higher than the gelling temperature (T_g) which is called thermal hysteresis and depends on the type and concentration of cations, see Figure 1.5b. Figure 1.8 shows an example of the dependence of transition temperatures on the concentration of K^+ , for κ -car. Below a critical polymer concentration (C_{crit}), T_m and T_g are similar and there is no hysteresis. The transition temperature of ι -car is most often lower than that of κ -car⁷⁴ and there is no hysteresis for ι -car¹⁴. The presence of biological precursor units (λ -, μ -, and ν -cars) in the extracts impede the helix formation, thereby negatively influencing the gelation properties^{43,46}.

1.2.4.3. Rheological properties

❖ Carrageenan solutions

Many factors influence the viscosity of Car solutions, such as molecular weight, concentration, temperature, type of Car, and cations in the solution^{65,88,89}. Figure 1.9 shows that the viscosity of Car in deionized water increases strongly with the increasing Car concentration.

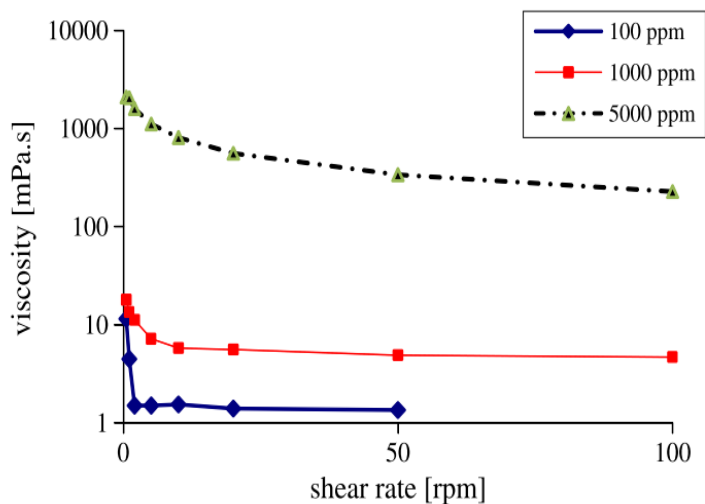


Figure 1.9. Viscosity of ι -car in deionized water (Stefan *et al*⁸⁸)

Research of Croguennoc *et al*⁹⁰ on semidilute κ -car solutions in the coil conformation (0.1 M NaCl, 20 °C) found that the low shear viscosity (η) increased following a power law at

higher polymer concentration, see Figure 1.10a. The presence of specific ions can cause aggregation of κ - and ι -car leading to more viscous systems. Núñez-Santiago *et al*⁷⁶ (Figure 1.10b) studied the viscosity of 5 g/L κ -car as a function of KCl concentration at 25°C and showed that there was first a decrease of η up to 4mM KCl, caused by screening of electrostatic interactions and subsequently a sharp increase caused by aggregation of the Car. Michele *et al*⁹¹ showed that η increased reversibly with decreasing temperature (Figure 1.11).

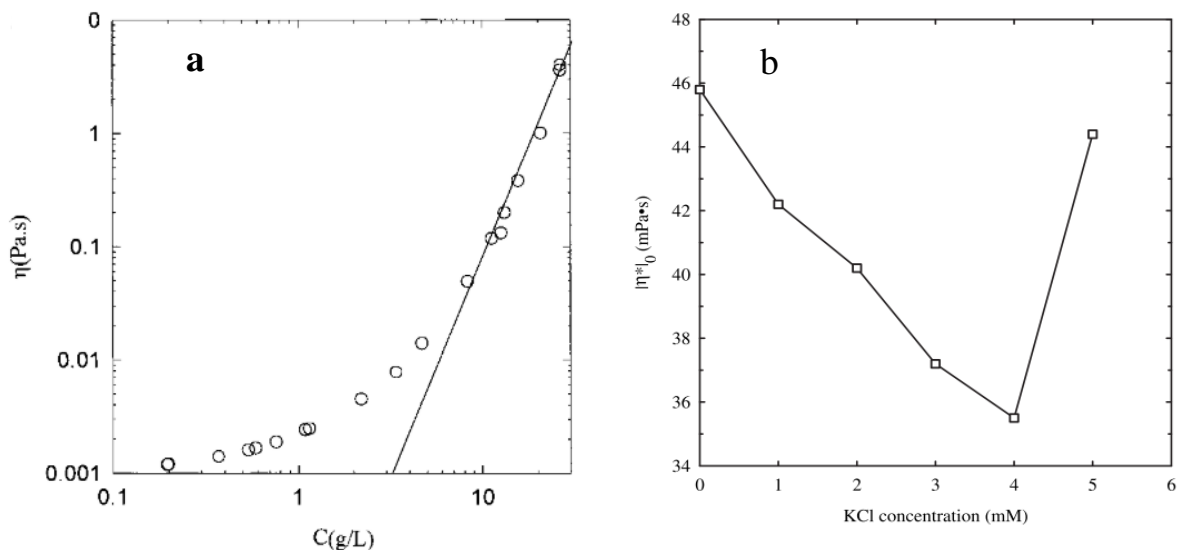


Figure 1.10a. The viscosity (η) of κ -car solution as a function of the concentration. The solid line represents the theoretical prediction for semidilute, flexible polymers in a good solvent (Croguennoc *et al*⁹⁰)

Figure 1.10b. Variations of the viscosity of 5 g/L κ -car as a function of KCl concentration (Núñez-Santiago *et al*⁷⁶).

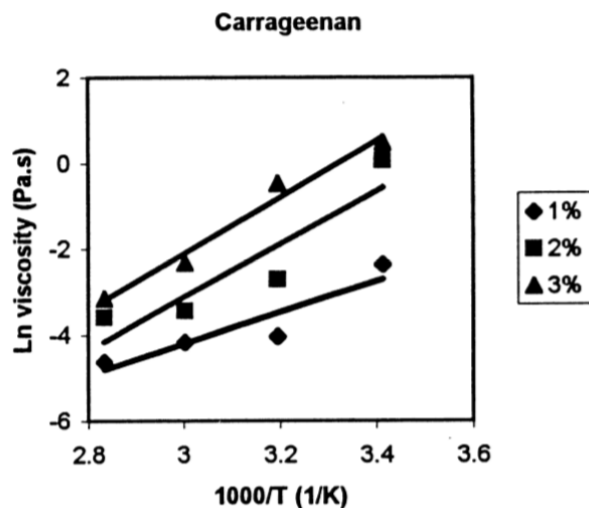


Figure 1.11. Arrhenius plots of the viscosity for κ -car solutions at different concentrations (Michel et al ⁹¹)

❖ Carrageenan gels

The differences in gel strength for different types of Car are mainly caused by the presence of 3,6-anhydro-D-galactose residues that are present in gelling κ - and ι -car, but not in non-gelling Car such as the λ -, μ -, and ν -car (Figure 1.2 & 1.3). The gel stiffness increases with increasing cation concentration, but saturates above a certain concentration ^{79,89}.

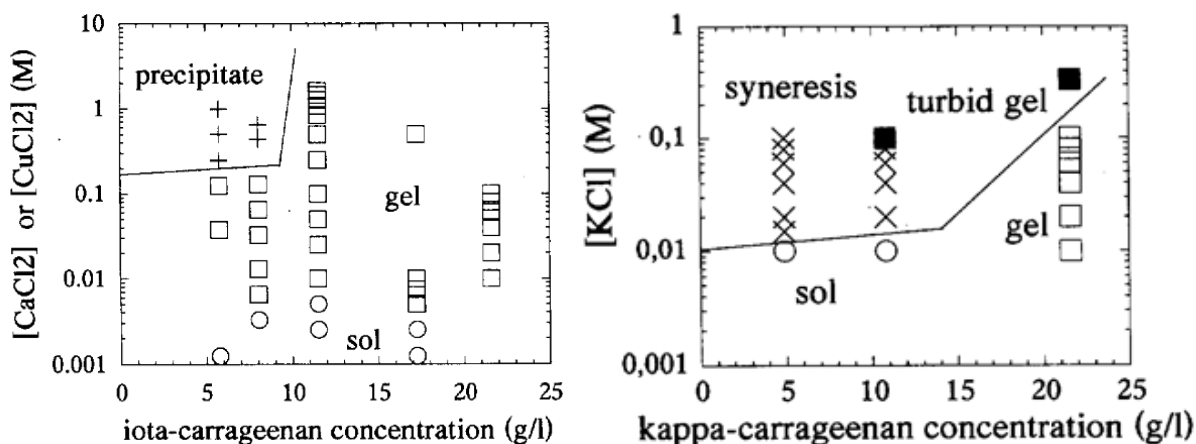


Figure 1.12. Phase diagram of ι - and κ -car in the presence of $\text{CaCl}_2/\text{CuCl}_2$ and KCl , respectively (■ turbid gel, □ clear gel, ○ clear sol, x syneresis, + precipitate) (Michel et al ⁸²)

Results of Michel *et al*⁸² showed that the sol-gel diagram of κ - and ι -car (see Figure 1.12) depends on the type of Car and the type and concentration of the cations. The homogeneity/ heterogeneity of the Car solutions and gels also depend on the type of ions and Car.

The gel stiffness increases with increasing Car concentration^{12,80,83,92}. The critical Car concentration to form a self supporting gel depends on the type of Car and ions present. Nguyen *et al*⁸⁰, for example, showed that in the presence of 10 mM KCl, κ -car at 2 g/L was enough to form a gel. Moreover, the investigations of Smidsrød *et al*⁹² and Rochas *et al*²¹ on the role of the molecular weight of κ -car found that gels are formed more easily with high molar mass Car. Below a critical value ($M_w < 3 \times 10^4$ Da) gelation did not occur.

1.2.5. Mixtures of different types of carrageenan

Mixtures of κ - and ι -car were in first instance studied in order to measure the effect of impurity of ι -car in κ -car gel¹⁵ and vice versa²¹. Rochas *et al*²¹ found that the elastic modulus of mixed gels decreased with increasing ι -car content. However, the yield stress of the mixed gels at a 50-50 ratio was higher than the sum of the individual Car gels. Later on, more studies were done on the behavior of Car in mixed systems by using other techniques such as DSC (Differential Scanning Calorimetry), NMR, turbidity and rheological measurements^{17-20,93,94}. These studies showed a two-step gelation process at temperatures that were equal to the coil-helix temperature (T_c) of the individual Car solutions at the same ion concentrations¹⁶⁻²⁰. This means that the coil-helix transition of the two types of Car chains is not influenced by the presence of the other type. The gel stiffness of ι -car gels in mixtures with κ -car in the coil conformation was found to be very close to that of the equivalent individual ι -car gels indicating that the gelation of ι -car was little influenced by the presence of κ -car coils. However, the gel stiffness of mixed gels was found to be much larger than the sum of the elastic moduli of the individual gels. This means that the two types of Car do not form independent homogeneously distributed networks²⁰.

It was suggested that the networks of each type of Car are microphase separated^{16,17,19,20}. Microphase separation causes the density of each network to be higher, which could explain the higher gel stiffness compared to a simple sum of the moduli of the individual networks. However, phase separation was not observed when solutions of κ -car and ι -car

were mixed in the coil conformation. In addition, the fact that the stiffness of ι -car gels is not influenced by the presence of κ -car coils suggests that phase separation does not occur in that case either. Therefore microphase separation, if it indeed occurs, is driven by formation of the κ -car network within the ι -car network when both Car are in the helical conformation.

Brenner *et al*²⁰ discussed in some details the issue of whether interpenetrated or microphase separated mixed gels are formed. They excluded on the basis of rheological measurements that non-interacting interpenetrated κ -car and ι -car networks are formed in the mixtures. Instead they concluded that the results were compatible with formation of bicontinuous microphase separated networks, but this hypothesis was not backed up by measurements of the microstructure. More recently, Hu *et al*⁹³ studied the diffusion of trace PEO chains in individual and mixed κ -car and ι -car gels using pulsed field gradient NMR. They observed a single diffusion process of PEO chains in mixed gels, which implies that if microphase separation occurs the κ -car and ι -car domains are smaller than 450 nm.

1.2.6. Microstructure of carrageenan gels

The microstructure of Car gels has been studied by Scanning Electron Microscopy (SEM), Atomic Force Microscopy (AFM), and Confocal Laser Scanning Microscopy (CLSM)⁹⁵⁻⁹⁹. Thrimawithana *et al*⁹⁹ have investigated the interaction between counter-ions and molecules of individual κ -car or ι -car by SEM. They could distinguish the absence or appearance of cross-linked structures by observing the absence or formation of rectangular pores on the images. The same technique was used by MacArtain *et al*⁷⁹ to observe the structure of κ -car in the presence of Ca^{2+} . Figure 1.13 shows SEM images of individual of κ -car and ι -car in the presence of calcium ions. The network of ι -car in the presence of calcium ion shows a dense structure (Figure 1.13a), whereas in the case of κ -car, it is a fine structure with thin filaments of κ -car linked together to form a continuous network (Figure 1.13b). However, a network of κ -car with excessive amount of KCl appeared as a rigid structure resulting presumably from large aggregates of helices⁹⁵. These observations are compatible with the investigations on rheological properties of Car gels in the literature that show that κ -car forms a strong gel with potassium ions, and ι -car gelation is induced by calcium ions.

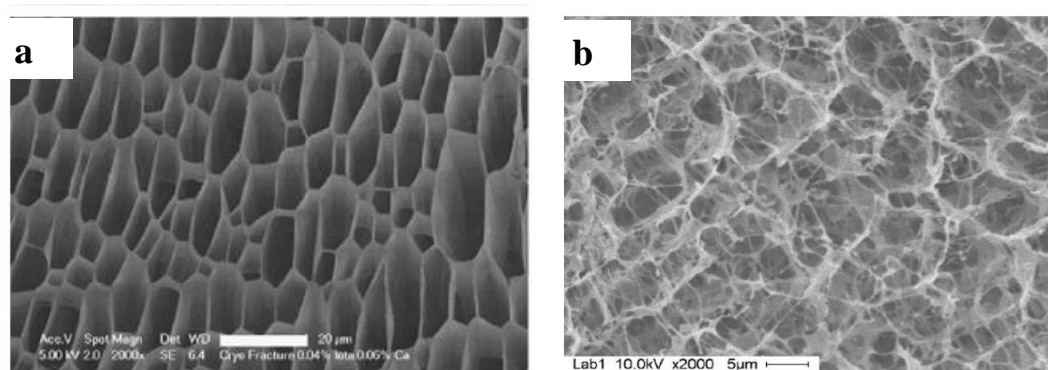


Figure 1.13. SEM images of ι -car gel at 4 g/L and 6 mM CaCl_2 (Thrimawithana *et al*⁹⁹) (a) and κ -car at 5 g/L and 5 g/L CaCl_2 (MacArtain *et al*⁷⁹) (b).

CLSM has been shown to be a useful method for investigating the structure of polymers. With this technique, the sample does not need to be dehydrated as for SEM or AFM, which might perturb the structure. However, CLSM requires labelling with fluorescent probes. Study of Núñez-Santiago *et al*⁷⁶ showed that κ -car (labeled with rhodamine B isothiocyanate) in the presence of KCl appeared as a homogeneous network on length scales accessible to light microscopy ($>100\text{nm}$) (Figure 1.14). Lundin *et al*¹⁷ showed a heterogeneous microstructure for a mixture of ι - and κ -car, see Figure 1.15, and interpreted this in terms of microphase separation between the two types of Car. However, a heterogeneous microstructure does not imply that microphase separation has occurred as similar heterogeneous microstructure can also be seen for individual Car gels.

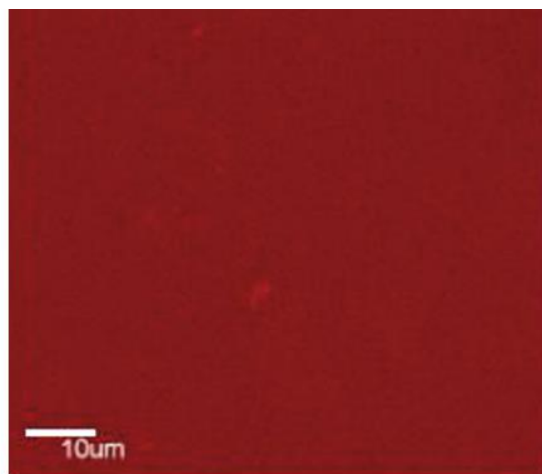


Figure 1.14. CLSM image of κ -car 5g/L and 100 mM KCl at 20°C (Núñez-Santiago *et al*).

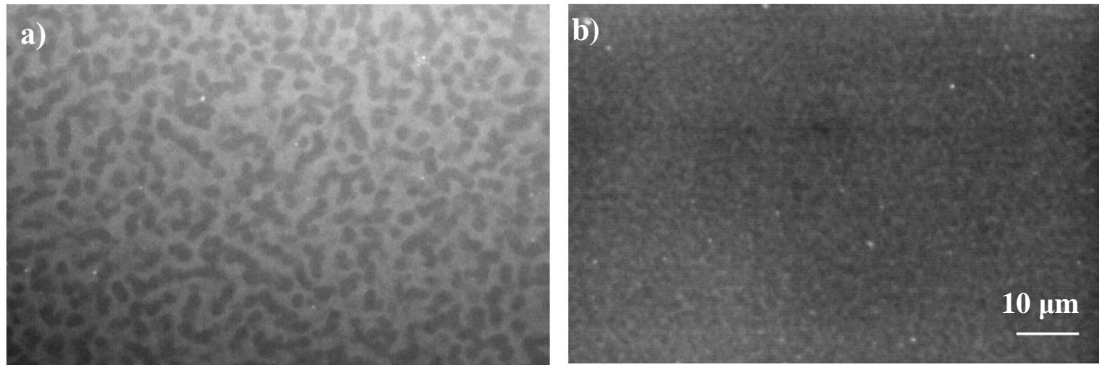


Figure 1.15. Confocal laser scanning micrographs of a mixture of 11.25 g/L ι -car and 15 g/L κ -car) in 400 mM NaCl (a) and mixture of 10 g/L ι -car and 15 g/L κ -car in 50 mM KCl (b) (Lundin *et al*¹⁷)

1.2.7. Applications

1.2.7.1. Food applications

Car has no nutritional value but it is widely utilized in the food industry due to its excellent physical functional properties such as thickening, gelling and stabilizing abilities. It is not significantly degraded in gastrointestinal tract in the stomach, but neither does it significantly affect absorption of nutrients¹⁰⁰. As a food additive (E407), Car is present in many processed foods, including dairy products, meat products, beverages, condiments, infant formula, and pet food^{6,30}.

Car has the ability to bind with milk proteins, hence the addition to dairy products can improve texture, thickness, and solubility¹⁰¹. Some typical products containing Car are whipped cream, yogurt, and liquid milk products⁷⁵.

Car is used as a fat substitute in processed meats and base-meat products^{4,101,102}. In these products, Car contributes to gel formation and water retention. It improves the water holding capacity leading to decreased toughness and increased juiciness, preserving the sensory quality during storage. By adding 3% Car during preparation of frankfurter sausages the sensory scores in the texture, color and taste were all higher than that of control sausages¹⁰³. Verbeke *et al*¹⁰⁴ indicated that the presence of Car in salt-soluble meat networks increased the gel strength and the water holding capacity. This was due to the network formed

by protein and Car upon cooling. Research on Alaska pollock surimi ¹⁰⁵ also showed that adding κ -car enhanced the gel strength of the product.

Edible coating produced by Car for fresh-cut packaged fruits is one example of novel use of the polymer in food industry ¹⁰⁶⁻¹⁰⁸. Car coatings function as a gas barrier, adhering to the cut surface of the fruit and reduce respiration. These studies have shown that Car reduced microbial contamination and prolonged shelf life.

1.2.7.2. Non- food application

Car is also used in various non-food products, such as pharmaceuticals, cosmetics, printing and textile formulations ^{6,27}. For example, Car is used in air freshener gels, toothpaste, shampoo and cosmetic creams. In recent years, it has been established that Car can control the release of bioactive compounds, flavors and probiotics ^{109,110}.

References

1. Juteau, A., Doublier, J. L. & Guichard, E. Flavor release from ι -carrageenan matrices: a kinetic approach. *J. Agric. Food Chem.* **52**, 1621–1629 (2004).
2. Yegappan, R., Selvaprithiviraj, V., Amirthalingam, S. & Jayakumar, R. Carrageenan based hydrogels for drug delivery, tissue engineering and wound healing. *Carbohydr. Polym.* **198**, 385–400 (2018).
3. Knutsen, S. H., Myslabodski, D. E., Larsen, B. & Usov, A. I. A. Modified System of Nomenclature for Red Algal Galactans. *Bot. Mar.* **37**, 163–169 (1994).
4. Trius, A. & Sebranek, J. G. Carrageenans and Their Use in Meat Products. *Crit. Rev. Food Sci. Nutr.* **36**, 69–85 (1996).
5. van De Velde, F., Pereira, L. & Rollema, H. S. The revised NMR chemical shift data of carrageenans. *Carbohydr. Res.* **339**, 2309–2313 (2004).
6. van De Velde, F., Knutsen, S. H., Usov, A. I., Rollema, H. S. & Cerezo, A. S. ^1H and ^{13}C high resolution NMR spectroscopy of carrageenans: application in research and industry. *Trends Food Sci. Technol.* **13**, 73–92 (2002).
7. Ask, E. I. & Azanza, R. V. Advances in cultivation technology of commercial eucheumatoid species: A review with suggestions for future research. *Aquaculture* **206**, 257–277 (2002).
8. Phang, S. M., Yeong, H. Y., Lim, P. E., Nor, A. R. M. & Gan, K. T. Commercial varieties of *Kappaphycus* and *Eucheuma* in Malaysia. *Malaysian J. Sci.* **29**, 214–224 (2010).
9. Ohno, M., Nang, H. Q. & Hirase, S. Cultivation and carrageenan yield and quality of *Kappaphycus alvarezii* in the waters of Vietnam. *J. of Applied Phycol.* **8**, 431–437 (1996).
10. Hung, L. D., Hori, K., Nang, H. Q., Kha, T. & Hoa, L. T. Seasonal changes in growth rate, carrageenan yield and lectin content in the red alga *Kappaphycus alvarezii* cultivated in Camranh Bay, Vietnam. *J. Appl. Phycol.* **21**, 265–272 (2009).
11. Morris, E. R. Molecular Interactions in Polysaccharide Gelation. *Br. Polym. J.* **18**, 14–21 (1986).
12. Landry, M. R. S. & Rochas, C. Role of the Molecular Weight on the Mechanical Cels Properties of Kappa Carrageenan previously. *Carbohydr. Polym.* **2**, 255–266 (1990).

13. Rochas, C. & Rinaudo, M. Activity Coefficients of Counterions and Conformation in Kappa-Carrageenan System. *Biopolymers* **19**, 1675–1687 (1980).
14. Yuguchi, Y., Thu Thuy, T. T., Urakawa, H. & Kajiwara, K. Structural characteristics of carrageenan gels: Temperature and concentration dependence. *Food Hydrocolloids* **16**, 515–522 (2002).
15. Piculell, L., Nilsson, S. & Muhrbeck, P. Effects of small amounts of kappa-carrageenan on the rheology of aqueous iota-carrageenan. *Carbohydr. Polym.* **18**, 199–208 (1992).
16. Piculell, L., Håkansson, C. & Nilsson, S. Cation specificity of the order-disorder transition in iota carrageenan: effects of kappa carrageenan impurities. *Int. J. Biol. Macromol.* **9**, 297–301 (1987).
17. Lundin, L., Odic, K., Foster, T. J., & Norton, I. T. Phase separation in mixed carrageenan systems. In *Supramolecular and colloidal structures in Biomaterials and Biosubstrates* 436–449 (ICP, 2000)
18. Parker, A., Brigand, G., Miniou, C., Trespoey, A. & Vallée, P. Rheology and fracture of mixed ι- and κ-carrageenan gels: Two-step gelation. *Carbohydr. Polym.* **20**, 253–262 (1993).
19. Du, L., Brenner, T., Xie, J. & Matsukawa, S. A study on phase separation behavior in kappa/iota carrageenan mixtures by micro DSC, rheological measurements and simulating water and cations migration between phases. *Food Hydrocoll.* **55**, 81–88 (2016).
20. Brenner, T., Tuvikene, R., Parker, A., Matsukawa, S. & Nishinari, K. Rheology and structure of mixed kappa-carrageenan/iota-carrageenan gels. *Food Hydrocoll.* **39**, 272–279 (2014).
21. Rochas, C., Rinaudo, M. & Landry, S. Relation between the molecular structure and mechanical properties of carrageenan gels. *Carbohydr. Polym.* **10**, 115–127 (1989).
22. Bixler, H. J. & Porse, H. A decade of change in the seaweed hydrocolloids industry. *J. Appl. Phycol.* **23**, 321–335 (2011).
23. FAO. The State of World Fisheries and Aquaculture. Contributing to food security and nutrition for all (2016). doi:92-5-105177-1
24. FAO. The State of World Fisheries and Aquaculture. Meeting the sustainable development goals (2018). doi:978-92-5-130562-1

25. Armisen, R. Agar and agarose biotechnological applications. *Hydrobiologia* **221**, 157–166 (1991).
26. Araki, C. & Arai, K. Studies on the Chemical Constitution a New Disaccharide as a Reversion of Agar-agar . Isolation Product from Acidic Hydrolysate. *Bull. Chem. Soc. Jpn.* **40**, 1452–1456 (1967).
27. Tye, Y. Y. *et al.* A review of extractions of seaweed hydrocolloids: Properties and applications. *eXPress Polym. Lett.* **12**, 296–317 (2018).
28. Rhein-Knudsen, N., Ale, M. T., Ajallouelian, F., Yu, L. & Meyer, A. S. Rheological properties of agar and carrageenan from Ghanaian red seaweeds. *Food Hydrocoll.* **63**, 50–58 (2017).
29. Cristiane, M. *et al.* Antioxidant activities of sulfated polysaccharides from brown and red seaweeds. *J. Appl. Phycol.* **19**, 153–160 (2007).
30. McHugh Dennis J. FAO Fisheries Technical Paper 441. A guide to the seaweed industry. (2003).
31. Sharma, A. & Gupta, M. N. Three phase partitioning of carbohydrate polymers: Separation and purification of alginates. *Carbohydr. Polym.* **48**, 391–395 (2002).
32. Torres, M. R. *et al.* Extraction and physicochemical characterization of *Sargassum vulgare* alginate from Brazil. *Carbohydr. Res.* **342**, 2067–2074 (2007).
33. Szekalska, M., B, A. P., N, E. S., Ciosek, P. & Winnicka, K. Alginate: Current Use and Future Perspectives in Pharmaceutical and Biomedical Applications. *Int. J. Polym. Sci.* 1–17 (2016).
34. Webber, V., De Carvalho, S. M. & Barreto, P. L. M. Molecular and rheological characterization of carrageenan solutions extracted from *Kappaphycus alvarezii*. *Carbohydr. Polym.* **90**, 1744–1749 (2012).
35. Estevez, J. M., Ciancia, M. & Cerezo, A. S. The system of low-molecular-weight carrageenans and agaroids from the room-temperature-extracted fraction of *Kappaphycus alvarezii*. *Carbohydr. Res.* **325**, 287–299 (2000).
36. van de Velde, F. & Rollema, H. S. High Resolution NMR of Carrageenans. in *Modern Magnetic Resonance* (ed. Webb, G. A.) 1605–1610 (Springer, Dordrecht, 2008).
37. Mccandless, E. L. Carrageenans in the Gametophytic and Sporophytic Stages of *Chondrus crispus*. *Planta (Berl.)* **112**, 201-212, (1973).

38. Falshaw, R., Bixlerb, H. J. & Johndrob, K. Structure and performance of commercial kappa-2 carrageenan extracts. Structure analysis. *Food Hydrocoll.* **15**, 441-452 (2001).
39. Tan, J. *et al.* *Kappaphycus malesianus* sp: a new species of Kappaphycus (Gigartinales, Rhodophyta) from Southeast Asia. *J. Appl. Phycol.* **26**, 1273–1285 (2014).
40. Collén, J. *et al.* *Chondrus crispus* - A present and historical model organism for red seaweeds. *Advances in Botanical Research* **71**, 53-89 (2014).
41. Aguilan, J. T. *et al.* Structural analysis of carrageenan from farmed varieties of Philippine seaweed. *Bot. Mar.* **46**, 179–192 (2003).
42. van de Velde, F. Structure and function of hybrid carrageenans. *Food Hydrocoll.* **22**, 727–734 (2008).
43. Azevedo, G., Torres, M. D., Sousa-pinto, I. & Hilliou, L. Effect of pre-extraction alkali treatment on the chemical structure and gelling properties of extracted hybrid carrageenan from *Chondrus crispus* and *Ahnfeltiopsis devoniensis*. *Food Hydrocoll.* **50**, 150–158 (2015).
44. Campo, V. L., Kawano, D. F., Silva, D. B. da & Carvalho, I. Carrageenans: Biological properties, chemical modifications and structural analysis - A review. *Carbohydr. Polym.* **77**, 167–180 (2009).
45. van De Velde, F. *et al.* The structure of κ/ι -hybrid carrageenans II. Coil-helix transition as a function of chain composition. *Carbohydrate Research* **340**, 1113–1129 (2005).
46. van De Velde, F. *et al.* Coil-helix transition of ι -carrageenan as a function of chain regularity. *Biopolymers* **65**, 299–312 (2002).
47. Chan, P. T. & Matanjun, P. Chemical composition and physicochemical properties of tropical red seaweed, *Gracilaria changii*. *Food Chem.* **221**, 302–310 (2017).
48. Smitha, J. L., Summers, G. & Wong, R. Nutrient and heavy metal content of edible seaweeds in New Zealand. *New Zeal. J. Crop Hortic. Sci.* **38**, 19–28 (2010).
49. Lars-Gosta Ekstrom, J. K. Optimality conditions for linear fractional bilevel programs. *Carbohydr. Res.* **116**, 89–94 (1983).
50. Viebke, C., Borgstrsm, J. & Piculell, L. Characterisation of kappa- and iota-carrageenan coils and helices by MALLS / GPC. **8617**, 145–154 (1995).
51. Hoffmann, R. A., Gidley, M. J., Cooke, D. & Frith, W. J. Effect of isolation procedures on the molecular composition and physical properties of *Eucheuma cottonii*

- carrageenan. *Top. Catal.* **9**, 281–289 (1995).
52. Meunier, V., Nicolai, T., Durand, D. & Parker, A. Light Scattering and Viscoelasticity of Aggregating and Gelling κ -Carrageenan. *Macromolecules* **32**, 2610–2616 (1999).
 53. Meunier, V., Nicolai, T. & Durand, D. Structure and Kinetics of Aggregating. *Macromolecules* **33**, 2497–2504 (2000).
 54. Sloodmaekers, D. & Mandel, M. Dynamic light scattering by iota- and kappa-carrageenan solutions. *Int. J. Biol. Macromol.* **13**, 17–25 (1991).
 55. Abad, L. V *et al.* Dynamic light scattering studies of irradiated kappa carrageenan. *Int. J. Biol. Macromol.* **34**, 81–88 (2004).
 56. Mangione, M. R., Giacomazza, D., Bulone, D., Martorana, V. & Biagio, P. L. S. Thermoreversible gelation of kappa-carrageenan: relation between conformational transition and aggregation. *Biophysical Chem.* **104**, 95–105 (2003).
 57. Lecacheux, D., Panaras, R., Brigand, G. & Martin, G. Molecular weight distribution of carrageenans by size exclusion chromatography and low angle laser light scattering. *Carbohydr. Polym.* **5**, 423–440 (1985).
 58. Brown, W. *Light Scattering: Principles and Developments.* (Oxford: Clarendon Press, 1996).
 59. Wittgren, B., Borgstrom, J., Picullel, L. & Wahlund, K., -G. Conformational Change and Aggregation of κ -Carrageenan Studied by Flow Field-Flow Fractionation and Multiangle. *Biopolymers* **45**, 85–96 (1997).
 60. Viebke, C. & Williams, P. A. Determination of molecular mass distribution of κ -carrageenan and xanthan using asymmetrical flow field-flow fractionation. *Food Hydrocoll.* **14**, 265–270 (2000).
 61. Thành, T. T. T. *et al.* Molecular Characteristics and Gelling Properties of the Carrageenan Family 1, Preparation of Novel Carrageenans and their Dilute Solution Properties. *Macromol. Chem. Phys.* 15–23 (2002).
 62. Tojo, E. & Prado, J. A simple ^1H NMR method for the quantification of carrageenans in blends. *Carbohydr. Polym.* **53**, 325–329 (2003).
 63. Bixle, H. J. Recent developments in manufacturing and marketing carrageenan. *Hydrobiologia* **326/327**, 35–57 (1996).
 64. Montolalu, R. I., Tashiro, Y., Matsukawa, S. & Ogawa, H. Effects of extraction

- parameters on gel properties of carrageenan from *Kappaphycus alvarezii* (Rhodophyta). *J. Appl. Phycol.* **20**, 521–526 (2008).
65. Bono, A., Anisuzzaman, S. M. & Ding, O. W. Effect of process conditions on the gel viscosity and gel strength of semi-refined carrageenan (SRC) produced from seaweed (*Kappaphycus alvarezii*). *J. King Saud Univ. - Eng. Sci.* **26**, 3–9 (2014).
66. Zinoun, M., Diouris, M., Potin, P., Floc, J. Y. & Deslandes, E. Evidence of Sulfohydrolase Activity in the Red Alga *Calliblepharis jubata*. **40**, 49–53 (1997).
67. Sabine M. Genicot; Agnès Groisiller, H  l  ne Rogniaux, Laurence Meslet-Cladi  re, Tristan Barbeyron, W. H. Discovery of a novel iota carrageenan sulfatase isolated from the marine bacterium *Pseudoalteromonas carrageenovora*. *Front. Chem.* **2**, 1–15 (2014).
68. E. V  zquez-Delf  n & D. Robledo & Y. Freile-Pelegr  n. Microwave-assisted extraction of the Carrageenan from *Hypnea musciformis* Microwave-assisted extraction of the Carrageenan from *Hypnea musciformis* (Cystocloniaceae, Rhodophyta). *J. Appl. Phycol.* **26**, 901–907 (2013).
69. Rafiquzzaman, S. M., Ahmed, R., Lee, M., Noh, G. & Jo, G. Improved methods for isolation of carrageenan from *Hypnea musciformis* and its antioxidant activity. *J. Appl. Phycol.* **28**, 1265–1274 (2015).
70. Moses, J., Anandhakumar, R. & Shanmugam, M. Effect of alkaline treatment on the sulfate content and quality of semi-refined carrageenan prepared from seaweed *Kappaphycus alvarezii* Doty (Doty) farmed in Indian waters. *African J. Biotechnol.* **14**, 1584–1589 (2015).
71. Karlsson, A. & Singh, S. K. Acid hydrolysis of sulphated polysaccharides. Desulphation and the effect on molecular mass. *Carbohydr. Polym.* **38**, 7–15 (1999).
72. Hayashi, L. *et al.* The effects of selected cultivation conditions on the carrageenan characteristics of *Kappaphycus alvarezii* (Rhodophyta, Solieriaceae) in Ubatuba Bay, S  o Paulo, Brazil. *J. Appl. Phycol.* **19**, 505–511 (2007).
73. Hilliou, L. *et al.* The impact of seaweed life phase and postharvest storage duration on the chemical and rheological properties of hybrid carrageenans isolated from Portuguese *Mastocarpus stellatus*. *Carbohydr. Polym.* **87**, 2655–2663 (2012).
74. Rochas, R. M. Calorimetric determination of the conformational transition of kappa

- carrageenan. *Carbohydr. Res.* **105**, 227–236 (1982).
75. Piculell, L. Gelling Carrageenans. in *Food Polysaccharides and Their Applications* (ed. A. Williams, A. M. Stephen and G. O. Phillips) 239–288 (Taylor & Francis, 2006)
 76. Núñez-Santiago, M. C., Tecante, A., Garnier, C. & Doublier, J. L. Rheology and microstructure of κ -carrageenan under different conformations induced by several concentrations of potassium ion. *Food Hydrocoll.* **25**, 32–41 (2011).
 77. Doyle, J., Giannouli, P., K. Philp & Morris, E. R. Effect of K^+ and Ca^{2+} cations on gelation of kappa-carrageenan. *Gums Stabilisers Food Ind.* **11**, 158–164 (2002).
 78. Norton, I. T., Goodall, D. M., Morris, E. R. & Rees, D. A. Role of cations in the conformation of iota and kappa carrageenan. *J. Chem. Soc. Faraday Trans. 1* **79**, 2475–2488 (1983).
 79. MacArtain, P., Jacquier, J. C. & Dawson, K. A. Physical characteristics of calcium induced κ -carrageenan networks. *Carbohydr. Polym.* **53**, 395–400 (2003).
 80. Nguyen, B. T., Nicolai, T., Benyahia, L. & Chassenieux, C. Synergistic effects of mixed salt on the gelation of κ -carrageenan. *Carbohydr. Polym.* **112**, 10–15 (2014).
 81. Robal, M. *et al.* Monocationic salts of carrageenans: Preparation and physico-chemical properties. *Food Hydrocoll.* **63**, 656–667 (2017).
 82. Michel, A. S., Mestdagh, M. M. & Axelos, M. A. V. Physico-chemical properties of carrageenan gels in presence of various cations. *International Journal of Biological Macromolecules* **21**, 195–200 (1997).
 83. Morris, E. R., Rees, D. A. & Robinson, G. Cation-specific aggregation of carrageenan helices: Domain model of polymer gel structure. *J. Mol. Biol.* **138**, 349–362 (1980).
 84. Viebke, C., Piculell, L. & Nilsson, S. On the Mechanism of Gelation of Helix-Forming *Biopolymers* **27**, 4160–4166 (1994).
 85. Kara, S., Tamerler, C. & Pekcan, Ö. Cation effects on swelling of κ -carrageenan: A photon transmission study. *Biopolymers* **70**, 240–251 (2003).
 86. Smidsrod, O. & Grasdalen, H. Some physical properties of carrageenan in solution and gel state. *Carbohydr. Polym.* **2**, 270–272 (1982).
 87. Schefer, L., Adamcik, J. & Mezzenga, R. Unravelling Secondary Structure Changes on Individual Anionic Polysaccharide Chains by Atomic Force Microscopy. *Angewandte Communications* **53**, 5376–5379 (2014).

88. Iglauer, S., Wu, Y., Shuler, P., Tang, Y. & Goddard, W. A. Dilute iota- and kappa-Carrageenan solutions with high viscosities in high salinity brines. *J. Pet. Sci. Eng.* **75**, 304–311 (2011).
89. Lai, V. M. F., Wong, P. A. L. & Lii, C. Y. Effects of cation properties on sol-gel transition and gel properties of κ -carrageenan. *J. Food Sci.* **65**, 1332–1337 (2000).
90. Croguennoc, P., Meunier, V., Durand, D. & Nicolai, T. Characterization of semidilute κ -carrageenan solutions. *Macromolecules* **33**, 7471–7474 (2000).
91. Marcotte, M., Taherian, A. R. & Ramaswamy, H. S. Rheological properties of selected hydrocolloids as a function of concentration and temperature. *Food Res. Int.* **34**, 695–703 (2001).
92. Smidsrød, O. & Grasdalen, H. Polyelectrolytes from seaweeds. *Hydrobiologia* **116–117**, 19–28 (1984).
93. Hu, B., Du, L. & Matsukawa, S. NMR study on the network structure of a mixed gel of kappa and iota carrageenans. *Carbohydr. Polym.* **150**, 57–64 (2016).
94. Ridout, M. J., Garza, S., Brownsey, G. J. & Morris, V. J. Mixed iota-kappa carrageenan gels. *Int. J. Biol. Macromol.* **18**, 5–8 (1996).
95. Ikeda, S., Morris, V. J. & Nishinari, K. Microstructure of aggregated and nonaggregated κ -carrageenan helices visualized by atomic force microscopy. *Biomacromolecules* **2**, 1331–1337 (2001).
96. Walther, B., Lorén, N., Nydén, M. & Hermansson, A. M. Influence of κ -carrageenan gel structures on the diffusion of probe molecules determined by Transmission Electron Microscopy and NMR diffusometry. *Langmuir* **22**, 8221–8228 (2006).
97. Lorén, N. *et al.* Dendrimer Diffusion in kappa-carrageenan Gel Structures. *Biomacromolecules* **10**, 275–284 (2009).
98. Hans Tromp, R., Van de Velde, F., Van Riel, J. & Paques, M. Confocal scanning light microscopy (CSLM) on mixtures of gelatine and polysaccharides. *Food Res. Int.* **34**, 931–938 (2001).
99. Thrimawithana, T. R., Young, S., Dunstan, D. E. & Alany, R. G. Texture and rheological characterization of kappa and iota carrageenan in the presence of counter ions. *Carbohydr. Polym.* **82**, 69–77 (2010).
100. Weiner, M. L. Food additive carrageenan: Part II: A critical review of carrageenan in

- vivo safety studies. *Crit. Rev. Toxicol.* **44**, 244–269 (2014).
101. McKim, J. M. Food additive carrageenan: Part I: A critical review of carrageenan in vitro studies, potential pitfalls, and implications for human health and safety. *Crit. Rev. Toxicol.* **44**, 211–243 (2014).
 102. Sarteshnizi, A. & Khaneghah, M. Mini Review A review on application of hydrocolloids in meat and poultry products. *Inter. Food Research J.* **22**, 872–887 (2015).
 103. Cierach, M., Modzelewska-kapituła, M. & Szaciło, K. The influence of carrageenan on the properties of low-fat frankfurters. *Meat Sci.* **82**, 295–299 (2009).
 104. Verbeken, D., Neirinck, N., Meeren, P. Van Der & Dewettinck, K. Meat Influence of kappa-carrageenan on the thermal gelation of salt soluble meat proteins. *Meat Science* **70**, 161–166 (2005).
 105. Eom, S. *et al.* Effects of Carrageenan on the Gelatinization of Salt-Based Surimi Gels. *Fish Aquat Sci* **16**, 143–147 (2013).
 106. Bico, S. L. S., Raposo, M. F. J., Morais, R. M. S. C. & Morais, A. M. M. B. Combined effects of chemical dip and / or carrageenan coating and / or controlled atmosphere on quality of fresh-cut banana. *Food Control* **20**, 508–514 (2009).
 107. Mustaffa, H., Osman, A., Ping, C. & Mohamad, F. Postharvest Biology and Technology Carrageenan as an alternative coating for papaya (*Carica papaya* L.cv. Eksotika). *Postharvest Biol. Technol.* **75**, 142–146 (2013).
 108. Lin, M. G., Lasekan, O., Saari, N. & Khairunniza-bejo, S. Effect of chitosan and carrageenan-based edible coatings on post-harvested longan (*Dimocarpus longan*) fruits. *CyTA - J. Food* **16**, 490–497 (2018).
 109. Ellis, A., Keppeler, S. & Jacquier, J. C. Responsiveness of κ -carrageenan microgels to cationic surfactants and neutral salts. *Carbohydr. Polym.* **78**, 384–388 (2009).
 110. Chakraborty, S. Carrageenan for encapsulation and immobilization of flavor, fragrance, probiotics, and enzymes: A review. *J. Carbohydr. Chem.* **36**, 1–19 (2017).

Chapter 2

Materials and Methods

2.1. Materials

2.1.1. Raw carrageenan extracted from red algae

2.1.1.1. Seaweed cultivation





Seaweeds were cultured following the method described by Hung *et al*¹ from September to January at Cam Ranh Bay, Khanh Hoa province of Vietnam (111°56'37.9"N 109°11'07.9"E). Briefly, mature specimens of *Kappaphycus alvarezii* (Ka), *Kappaphycus striatum* (Ks), *Kappaphycus malesianus* (Km), and *Eucheuma denticulatum* (Ed) were donated from one farm owner at Cam Ranh Bay. Specimens were selected for which the radius of the main stems was 3-5 mm and the length of the branches was 5-7 cm. The seaweed was immersed in the seawater attached to strings (see Figure 2.1), and the cultivation area was surrounded with fishing nets to avoid fragment dispersion and attack by fish.



Figure 2.1. An example of setting up of seaweed cultivation on the farm

The seaweed was collected after 60 days and washed immediately with tap water to remove salt and sand. It was dried first 6 hours in the sun and subsequently dried at 60°C for 24 hours in a ventilated oven. The dried products were stored under vacuum condition at room temperature. Images of the seaweed and the residual water content after drying are shown in Table 2.1.

Table 2.1. Images of Ka, Ks, Km and Ed and residual water content of the dried seaweeds

<i>Sample</i>	Ka	Ks	Km	Ed
<i>Moisture (wt%)</i>	30	28	28	29
<i>Pictures</i>				

2.1.1.2. Carrageenan extraction

Raw Car was extracted according to the method described by Montolalu *et al*² with some modifications. Briefly, 30 g dried seaweed was soaked and washed in distilled water for two hours to remove pigments, salts and other material dispersible in water at ambient temperatures. The washed seaweed was then cut and minced into small pieces (≈ 1 mm) and added to 2.1 L of distilled water at 70°C and kept at this temperature during 75 minutes for Ka, Ks, Km and during 100 minutes for Ed while stirring continuously. The hot suspension was filtered through a membrane with pore size 25 μ m. Finally, the solution was freeze-dried to obtain the raw Car.

In preliminary work (not shown) we investigated the effects of temperature, duration and ratio of volume of water to dried algae on the Car yield and the viscosity of Car from Ka by using a statistical method (Response Surface Methodology). We found that optimum conditions of yield and viscosity were obtained at temperatures between 70 and 75°C during 75 minutes. In the case of *Eucheuma denticulatum*, however the optimum extraction time to have best viscosity was found to be longer, 100 minutes.

2.1.2. Purification of raw carrageenan

Raw carrageenan and commercial carrageenan (a gift from Cargill, Baupte, France) were purified by centrifugation of aqueous suspensions at $C = 5$ g/L at 1.5×10^4 g for 15 minutes at 35°C in order to remove insoluble part, followed by dialysis first against 0.1 M NaCl for 18 hours in order to exchange K^+ for Na^+ and subsequently against Milli-Q water for 1 day in

order to remove excess salt. Finally, the purified carrageenan solution was freeze-dried and stored at room temperature for further analysis.

2.1.3. Fluorescent labelling of carrageenan

The purified Car was covalently labelled with Fluorescein isothiocyanate (FITC) and rhodamine B isothiocyanate (RBITC) following the method described by Heilig, Göggerle and Hinrichs³ with minor modifications. Briefly, 20 ml DMSO and 80 μ l pyridine were mixed with 1 g carrageenan and stirred at 70°C for 30 min. After adding 0.1 g FITC or RBITC and 40 μ l dibutyltin dilaurate, the mixture was incubated for 3 h at 70°C. The Car was then precipitated and washed many times with ethanol 95% until the waste solvent became colorless. The precipitate was dissolved and dialyzed against Milli-Q water in order to remove any residual free FITC. The FITC absorbance at 480 nm of the bath water was checked and the dialysis process was considered complete when the absorbance was negligible. After purification the labelled Car was freeze-dried. Comparison of the absorbance of labelled Car with that of known concentrations of the fluorophore showed that about 1 in 100 sugar units was labelled. M_w and R_h were reduced during the labelling process: $M_w = 5.0 \times 10^5$ g/mol, $R_h = 67$ nm for κ -car, $M_w = 5.0 \times 10^5$ g/mol, $R_h = 75$ nm for ι -car and $M_w = 2.1 \times 10^5$ g/mol, $R_h = 60$ nm for the commercial κ -car. We speculate that the labelling treatment led to breakage of one or two covalent bonds in the larger Car chains. It was verified that the rheological properties of the labelled Car were the same as for unlabelled Car.

2.1.4. Preparation of solutions

Stock solutions of non-labelled and labelled Car solutions were prepared by dissolving the freeze-dried Car at a concentration of 30 g/L in Milli-Q water with 200 ppm sodium azide added as a bacteriostatic agent with stirring for few hours at 70°C.

For light scattering measurements on diluted solutions, the stock solution of Car was diluted with 0.1 M NaCl to between 0.2 and 1 g/L and subsequently filtered through 0.45 μ m pore size filters (Anatop). The concentration of the Car solutions was determined by measuring the refractive index using a refractive index increment $dn/dc = 0.145$ mL/g.

For measurements on individual and mixed Car solutions that gelled during cooling, individual Car solutions were first heated to 90°C before mixing and addition of aliquots of 0.4 M KCl or CaCl₂ solutions in the required amounts while stirring. The solutions were kept at 90°C for 30 minutes before cooling.

For Confocal Laser Scanning Microscopy (CLSM) observations 10% of the Car was replaced by labelled Car.

2.2. Methods

2.2.1. Light Scattering

Light Scattering (LS) is a technique that can be used to measure the average molar mass (M_w), z-average radius of gyration (R_g) and z-average hydrodynamic radius (R_h) of polymers in solution. In this study the size and molar mass were determined by using a commercial static and dynamic light scattering equipment (ALV-5000, ALV-Langen, Germany). The light source was a He–Ne laser with wavelength of 632 nm. The temperature was controlled by a thermo-stat bath within $\pm 0.1^\circ\text{C}$. The relative scattering intensity (I_r) was calculated as the measured intensity minus the solvent scattering divided by the scattering intensity of toluene at 20°C.

In dilute solutions, I_r is related to M_w and the structure factor ($S(q)$) of the solute:

$$\frac{I_r}{KC} = M_w S(q) \quad (2.1)$$

with K an optical constant

$$K = \frac{4\pi^2 n_s^2}{\lambda^4 N_a} \left(\frac{\partial n}{\partial C} \right)^2 \left(\frac{n_{\text{tol}}}{n_s} \right)^2 \frac{1}{R_{\text{tol}}} \quad (2.2)$$

Here, N_a is Avogadro's number and $R_{\text{tol}} = 1.35 \times 10^{-5} \text{ cm}^{-1}$ is the Rayleigh constant of the toluene standard. The structure factor describes the dependence of the intensity on the scattering wave vector (q) and depends on the structure and the size of the solute. The initial q -dependence can be used to obtain the z-average radius of gyration (R_g):

$$S(q)=(1+q^2.R_g^2/3)^{-1} \quad (2.3)$$

If interaction between the solute molecules is not negligible, eq. 2.3 can be used to obtain an apparent molar mass (M_a) and radius of gyration (R_a). The true molar mass and radius of gyration are obtained by extrapolation to $C = 0$:

$$\frac{1}{M_a} = \frac{1}{M_w} + 2A_2C \quad (2.4)$$

where A_2 is the second virial coefficient.

Examples of $S(q)$ as a function of $q.R_a$ are shown in Figure 2.2 for Car at different concentrations in 0.1 M NaCl. The solid curve in Figure 2.2 represents eq 2.3. Figure 2.3 shows M_a and R_a as a function of C from which M_w , R_g and A_2 can be obtained.

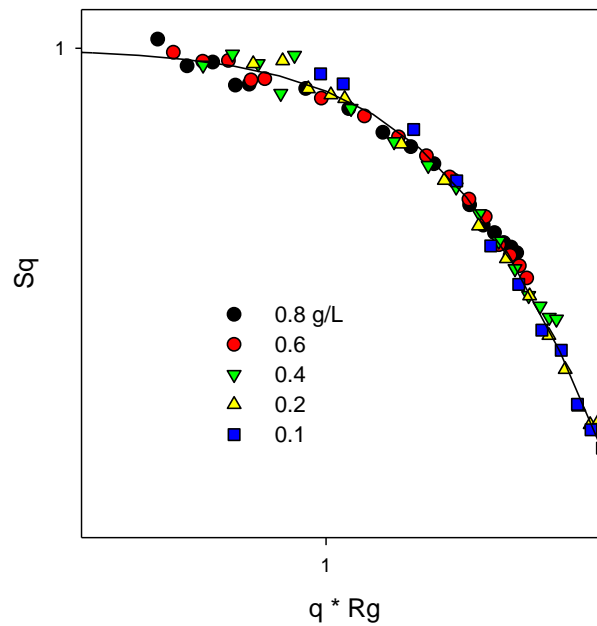


Figure 2.2. Structural factor of different Car concentration in function of angle

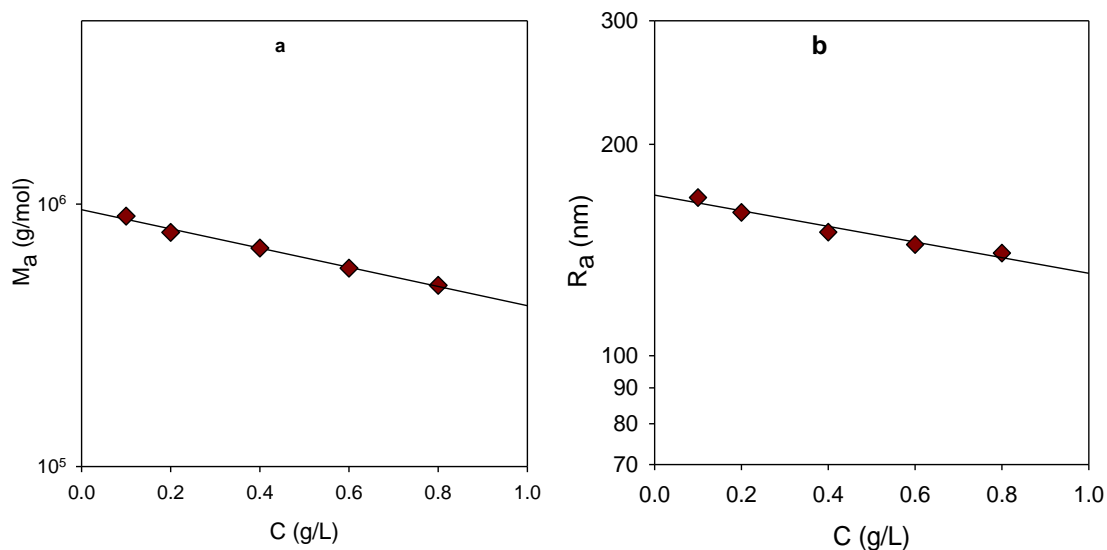


Figure 2.3. Dependence of M_a and R_a on the Car concentrations.

With the dynamic light scattering technique intensity auto correlation functions are determined, which can be analyzed in terms of a sum of exponential relaxations with a corresponding distribution of relaxation times⁴. For polymer solutions, relaxation times can be related to translational diffusion coefficients (D), which in terms can be related to apparent hydrodynamic radius using the Stokes-Einstein equation:

$$R_{ha} = \frac{kT}{6\pi\eta D} \quad (2.5)$$

with η the viscosity of the solvent, k Boltzman's constant, and T the absolute temperature.

The z-average hydrodynamic radius (R_h) of the solute is obtained by extrapolating R_{ha} to $q=0$ and $C=0$. Examples of R_{ha} as a function of q are shown in Figure 2.4a for Car at different concentrations in 0.1 M NaCl. R_{ha} taken at low q -values is plotted as a function of C in figure 2.4b. R_h can be obtained by extrapolating to $C = 0$.

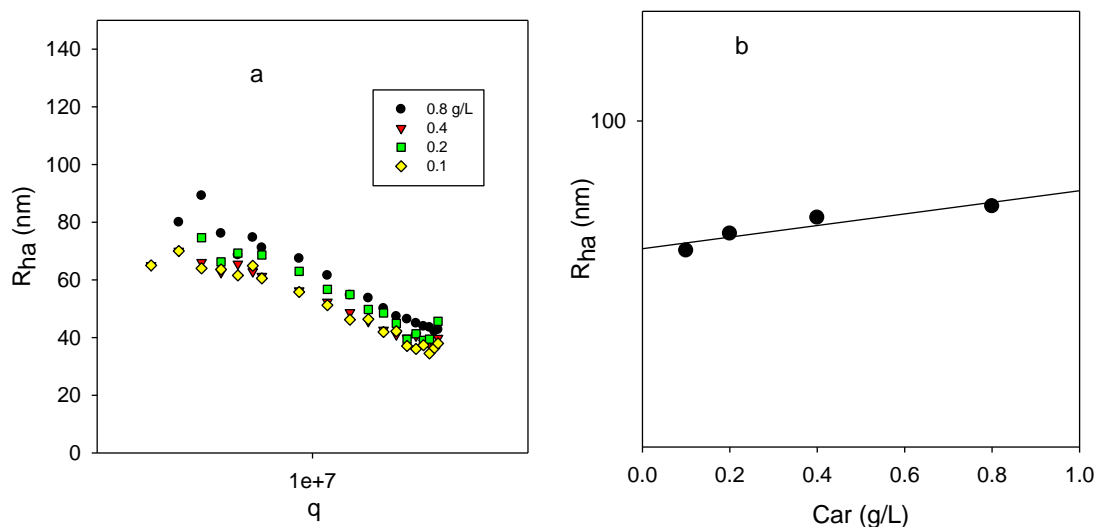


Figure 2.4. q -dependence of R_{ha} (a) and R_{ha} taken at low q -values (took at plateau regime) as a function of Car concentration (b).

2.2.2. NMR spectroscopy

^1H NMR spectroscopy analyses was done following the methods described by van De Velde et al ⁵ and Tojo and Prado ⁶ with some modifications. 0.05 g of purified Car powder was dissolved in 2 ml D_2O at 70 °C by stirring for 10 minutes. In order to reduce the viscosity, the solution was sonicated during 10 minutes using an ultrasound sonicator (Vibra-cellTM 75115) operating at 30% amplitude. The solution was filtered through 0.45 μm pore size filters. ^1H NMR spectra were obtained for solutions at 80 °C with a Bruker spectrometer operating at 400 MHz. The number of scans was 256.

2.2.3. Yield, moisture and mineral content determination

The residual water in dried seaweed was obtained by weighing before and after drying process. Moisture content (W %) was calculated as:

$$W (\%) = \frac{W_b - W_a}{W_b} \times 100 \quad (2.6)$$

where W_b and W_a are the weight of seaweed before and after drying.

The moisture content of the raw and purified Car powders was determined by thermogravimetric analysis (TGA). Approximately 7 mg of the samples was heated from room temperature at 20°C per minute up to 200°C in a Q500 TA instrument (USA), combined with TA instrument universal analysis 2000 software. The moisture content (%) was determined by the stable weight loss (%) at a temperature around 170°C.

The yield of Car before and after purification was defined as the mass of extracted material divided by the mass of dry seaweed .

The quantity of sodium, potassium and calcium in the powders was determined using flame atomic absorption spectrometry as described by Noël et al ⁷. The concentrations of the elements were determined from calibration curves of the standard elements. The results were expressed in mg per gram powder.

2.2.4. Rheology

The rheological properties were determined using a stress-controlled rheometer (ARG2, TA Instruments) in combination with a cone – plate or plate – plate geometry. The temperature was controlled by a Peltier system and the periphery of the samples was covered with a thin layer of paraffin oil to prevent water evaporation. Carrageenan solutions were loaded onto the rheometer at high temperatures where they were liquid. Oscillatory storage (G') and loss (G'') moduli were determined as a function of time, the frequency and the temperature in the linear response regime. The viscosity was measured as a function of the shear rate and the zero shear viscosity (η_0) value was taken in the linear response regime. Results obtained with increasing and decreasing shear rates were the same.

2.2.5. Turbidity

The turbidity of individual carrageenan solutions and mixtures was done at a wavelength of 600 nm as a function of the temperature in 1 cm quartz cuvettes using a UV-visible spectrometer Varian Cary - 50 Bio. The temperature was varied from 80°C to 5°C at a rate of approximately 1°C/ min.

2.2.6. Confocal Laser Scanning Microscopy (CLSM)

2.2.6.1. CLSM observations

The κ - and ι -car were visualized separately by using different fluorescent labelling: FITC or RBITC. CLSM observations were made with a Zeiss LSM800 (Germany). The images of 512 x 512 pixels were produced at different zooms with objective 63. The solutions were inserted between a concave slide and a coverslip and hermetically sealed. The incident light was emitted by a laser beam at 543 and/or 488 nm. The signal from FITC was collected at wavelengths below 520 nm where RBITC does not emit light. The signal from RBITC was detected at wavelengths above 550 nm where FITC emits relatively little light.

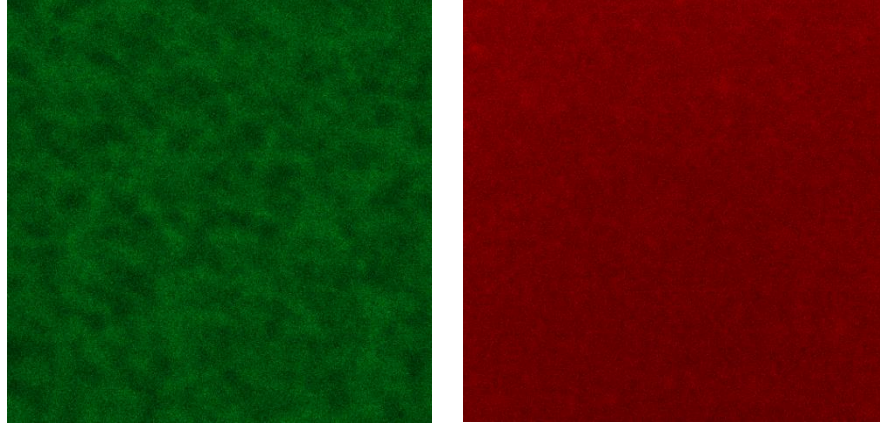


Figure 2.5. An example of CLSM images ($25 \times 25 \mu\text{m}$) of mixed Car in the presence of CaCl_2 of labelled κ -carrageenan with FITC (left) and labelled ι -car with RBITC (right).

2.2.6.2. Pair correlation function of CLSM images

The differences in the microstructure can be quantified by calculating the pair correlation function ($g(r)$) of the fluorescence intensity fluctuations from the CSLM images:

$$g(r) = \frac{\sum_{i=1}^n \sum_{j=1}^m A_i A_j}{\sum_{i=1}^n A_i \sum_{j=1}^m A_j} \quad \text{with } r = |\vec{i} - \vec{j}|, \quad (2.7)$$

where A_i is the fluorescence intensity of pixel i and r is the distance between pixels i and j . Figure 2.6 shows an example of $g(r)$ for different zooms and objectives before (a) and after superposition (b). Results from three magnifications were combined to increase the range of r (figure 2.6c), see ref ⁸ for more detail on this method. It was verified that the fluorescence

intensity was linearly proportional to the carrageenan concentration in the range observed here. This means that $g(r)$ represents the pair correlation function of the carrageenan concentration fluctuations. The value of $g(r \rightarrow 0)$ characterizes the amplitude of concentration fluctuations and the distance r at which $g(r)$ become zero characterizes the length scale of the concentration fluctuations.

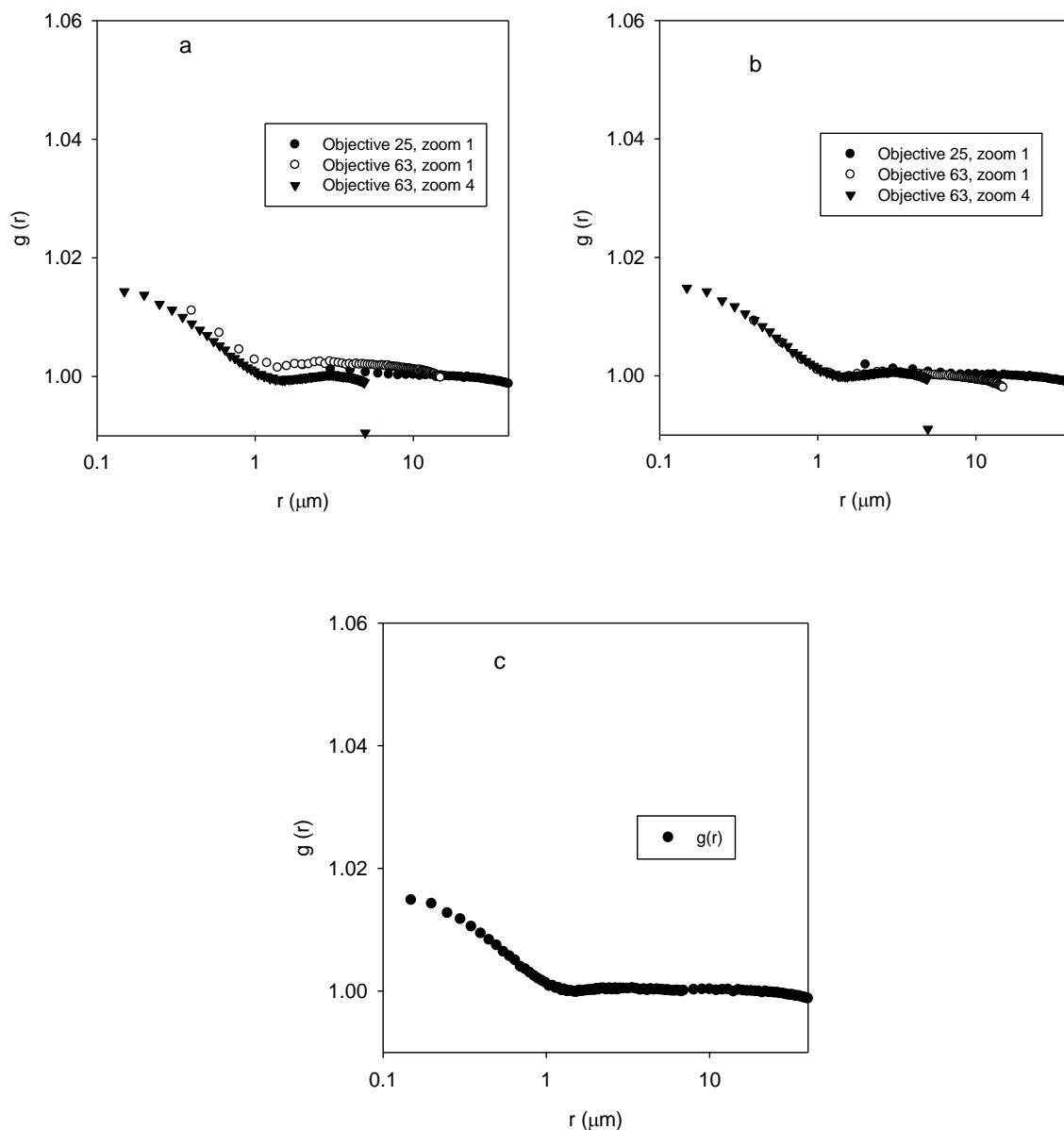


Figure 2.6. $g(r)$ as a function of r for different zooms and objectives before (a) and after superposition (b), (c)

2.2.6.3. Fluorescence recovery after photobleaching

Fluorescence recovery after photobleaching (FRAP) is a widely used method to obtain information on the dynamics of fluorescently labelled molecules. Experimentally, the sample is imaged with a low intensity laser to verify that the sample is not bleached by the laser during the recovery phase ⁹. Subsequently, the intensity is increased to maximum to bleach interesting regions for a very short time. After bleaching, unbleached fluorescent molecules from the surroundings gradually diffuse into the bleached region, whereas bleached fluorescent molecules diffuse out. The rate of fluorescence recovery depends on the mobility of molecules. If the exchange is caused by Brownian motion, the diffusion coefficient can be evaluated from analyzing the fluorescence recovery. If not all fluorescent molecules are mobile the recovery is only partial and the fraction of mobile molecules is equal to the fraction of the fluorescence that is recovered.

In a typical FRAP measurement, the images and fluorescence recovery are shown in Figure 2.7. The fraction of molecules that has exchange in time t ($F(t)$) can be calculated from fluorescence intensity after bleaching at the time t (I_t) ¹⁰:

$$F(t) = \frac{I_t - I_b}{I_i - I_b} \times 100 \quad (2.8)$$

where I_i is the intensity before bleaching and I_b that just after bleaching. If all labelled molecules diffuse with the same diffusion coefficient the intensity cross profile of a cylindrical bleached area is Gaussian with a minimum at the centre of the area. Fits to the intensity distribution of the image as a function of time yields the diffusion coefficient (D). The time dependence of the intensity of all the pixels in the image was analyzed using a fit routine developed by Jonasson *et al* ¹¹. The time dependence of the recovery is given by:

$$F(t) = \exp(-2\tau/t) [I_0(2\tau/t) + I_1(2\tau/t)], \quad (2.9)$$

where $\tau = w^2/4D$ is the characteristic time needed to diffuse out of the bleached area with radius w and I_0 and I_1 are Bessel functions ¹².

If a sample is heterogeneous, the observed recovery depends where the sample is bleached and the size of the bleached area¹³. However, if the bleached area is much larger than the length scale of the heterogeneities an average mobility will be detected.

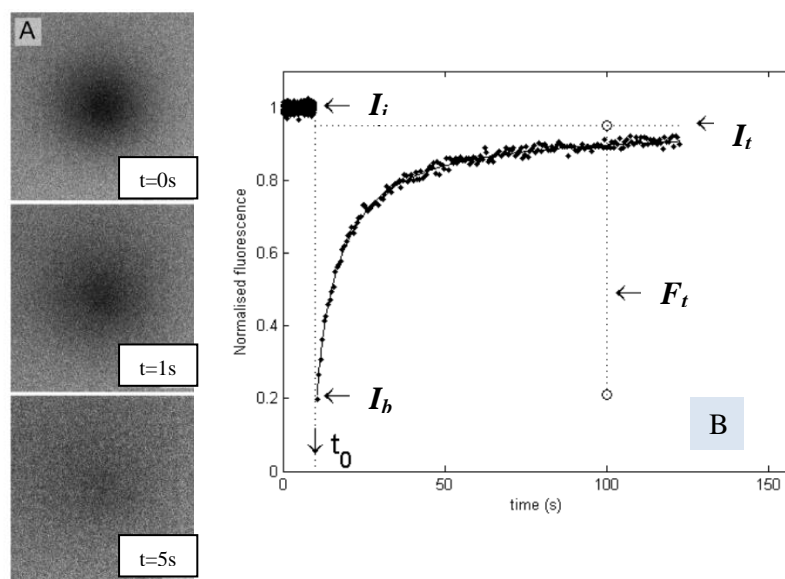


Figure 2.7. Typical fluorescence recovery images of 2% gelatin gel at 25 °C (A)(Hagman et al¹⁴), and curves (B) (Klein et al¹⁰) in a FRAP experiment

In our experiments, the Car solutions were inserted at high temperatures, where they were liquid, between a concave slide and a cover slip that was sealed and then cooled down to 20°C at which temperature all FRAP measurements were done. Circular areas with radius $w = 10 \mu\text{m}$ were bleached and the fluorescence recovery was probed by taking images of size $110 \times 110 \mu\text{m}$. After bleaching first 33 images were taken at time intervals of $\Delta t = 0.6 \text{ s}$, followed by images with increasing Δt in order to obtain representative images of the recovery on a logarithmic time scale. Care was taken that the total number of images taken during detection of the recovery did not lead to significant additional bleaching.

2.2.7. Release of unbound carrageenan from gels

In order to investigate the release of unbound Car from the gels, 50g of κ -car gel at $C=10\text{g/L}$ and $\text{KCl}=50 \text{ mM}$ was cut into small pieces ($\pm 2\text{mm}^3$) and added to 350ml water containing the same salt concentration as in the gel, see Figure 2.8. The suspension was kept

while stirring at 10 rpm. At regular intervals the release of Car into the supernatant was checked by measuring the light scattering intensity. The same protocol was applied for a ι -car gel at $C=10\text{g/L}$ and $\text{CaCl}_2=50\text{ mM}$.

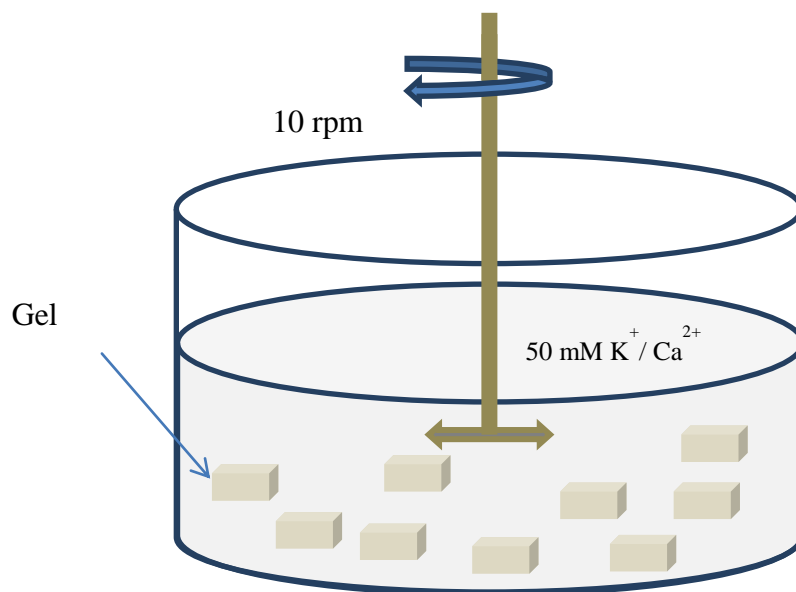


Figure 2.8. Schematic representation of the method to release of unbound Car from the gels

References

1. Hung, L. D., Hori, K., Nang, H. Q., Kha, T. & Hoa, L. T. Seasonal changes in growth rate, carrageenan yield and lectin content in the red alga *Kappaphycus alvarezii* cultivated in Camranh Bay, Vietnam. *J. Appl. Phycol.* **21**, 265–272 (2009).
2. Montolalu, R. I., Tashiro, Y., Matsukawa, S. & Ogawa, H. Effects of extraction parameters on gel properties of carrageenan from *Kappaphycus alvarezii* (Rhodophyta). *J. Appl. Phycol.* **20**, 521–526 (2008).
3. Heilig, A., Göggerle, A. & Hinrichs, J. Multiphase visualisation of fatcontaining β -lactoglobulin- κ -carrageenan gels by confocal scanning laser microscopy, using a novel dye, V03-01136, for fat staining. *LWT - Food Sci. Technol.* **42**, 646–653 (2009).
4. Berne, B. J. & Pecora, R. Dynamic Light Scattering. *Br. Polym. J.* 177 (1976).
5. van De Velde, F., Pereira, L. & Rollema, H. S. The revised NMR chemical shift data of carrageenans. *Carbohydr. Res.* **339**, 2309–2313 (2004).
6. Tojo, E. & Prado, J. A simple ^1H NMR method for the quantification of carrageenans in blends. *Carbohydr. Poly.* **53**, 325–329 (2003).
7. Noël, L., Carl, M., Vastel, C. & Guérin, T. Determination of sodium, potassium, calcium and magnesium content in milk products by flame atomic absorption spectrometry (FAAS): A joint ISO/IDF collaborative study. *Int. Dairy J.* **18**, 899–904 (2008).
8. Ako, K., Durand, D., Nicolai, T. & Becu, L. Quantitative analysis of confocal laser scanning microscopy images of heat-set globular protein gels. *Food Hydrocoll.* **23**, 1111–1119 (2009).
9. Lorén, N. *et al.* Fluorescence recovery after photobleaching in material and life sciences : putting theory into practice. *Q. Rev. Biophys.* **3**, 323–387 (2015).
10. Klein, C. & Waharte, F. Analysis of molecular mobility by fluorescence recovery after photobleaching in living cells. In *Microscopy: Science, Technology, Applications and Education*, 772–783 (Formatex, 2010).
11. Jonasson, J. K., Lorén, N., Olofsson, P., Nydén, M. & Rudemo, M. A pixel-based

- likelihood framework for analysis of fluorescence recovery after photobleaching data. *J. Microsc.* **232**, 260–269 (2008).
12. Soumpasis, D. M. Brief communication theoretical analysis of fluorescence photobleaching recovery experiments. *Biophys. J.* **41**, 95–97 (1983).
 13. Lorén, N., Nydén, M. & Hermansson, A. Determination of local diffusion properties in heterogeneous biomaterials. *Adv. Colloid Interface Sci.* **150**, 5–15 (2009).
 14. Hagman, J., Lorén, N. & Hermansson, A. M. Effect of gelatin gelation kinetics on probe diffusion determined by FRAP and rheology. *Biomacromolecules* **11**, 3359–3366 (2010).

Chapter 3

Characterization and Rheological Properties of Carrageenan Extracted from Different Red Algae Species

3.1. Introduction

The various species of Rhodophyta including *Gigartina*, *Chondrus*, *Kappaphycus*, *Eucheuma* and *Hypnea*¹⁻⁴ are well known for extraction of Car. Extracts from different species yield different types of Car with different functional properties. The genera *Kappaphycus* and *Hypnea* are principally used for extraction of κ -car⁴⁻⁷, *Eucheuma* is the main source of ι -car^{4,8} and *Chondrus* is used to extract λ -car⁹. Ruth *et al*^{10,11} showed that extracts from *Gigartina* predominantly contained λ - and ξ -car. β -, θ -, μ -, ξ - and ν -car are known as bioprecursors and are present in low amounts in the extracts of all mentioned species. Their presence in Car powder has undesirable effects on the gelling properties.

Many parameters influence the yield and quality of Car including processing methods¹²⁻¹⁵, cultivation conditions^{16,17} and storage conditions¹⁸. For instance, using alkali treatment removes some of the sulfate groups and modifies the functional properties^{12,14,16,19}. Hoffman *et al*²⁰ compared alkali treated Car with untreated Car. The results showed that there was an increase in 3,6-anhydro-D-galactose residues from 37.4 to 44.8 (mol%) and a decrease of sulfate groups from 25.5 to 17.5 wt%. Moses *et al*¹⁴ found that the optimum concentration of KOH solution to treat *Kappaphycus alvarezii* was 6-12% (w/v). Studies of the parameters affecting the yield and quality of *Kappaphycus alvarezii* by Hung *et al*¹⁶ and Hayashi *et al*¹⁷ showed that the highest productivity was obtained from seaweed when cultured in the winter season between 44 and 59 days^{17,21}. Hayashi *et al*¹⁷ also found that from the 59th day of cultivation there was a significantly increase of the iota Car fraction in the extract from *Kappaphycus alvarezii*.

In this chapter, four species of red algae cultured at Cam Ranh Bay in Khanh Hoa province of Vietnam: *Kappaphycus alvarezii* (Ka), *Kappaphycus striatum* (Ks), *Kappaphycus melasianus* (Km) and *Eucheuma denticulatum* (Ed) were selected. We aimed to characterize the chemical structure and the physico-chemical properties of the extracted Car in the native state.

Therefore mild water extraction methods were used in order to avoid as much as possible changes to the structure and size of the Car. The extracted raw Car was purified by centrifugation and extensive dialysis in order to eliminate insoluble material and excess minerals or other small components. Car obtained by alkaline treatment was also used to compare the rheological properties with commercial products.

3.2. Results

3.2.1. Yield, mineral content and moisture content

Table 3.1. Yield, moisture and main mineral content of the Car samples

	Yield (%)		Moisture (%)	Potassium (mg g ⁻¹)		Calcium (mg g ⁻¹)		Sodium (mg g ⁻¹)	
	<i>Raw</i>	<i>Purified</i>		<i>Raw</i>	<i>Purified</i>	<i>Raw</i>	<i>Purified</i>	<i>Raw</i>	<i>Purified</i>
<i>Ed</i>	32	20	7.2	18	0	2.9	0.4	17	55
<i>Ka</i>	42	26	7.1	27	0	1.5	0.07	16	42
<i>Km</i>	37	22	7.4	36	0	1.8	0.07	18	41
<i>Ks</i>	33	19	7.3	40	0	1.4	0.06	17	50

The yield defined as the mass of extracted material divided by the mass of dry seaweed and the mineral composition before and after purification are summarized in Table 3.1. The highest yield was obtained with *Ka*. The obtained yields of raw material are close to those commonly reported (~30%)¹⁶⁻¹⁹. A significant amount of material in the form of insolubles, excess minerals and other small molecules was lost after purification. After purification, no residual potassium could be detected and the calcium content was found to be very low in all four samples.

3.2.2. Structure

The molecular structure of the Car chains was characterized by ¹H NMR at 80°C. The different types of Car can be identified by their chemical shifts (ppm) between 5 and 6 ppm²²⁻²⁵. Tojo *et al*²³ reported that the ¹H NMR spectra of κ- and ι-car recorded at 80°C showed distinctive peaks at 5.73 ppm and 5.97 ppm, respectively, relative to that of the residual HOD at 4.82 ppm. van De Velde *et al*²⁴ recorded ¹H NMR chemical shifts of κ- and ι-car at 65°C at

5.093 ppm and 5.292 ppm, respectively, relative to DSS as an internal standard at 0 ppm. Here we compared the spectra of isolated Car fractions with that of commercial κ - and ι -car samples at 80°C, see Figure 3.1. The spectra of Car extracted from the three species of *Kappaphycus* and a commercial κ -car sample were almost the same and showed that these samples contained predominantly κ -car with a large peak at 5.5 ppm (Figure 3.1a). The spectrum of Car extracted from *Euchuma denticulatum* was similar to that of a commercial ι -car sample with a large peak at 5.7 ppm (Figure 3.1b). The relative amplitudes of the peaks at 5.5 ppm and 5.7 ppm showed that the Car extracted from *Kappaphycus* contained only trace amounts of ι -car and the Car extracted from *Euchuma denticulatum* contained only trace amounts of κ -car. These results agree with analyses reported in the literature for Car extracted from Ka, Ks, Km and Ed^{22,26–29}.

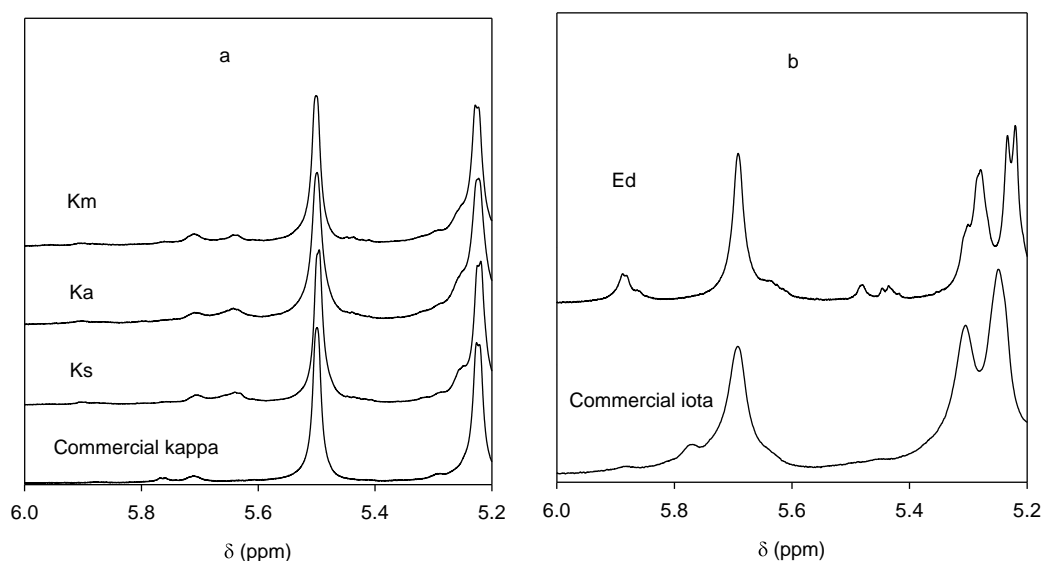


Figure 3.1. ^1H NMR spectra (80°C) of Car extracted from Km, Ka and Ks and commercial κ -car (a); Car extracted from Ed and commercial ι -car (b)

The average molar mass (M_w), second virial coefficient (A_2) and z-average radius of gyration (R_g) of the Car chains was characterized by light scattering as described in Chapter 2. In order to avoid strong electrostatic repulsion between the chains, light scattering measurements were done in 0.1 M NaCl. The apparent molar mass (M_a) and radius of gyration (R_a) were determined at different Car concentrations by fitting the q-dependence of I_T/KC to eq. 2.3. The concentration dependence of $1/M_a$ is shown in Figure 3.2a. The results obtained

for the three κ -car samples extracted from Ks, Ka and Km were the same within the experimental error and applying eq. 2.4 we obtain: $M_w = 1.1 \times 10^6$ g/mol and $A_2 = 1.9 \times 10^{-6}$ mol L/g². For the ι -car extracted from Ed we obtained approximately the same molar mass: $M_w = 1.0 \times 10^6$ g/mol, but a smaller second virial coefficient $A_2 = 1.6 \times 10^{-6}$ mol L/g². It appears that the repulsive interaction between the ι -car chains was weaker than between the κ -car chains. This may seem surprising in view of the higher charge density of ι -car. However, the measurements were done in 0.1 M NaCl so that charge interactions were screened. Repulsion between Car chains explains why R_a decreased with increasing concentration, see Figure 3.2b. As was found for M_a , the concentration dependence of R_a was the same for the three κ -car samples within the experimental error and it was stronger than for ι -car. Extrapolation to $C = 0$ yielded approximately the same z-average radii for the three κ -car samples ($R_g = 180$ nm) and for ι -car ($R_g = 170$ nm).

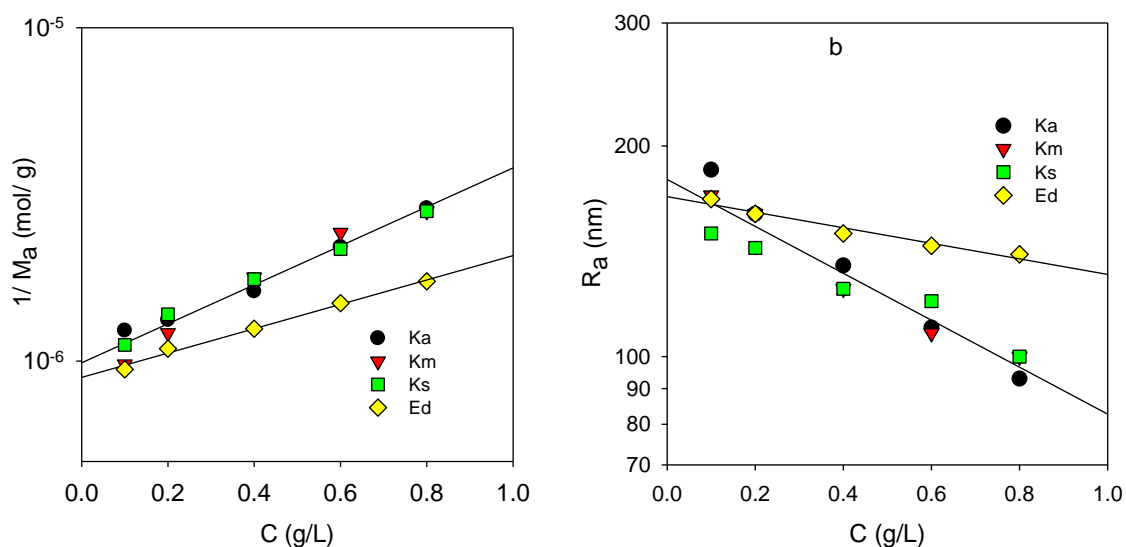


Figure 3.2. Concentration dependence of $1/M_a$ (a) and R_a (b) for κ -car extracted from Ka, Km and Ks and ι -car extracted from Ed

3.2.3. Rheological properties

The shear viscosity of Car solutions was determined as a function of the shear rate. Shear thinning was observed above a shear rate that decreased with increasing concentration as is shown for κ -car extracted from Ka in Figure 3.3. Figure 3.4 compares the concentration dependence of the zero shear viscosity (η) at 20°C of κ -car extracted from Ks, Ka and Km as well as ι -car extracted from Ed. η increased more strongly with increasing concentration for

Ka than Km, which in turn increased more strongly than Ks. These differences cannot be explained by differences in M_w and R_g and were perhaps caused by differences in the size distribution or the molecular structure or interaction. The concentration dependence of η for ι -car extracted from Ed was close to that of κ -car extracted from Ks.

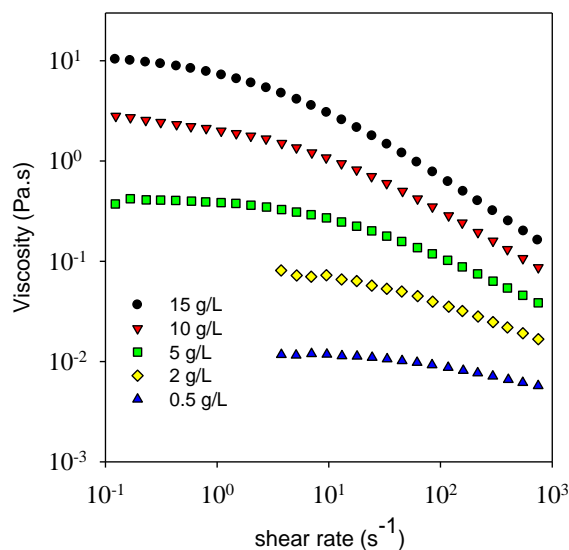


Figure 3.3. Shear rate dependence of the viscosity of solutions of κ -car extracted from Ka at different concentrations.

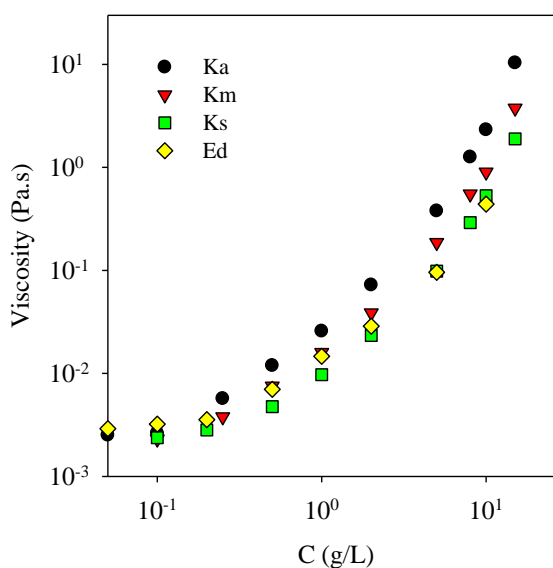


Figure 3.4. Comparison of the concentration dependence of the zero-shear viscosity of Car solutions extracted from Ka, Km, Ks and Ed.

Gelation of κ -car solutions can be induced by cooling in the presence of salt. The critical gel temperature is strongly dependent on the concentration and type of cations. Potassium is particularly effective and therefore KCl is generally used to induce gelation of κ -car solutions. The gelling capacity of the κ -car samples extracted from Ka, Km and Ks was compared at a fixed Car concentration ($C = 10$ g/L) and a fixed concentration of added KCl (10 mM). The oscillatory shear moduli were probed at 0.1 Hz during cooling and subsequent heating between 60°C and 5°C at a rate of 2°C per minute. Figure 3.5 shows that for all κ -car samples G' increased sharply below a critical temperature because gels were formed. κ -Car extracted from Km gelled at a slightly higher temperature (23°C) than κ -car extracted from Ks or Ka (19°C). During heating the gels melted at temperatures that were 13°C higher than the gel temperature.

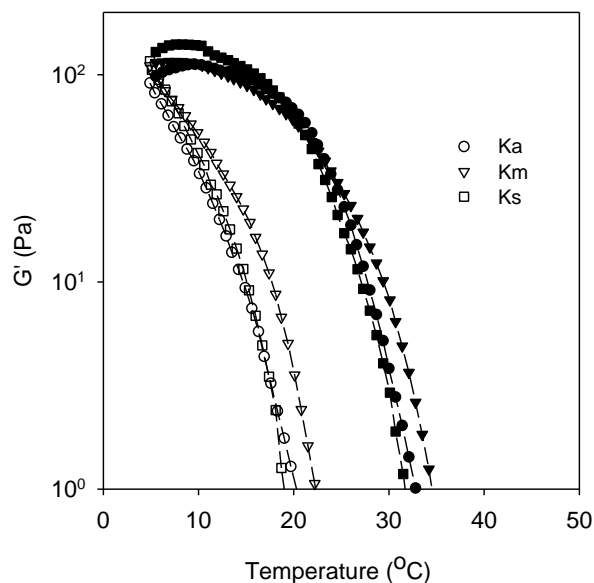


Figure 3.5. Storage shear modulus at 0.1 Hz as a function of the temperature for solutions of κ -car extracted from Ka, Km and Ks at $C = 10$ g/L and 10 mM KCl during cooling (open symbols) and subsequent heating (closed symbols) at a rate of 2°C per minute.

The effect of time on the gel stiffness was determined by measuring G' of the three κ -car solutions at 5°C after rapid cooling from 80°C (Figure 3.6). A rapid increase of G' was observed when the temperature was decreased below 20°C. The initial increase was stronger for κ -car extracted from Km than for κ -car extracted from Ka and the weakest for κ -car

extracted from Ks. The rapid increase of G' was followed by a weak decrease for κ -car extracted from Km and Ka which we attribute to an effect of syneresis that causes some loss of contact between the gel and the plate. The storage modulus of the gel formed by κ -car extracted from Ks continued to increase weakly and as a consequence the moduli of all three samples were similar after standing for two hours. It may be concluded from these measurements and the temperature ramps shown that the elasticity of KCl induced gels does not depend strongly on the species of algae from which they were extracted.

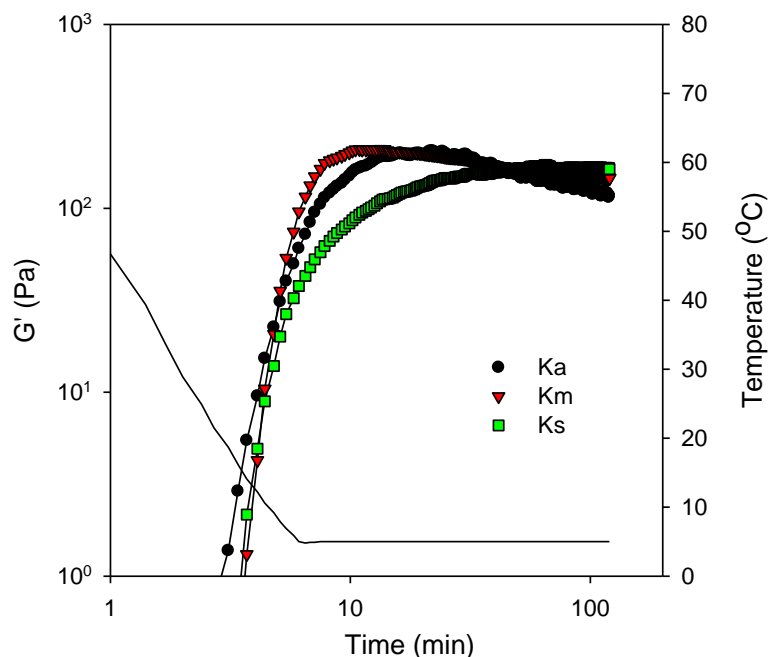


Figure 3.6. Storage shear modulus at 0.1 Hz as a function of time during and after rapid cooling to 5°C for solutions of κ -car extracted from Ka, Km and Ks at $C = 10$ g/L and 10 mM KCl.

Gelation of ι -car solutions is sensitive to divalent cations hence CaCl_2 at different concentrations was used to study the gelling behavior. Figure 3.7a shows that the gelling temperature (T_g) and G' increased with increasing $[\text{CaCl}_2]$ to 30 mM, adding more salt did not lead to a further increase of the storage modulus. The melting temperature (T_m) was close to T_g for $[\text{CaCl}_2] > 20$ mM, which confirms that the ι -car shows little thermal hysteresis and contains little κ -car (Figure 3.7b). Measurements as a function of time at 5°C showed no effect of syneresis (Figure 3.8).

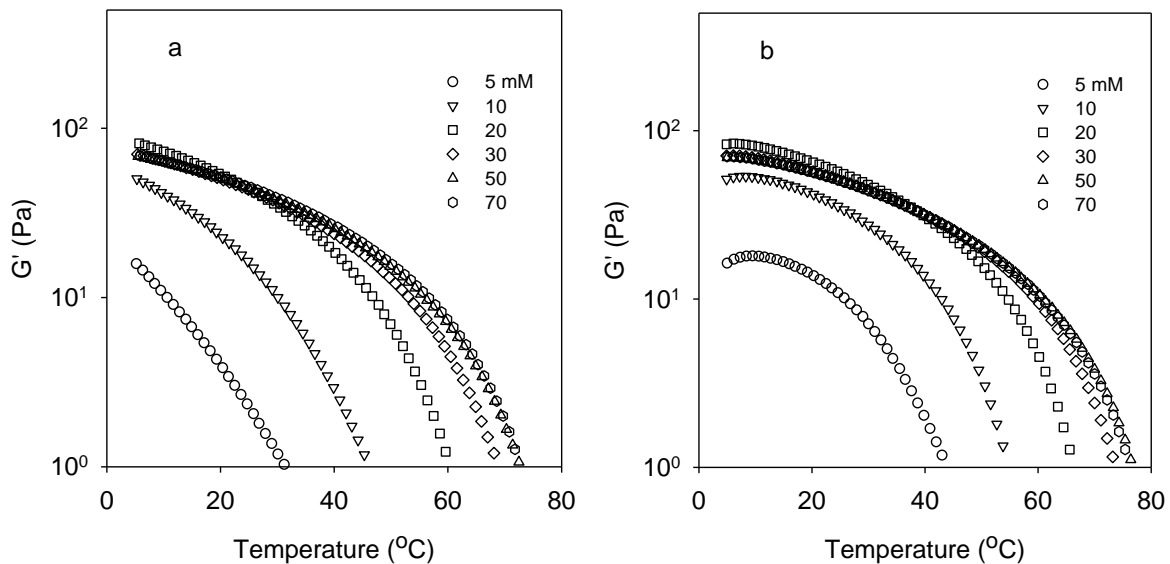


Figure 3.7. Storage shear modulus at 0.1 Hz as a function of the temperature for solutions of *t*-car ($C = 10$ g/L) extracted from Ed at different CaCl_2 concentrations during cooling (a) and heating (b) ramps at a rate of 2°C per minute.

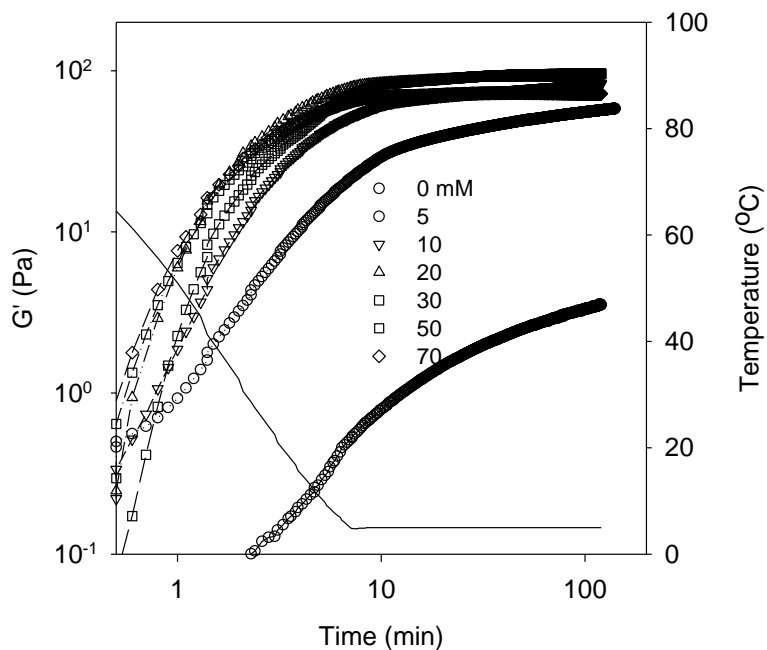


Figure 3.8. Storage shear modulus at 0.1 Hz as a function of time during and after rapid cooling to 5°C for solutions of *t*-car extracted from Ed at $C = 10$ g/L and different CaCl_2 concentrations.

3.2.4. Comparison of the rheological properties of alkali extracted carrageenan and commercial carrageenan

In order to compare the rheological properties of selected Car with commercial samples, we used the alkali treatment method to isolate the κ - and ι -car from Ka and Ed, respectively. The extraction was done following Moses *et al* ¹⁴. Briefly, 20 g dried seaweed was washed in water to remove salt and sand, followed by soaking it in 1.2 L of a KOH solution at 10% (w/v) for 2 hours at 80°C. The seaweed was subsequently washed with water several times to reduce the pH to near neutral value and cooked with 1.5 L of distilled water at 80°C for 2 hours. The extracted Car was recovered and purified as described in Chapter 2. The results in table 3.2 show that after purification, the amount of calcium was very low in all four samples and no residual potassium could be detected.

Table 3.2. Yield, moisture and main mineral contents in the purified Car samples extracted by alkali method and commercial κ - and ι -car

Samples	Yield (%)	Moisture (%)	Potassium (mg g ⁻¹)	Calcium (mg g ⁻¹)	Sodium (mg g ⁻¹)
<i>Ed</i>	22.4	7.4	0	0.21	48
<i>Ka</i>	25	7.3	0	0.06	39
<i>Commercial Kappa</i>	-	7.2	0	0.09	40
<i>Commercial Iota</i>	-	7.5	0	0.19	44

The concentration dependence of $1/M_a$ and R_a of alkali treated κ - and ι -car are shown in Figure 3.9. From extrapolation to $C = 0$ we obtain: $M_w = 6.1 \times 10^5$ g/mol and $R_g = 130$ nm for the κ -car from Ka and $M_w = 8.5 \times 10^5$ g/mol and $R_g = 142$ nm for ι -car from Ed. M_w and R_g of alkali treated Car are smaller than that of samples extracted in water, which confirms reports in the literature ^{12,19,30} that the alkali treatment reduces the size of polymer chains.

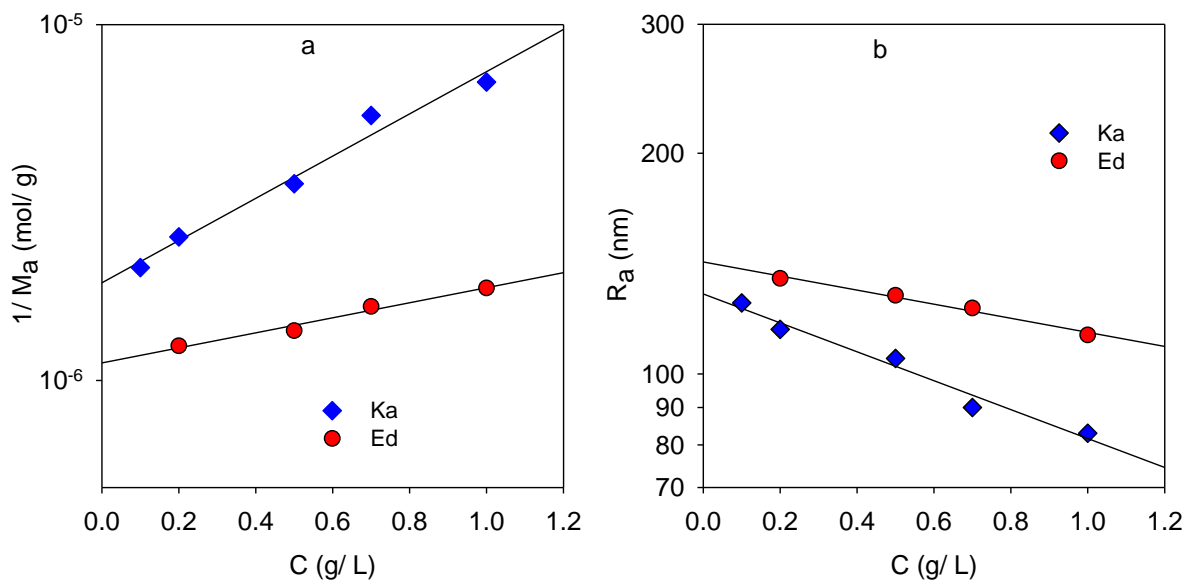


Figure 3.9. Concentration dependence of $1/M_a$ (a) and R_a (b) for alkali treated t - and κ -car extracted from Ed and Ka, respectively.

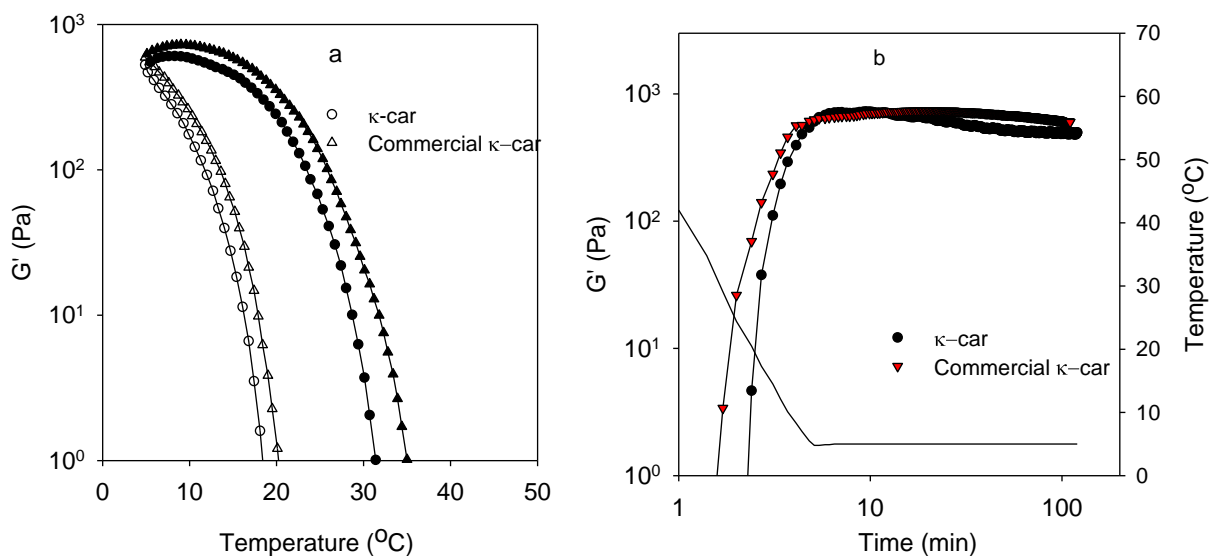


Figure 3.10. Storage shear modulus at 0.1 Hz as a function of the temperature during cooling (open symbols) and subsequent heating (closed symbols) at a rate of $2^{\circ}\text{C}/\text{min}$ (a) and as a function of time during and after rapid cooling to 5°C (b) for solutions of κ -car from Ka (alkali treatment) and a commercial product at $C = 10$ g/L and 10 mM KCl.

Figure 3.10 compares G' of alkali treated κ -car from Ka with commercial κ -car at $C = 10$ g/L and 10 mM KCl. Commercial κ -car gelled at a slightly higher temperature (20°C) than κ -car extracted from Ka (19°C) (Figure 3.10a), but the gel stiffness measured after keeping the samples at 5°C for 2 hours were not different (Figure 3.10b). The comparison was done also for alkali treated and commercial ι -car at $C = 10$ g/L and 10 mM CaCl_2 , see Figure 3.11. Interestingly, the gelling and melting temperatures of these two samples were exactly the same, but the storage modulus of the commercial sample was lower than that extracted from Ed.

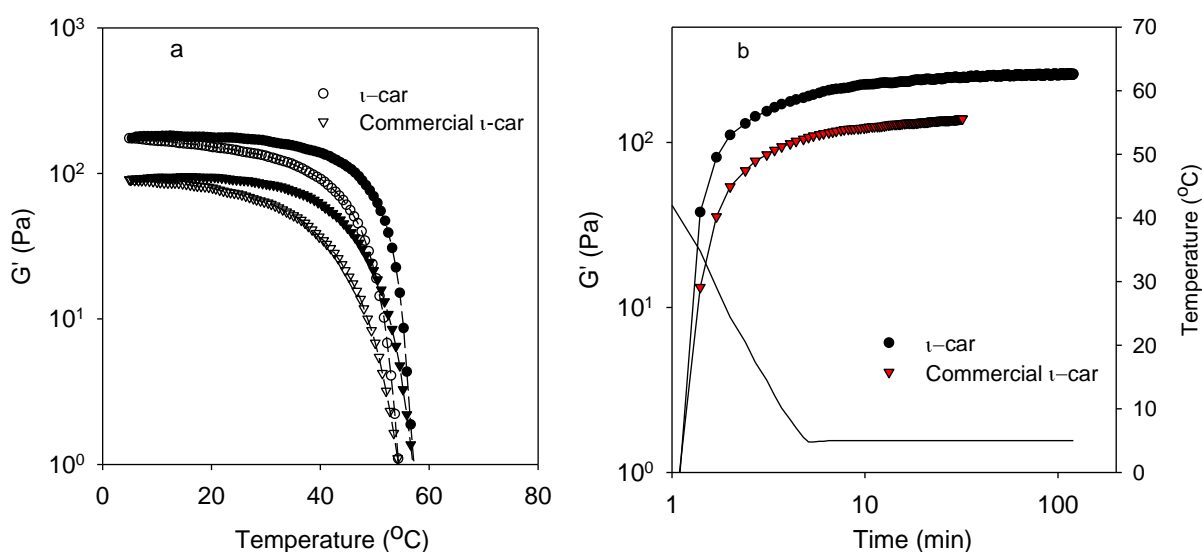


Figure 3.11. Storage shear modulus at 0.1 Hz as a function of the temperature during cooling (open symbols) and subsequent heating (closed symbols) at a rate of $2^\circ\text{C}/\text{min}$ (a) and as a function of time during and after rapid cooling to 5°C (b) for solutions of alkali treated ι -car from Ed and a commercial products at $C = 10$ g/L and 10 mM CaCl_2 .

Comparing the rheological properties of κ - and ι -car obtained with (Figures 3.10, 3.11) and without (Figures 3.5-3.8) alkali treatment shows that alkali treatment causes a strong increase of G' . The increase of the gel stiffness is caused by a decrease of the content of sulfate groups, which favors formation of stronger gels.

3.3. Conclusions

The yield of κ -car extracted from Ks and Km and ι -car extracted from Ed was between 32 and 37% and is somewhat higher (42%) for κ -car extracted from Ka. The size and molar mass of the κ -car chains extracted from the three different subspecies of *Kappaphycus* was within the experimental error the same and was slightly smaller for ι -car extracted from Ed. Small differences were observed in the concentration dependence of the zero shear viscosity with κ -car extracted from Ka giving the highest viscosity followed by κ -car extracted from Ks and Km. The viscosity of ι -car extracted from Ed was close to that of κ -car extracted from Km. Gelation of κ -car solutions could be induced by addition of small amounts of KCl. The critical gel temperature depended weakly on the origin and was higher for κ -car extracted from Ka than Ks, which was in turn a few degrees lower than for κ -car extracted from Km. Gel stiffness of Car extracted from Ka and Ed after alkali treatment was larger than for water extracted Car and close to that of commercial ι - and κ -car. The principal conclusion is that *K. alvarezii* is the best choice for cultivation to yield κ -car at the Cam Ranh Bay in Khanh Hoa province of Vietnam as it has the highest yield and has the best viscosifying and gelling properties. Most likely, the same conclusion is valid also for cultivation in other areas.

References

1. Webber, V., Carvalho, S. M. de, Ogliari, P. J., Hayashi, L. & Barreto, P. L. M. Optimization of the extraction of carrageenan from *Kappaphycus alvarezii* using response surface methodology. *Food Sci. Technol.* **32**, 812–818 (2012).
2. Estevez, J. M., Ciancia, M. & Cerezo, A. S. The system of low-molecular-weight carrageenans and agaroids from the room-temperature-extracted fraction of *Kappaphycus alvarezii*. *Carbohydr. Res.* **325**, 287–299 (2000).
3. van de Velde, F. & Rollema, H. S. High Resolution NMR of Carrageenans. In *Modern Magnetic Resonance* (ed. Webb, G. A.) 1605–1610 (Springer, Dordrecht, 2008).
4. van de Velde, F., Knutsen, S. H., Usov, A. I., Rollema, H. S. & Cerezo, A. S. ¹H and ¹³C high resolution NMR spectroscopy of carrageenans: application in research and industry. *Trends Food Sci. Technol.* **13**, 73–92 (2002).
5. McHugh Dennis J. FAO Fisheries Technical Paper 441. A guide to the seaweed industry, (2003).
6. E. Vázquez-Delfín & D. Robledo & Y. Freile-Pelegrín. Microwave-assisted extraction of the carrageenan from *Hypnea musciformis* (Cystocloniaceae, Rhodophyta). *J. Appl. Phycol.* **26**, 901–907 (2013).
7. Vanina A. Cosenzaa, Diego A. Navarroa, Eliana N. Fissoreb, Ana M. Rojasb, C. A. S. Chemical and rheological characterization of the carrageenans from *Hypnea musciformis* (Wulfen) Lamoroux. *Carbohydr. Polym.* **102**, 780–789 (2014).
8. Piculell, L., Nilsson, S. & Muhrbeck, P. Effects of small amounts of kappa-carrageenan on the rheology of aqueous iota-carrageenan. *Carbohydr. Polym.* **18**, 199–208 (1992).
9. Collén, J. et al. *Chondrus crispus* - A present and historical model organism for red seaweeds. In *Advances in Botanical Research* **71**, 53–89 (Elsevier, 2014).
10. Falshaw, R. & Furneaux, R. H. Carrageenans from the tetrasporic stages of *Gigartina clavifera* and *Gigartina alveata*. *Carbohydr. Res.* **276**, 155–165 (1995).
11. Falshaw, R. & Furneaux, R. H. Carrageenan from the tetrasporic stage of *Gigartina decipiens* (Gigartinaceae , Rhodophyta). *Carbohydr. Res.* **252**, 171–182 (1994).

12. Bono, A., Anisuzzaman, S. M. & Ding, O. W. Effect of process conditions on the gel viscosity and gel strength of semi-refined carrageenan (SRC) produced from seaweed (*Kappaphycus alvarezii*). *J. King Saud Univ. - Eng. Sci.* **26**, 3–9 (2014).
13. Chan, P. T. & Matanjun, P. Chemical composition and physicochemical properties of tropical red seaweed, *Gracilaria changii*. *Food Chem.* **221**, 302–310 (2017).
14. Moses, J., Anandhakumar, R. & Shanmugam, M. Effect of alkaline treatment on the sulfate content and quality of semi-refined carrageenan prepared from seaweed *Kappaphycus alvarezii* Doty (Doty) farmed in Indian waters. *African J. Biotechnol.* **14**, 1584–1589 (2015).
15. Karlsson, A. & Singh, S. K. Acid hydrolysis of sulphated polysaccharides. Desulphation and the effect on molecular mass. *Carbohydr. Polym.* **38**, 7–15 (1999).
16. Hung, L. D., Hori, K., Nang, H. Q., Kha, T. & Hoa, L. T. Seasonal changes in growth rate, carrageenan yield and lectin content in the red alga *Kappaphycus alvarezii* cultivated in Camranh Bay, Vietnam. *J. Appl. Phycol.* **21**, 265–272 (2009).
17. Hayashi, L. *et al.* The effects of selected cultivation conditions on the carrageenan characteristics of *Kappaphycus alvarezii* (Rhodophyta, Solieriaceae) in Ubatuba Bay, São Paulo, Brazil. *J. Appl. Phycol.* **19**, 505–511 (2007).
18. Hilliou, L. *et al.* The impact of seaweed life phase and postharvest storage duration on the chemical and rheological properties of hybrid carrageenans isolated from Portuguese *Mastocarpus stellatus*. *Carbohydr. Polym.* **87**, 2655–2663 (2012).
19. Rhein-Knudsen, N., Ale, M. T., Ajalloueiian, F., Yu, L. & Meyer, A. S. Rheological properties of agar and carrageenan from Ghanaian red seaweeds. *Food Hydrocoll.* **63**, 50–58 (2017).
20. Hoffmann, R. A., Gidley, M. J., Cooke, D. & Frith, W. J. Effect of isolation procedures on the molecular composition and physical properties of *Eucheuma cottonii* carrageenan. *Top. Catal.* **9**, 281–289 (1995).
21. Ohno, M., Nang, H. Q. & Hirase, S. Cultivation and carrageenan yield and quality of *Kappaphycus alvarezii* in the waters of Vietnam. *J. of Applied Phycol.* **8**, 431–437 (1996).

22. van De Velde, F. *et al.* Coil-helix transition of ι -carrageenan as a function of chain regularity. *Biopolymers* **65**, 299–312 (2002).
23. Tojo, E. & Prado, J. A simple ^1H NMR method for the quantification of carrageenans in blends. *Carbohydr. Polym.* **53**, 325–329 (2003).
24. van De Velde, F., Pereira, L. & Rollema, H. S. The revised NMR chemical shift data of carrageenans. *Carbohydr. Res.* **339**, 2309–2313 (2004).
25. van De Velde, F. *et al.* The structure of κ/ι -hybrid carrageenans II. Coil-helix transition as a function of chain composition. *Carbohydrate Research* **340**, 1113–1129 (2005).
26. Aguilan, J. T. *et al.* Structural analysis of carrageenan from farmed varieties of Philippine seaweed. *Bot. Mar.* **46**, 179–192 (2003).
27. Campo, V. L., Kawano, D. F., Silva, D. B. da & Carvalho, I. Carrageenans: Biological properties, chemical modifications and structural analysis - A review. *Carbohydr. Polym.* **77**, 167–180 (2009).
28. Chan, S. W., Mirhosseini, H., Taip, F. S., Ling, T. C. & Tan, C. P. Comparative study on the physicochemical properties of κ -carrageenan extracted from *Kappaphycus alvarezii* (doty) doty ex Silva in Tawau, Sabah, Malaysia and commercial κ -carrageenans. *Food Hydrocoll.* **30**, 581–588 (2013).
29. Mendoza, W. G., Montaña, N. E., Ganzon-Fortes, E. T. & Villanueva, R. D. Chemical and gelling profile of ice-ice infected carrageenan from *Kappaphycus striatum* (Schmitz) Doty ‘sacol’ strain (Solieriaceae, Gigartinales, Rhodophyta). *J. Appl. Phycol.* **14**, 409–418 (2002).
30. Azevedo, G., Torres, M. D., Sousa-pinto, I. & Hilliou, L. Effect of pre-extraction alkali treatment on the chemical structure and gelling properties of extracted hybrid carrageenan from *Chondrus crispus* and *Ahnfeltiopsis devoniensis*. *Food Hydrocoll.* **50**, 150–158 (2015).

Chapter 4

Mixtures of Iota and Kappa-Carrageenan

4.1. Introduction

There are many types of Car, but only κ and ι -car are used widely in industry due to their gelling properties. As was mentioned in Chapter 1, gels of κ -car or ι -car in aqueous solution are formed below a critical temperature (T_c) caused by a conformational transition from a random coil to a helix followed by association of the helices into a system spanning network. T_c and the gel stiffness strongly depend on the type of Car, and the type and concentration of ions that are present¹⁻⁸. There is a huge number of reports on the gelling properties of individual κ -car or individual ι -car in presence of typical ions, whereas few reports have done on mixtures of these Car and the structure of mixed Car gels has not yet been established.

Understanding gelation of mixtures of κ -car and ι -car is important not only because the two types of Car are often present together in commercial samples, but also because the synergetic rheological properties of mixtures compared to individual systems can potentially be exploited in applications. Furthermore there is the interesting fundamental issue of how these polysaccharides with the same chemical structure, but a different charge density, interact during gelation.

As mentioned in Chapter 1, earlier studies of mixtures suggested formation of bicontinuous microphase separated networks in mixed Car gels, but there is lack of microscopic evidence to support this hypothesis. In this chapter, therefore gelation of mixtures of κ -car and ι -car was investigated using confocal laser scanning microscopy and rheology in parallel. All previous investigations on gelation of mixtures of κ -car and ι -car were done in the presence of NaCl or KCl. Here we have used CaCl₂ which leads to κ -car gels with a more heterogeneous microstructure than in the presence of KCl and therefore allows us to better observe the effect of ι -car on the gel structure. A few measurements were repeated using KCl in order to assess the generality of the conclusions.

4.2. Results and discussion

4.2.1. Mixtures of iota and kappa carrageenan in presence of calcium ions

4.2.1.1. Rheology

Shear moduli of κ -car and ι -car solutions at $C = 10$ g/L and mixtures containing 10 g/L of each Car were measured at 0.1 Hz during cooling and heating ramps at a rate of 2°C per minute. As an example, Figure 4.1a shows the results during cooling for G' in the presence of 50 mM CaCl_2 . G' increased sharply below $T_c = 22^\circ\text{C}$ for pure κ -car and more gradually for ι -car below $T_c \approx 80^\circ\text{C}$ and became much larger than G'' , which was caused by gelation of the Car.

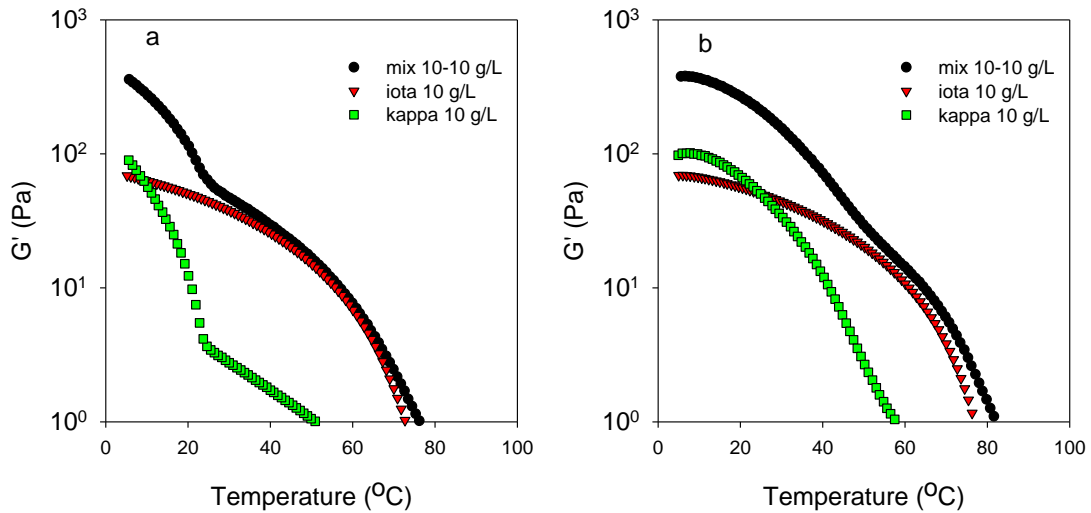


Figure 4.1. Storage moduli measured during cooling (a) and subsequent heating (b) ramps at a rate of $2^\circ\text{C}/\text{min}$ for solutions of ι -car (10 g/L), κ -car (10 g/L) and a mixture (10-10 g/L) at 50 mM CaCl_2 .

The mixture showed a two step gelation process corresponding to that of ι -car below 80°C followed by that of κ -car below 23°C . These results agree with observations reported in the literature that T_c of κ -car and ι -car in the presence of KCl or NaCl is the same in mixtures and in the corresponding individual solutions^{9–12}. The gelation process of ι -car was only weakly influenced by the presence of κ -car, but the subsequent gelation of κ -car led to a much stiffer gel than the sum of the moduli of the individual gels. For independent interpenetrated networks the elastic modulus is equal to the sum of that of each individual network. This was

clearly not the case when both ι -car and κ -car had gelled confirming the conclusion of Brenner *et al*¹¹ for gels formed in the presence of KCl. Subsequent heating ramps showed that melting of the κ -car and ι -car gels also occurred at the same temperatures as for the individual Car solutions, see Figure 4.1b. κ -Car gels melted at significantly higher temperatures than T_c , whereas for ι -car gelation and melting temperatures were close.

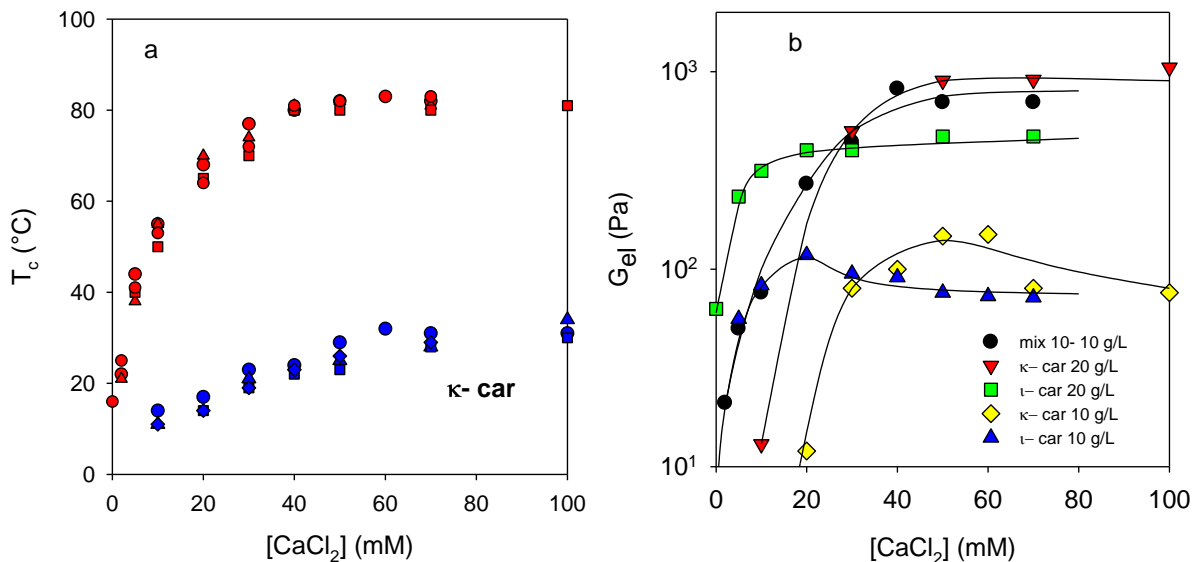


Figure 4.2a. Critical temperature as a function of the CaCl_2 concentration for κ -car (blue) and ι -car (red) in individual solutions at $C = 10$ g/L (circles) or $C = 20$ g/L (triangles) as well as in mixtures containing 5 g/L (squares) or 10 g/L (diamonds) of each Car.

Figure 4.2b. Elastic modulus after one hour at 5°C as a function of the CaCl_2 concentration for individual κ -car and ι -car gels at $C = 10$ g/L and 20 g/L and mixed Car gels containing 10 g/L of each Car.

Similar results were obtained at other CaCl_2 concentrations ($[\text{CaCl}_2]$). The dependence of T_c on $[\text{CaCl}_2]$ is shown in Figure 4.2a. Additional results for T_c obtained for individual Car solutions at $C = 20$ g/L and mixtures at $C = 10$ g/L are also shown. The experimental uncertainty in the measured values of T_c can be estimated from the spread in the data and is about $\pm 3^\circ\text{C}$. T_c is within the experimental uncertainty the same in mixtures and in individual solutions and is independent of the Car concentration. For both types of Car, T_c increased with

increasing $[\text{CaCl}_2]$ up to 50 mM and remained constant at higher concentrations, but T_c values were much higher for ι -car than for κ -car.

The evolution of G' at 5°C was measured at 0.1 Hz after rapid cooling starting from 90°C . G' increased initially rapidly followed by a weak slow increase. After keeping the systems at 5°C for one hour the frequency (f) dependence was determined, which showed for gelled systems that $G' > G''$ independent of f at low frequencies. Examples of time and frequency sweeps are shown in Figures 4.3 and 4.4, respectively.

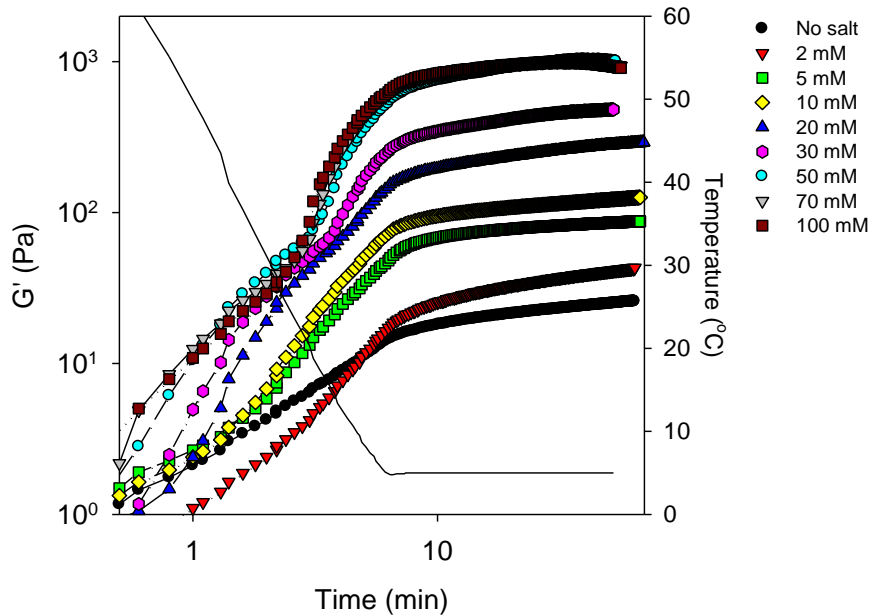


Figure 4.3. Time dependence of G' at 0.1 Hz for mixed gels containing 10 g/L of each Car at different CaCl_2 concentrations. The solid line indicates how the temperature decreased to 5°C .

The elastic modulus (G_{el}) of the gels, defined as the plateau value of G' at low frequencies, increased sharply above a critical CaCl_2 concentration. It reached a maximum at about $[\text{CaCl}_2] \approx 20$ mM in the case of ι -car and $[\text{CaCl}_2] \approx 50$ mM in the case of κ -car, see Figure 4.2b. The experimental uncertainty in the measured values of G_{el} can be estimated from the spread in the data and was about 20%. At higher $[\text{CaCl}_2]$, G_{el} remained constant at $C = 20$ g/L, but at $C = 10$ g/L it decreased weakly. A constant gel stiffness at high $[\text{CaCl}_2]$ for larger Car concentrations⁴ and a decrease with increasing $[\text{CaCl}_2]$ at lower C have been reported before in the literature^{5,7}. We note that at low $[\text{CaCl}_2]$ where κ -car did not gel at 5°C , G_{el} of the

mixtures was close to that of individual ι -car at the same concentration as in the mixture (10 g/L), which confirms that the presence of κ -car coils did not influence the gel stiffness of the ι -car network.

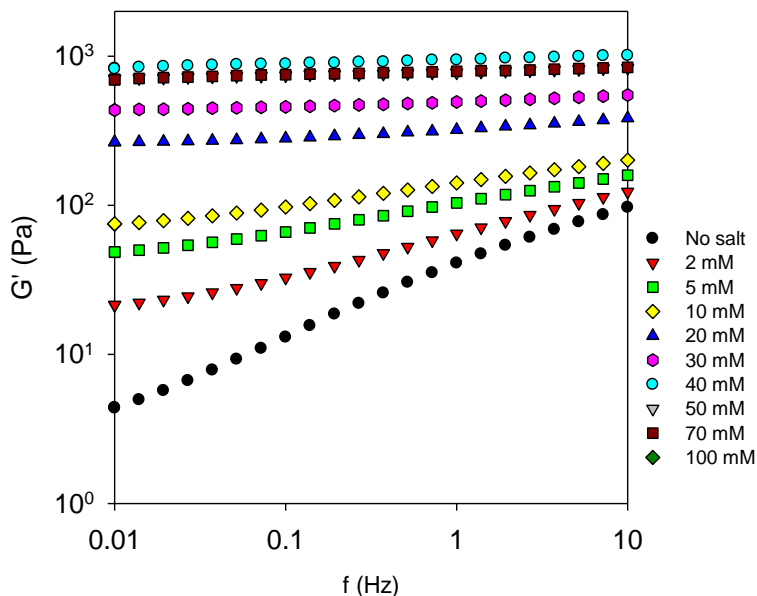


Figure 4.4. Frequency dependence of G' for mixed gels containing 10 g/L of each Car at different CaCl_2 concentrations.

4.2.1.2. Microstructure

The microstructure of individual Car systems at $C = 10$ g/L and 20 g/L and mixtures containing 10 g/L of each type were observed with CLSM at 20°C after cooling from 90°C. The solutions contained a small amount of κ -car or ι -car labelled with FITC and RBITC, respectively. Figure 4.5 shows the effect of $[\text{CaCl}_2]$ on the microstructure of individual ι -car and κ -car systems at $C = 10$ g/L. The presence of more CaCl_2 led to formation of more heterogeneous κ -car gels, but the amplitude of the concentration fluctuations was small even at the highest $[\text{CaCl}_2]$. We did not artificially increase the contrast which means that the grey scale of images corresponds to the polymer concentration. The ι -car gels remained homogenous on length scales accessible to CLSM, i.e. larger than 100 nm, except at the highest $[\text{CaCl}_2]$ where a faint structure can be observed. Notice that in homogeneous systems a few dense aggregates can be seen as bright spots.

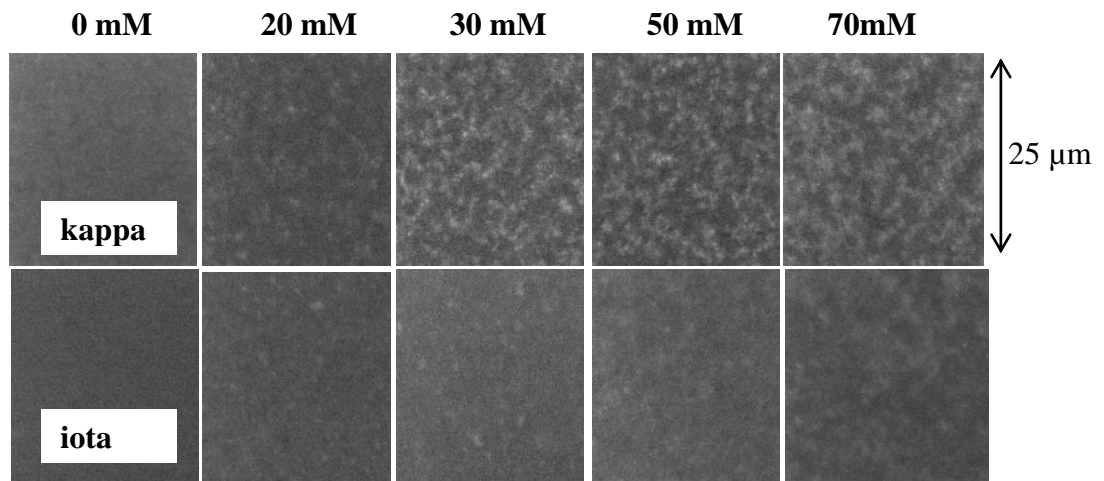


Figure 4.5. CLSM images at 20°C of κ -car and ι -car systems at $C = 10$ g/l at different CaCl_2 concentrations.

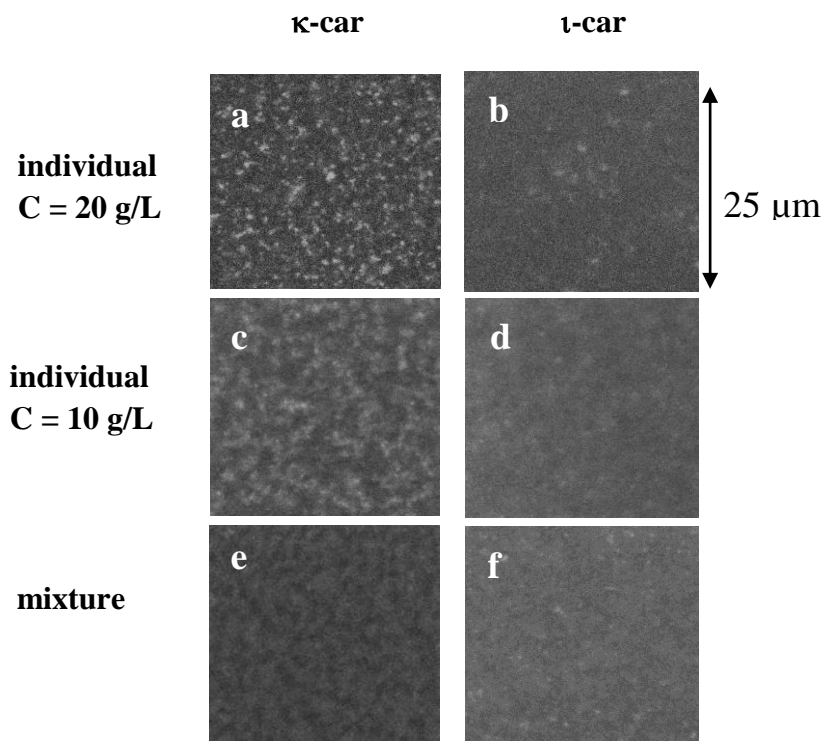


Figure 4.6. CLSM images of the structure of κ -car (a,c) and ι -car (b,d) in individual gels at $C = 20$ g/L (a,b) and 10 g/L (c,d) and in a mixed gel (e,f) containing 10 g/L of each Car in the presence of 50 mM CaCl_2 at 20°C. Images e on the right show the signal from FITC corresponding to labelled κ -car and image f shows the signal from RBITC corresponding to labelled ι -car.

The effect of mixing κ -car and ι -car was tested at $[\text{CaCl}_2] = 50 \text{ mM}$. Figure 4.6 compares images of individual κ -car and ι -car gels at $C = 20 \text{ g/L}$ (a and b) and $C = 10 \text{ g/L}$ (c and d) with the FITC signal corresponding to κ -car (e) and the RBTIC corresponding to ι -car (f) chains in the gelled mixture containing 10 g/L of each car. At these conditions ι -car chains were homogeneously distributed on length scales accessible to CLSM both in the individual systems and the mixture. The distribution of κ -car chains was heterogeneous both in the individual gels and in the mixture, but it appears to be less heterogeneous in the latter.

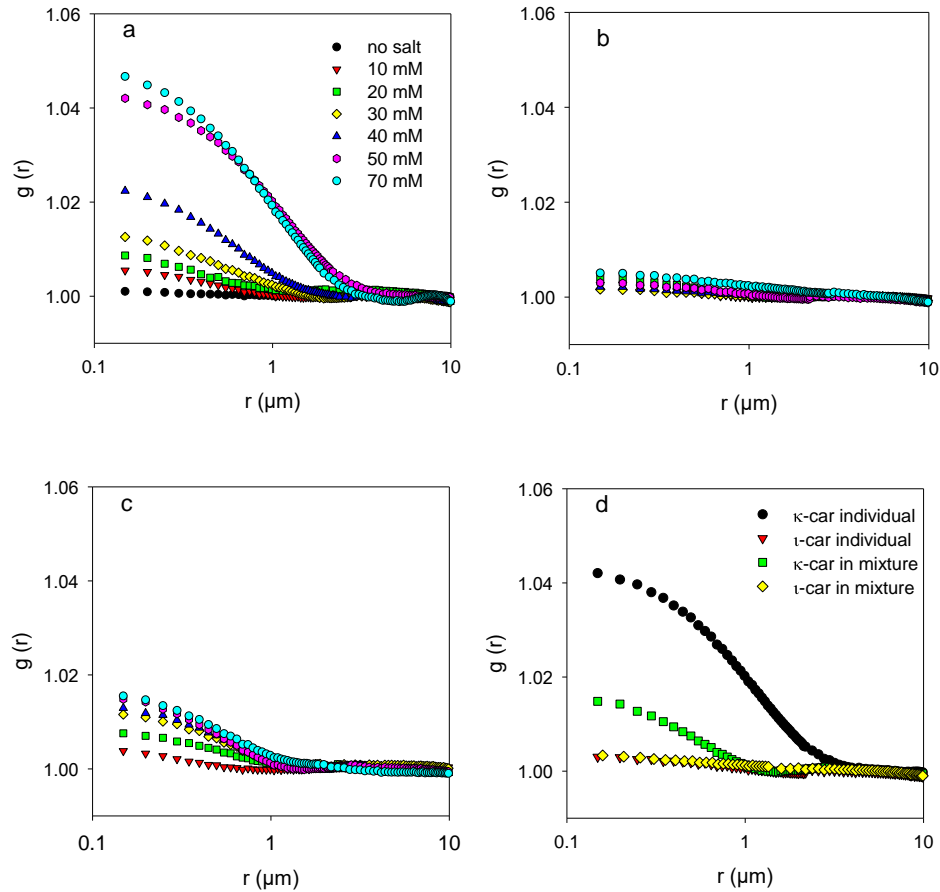


Figure 4.7. Pair correlation functions of the Car concentration fluctuations for individual κ -car (a) and ι -car (b) gels at $C = 10 \text{ g/L}$ and different $[\text{CaCl}_2]$ indicated in the figure. Figure 4.7c shows $g(r)$ of κ -car concentration fluctuations in the mixed gels containing 10 g/L of each Car. Figure 4.7d compares $g(r)$ for individual κ -car and ι -car gels with that of the mixed gel at $[\text{CaCl}_2] = 50 \text{ mM}$.

As was noted in section 2.2.6.1 (Chapter 2), a small amount of FITC signal corresponding to κ -car was detected together with the RBITC signal corresponding to ι -car. However, this effect was too small to have a visible effect on the image corresponding to ι -car in the mixture.

Figure 4.7 shows $g(r)$ for individual κ -car and ι -car gels as well as mixed gels at different $[\text{CaCl}_2]$. For the mixed gels two pair correlation functions were calculated one for the FITC signal corresponding to κ -car and one for the RBITC signal corresponding to ι -car in the mixture. The amplitude of concentration fluctuations of ι -car in individual (Figure 4.7b) as well as in mixed gels (Figure 4.8) was close to zero for all CaCl_2 concentrations confirming the visual impression of homogeneous distribution on length scales accessible to CLSM. The amplitude of $g(r)$ increased with increasing $[\text{CaCl}_2]$ both for individual κ -car gels (Figure 4.7a) and for κ -car in the 50/50 mixture (Figure 4.7c), but it was systematically lower for the mixtures. The characteristic length scale of the concentration fluctuations increased weakly (between 1 and 2 μm) with increasing $[\text{CaCl}_2]$ for individual κ -car gels, whereas it remained about 1 μm for κ -car in the mixed gel. A comparison of $g(r)$ for κ -car and ι -car in individual and mixed gels is shown in Figure 4.7d.

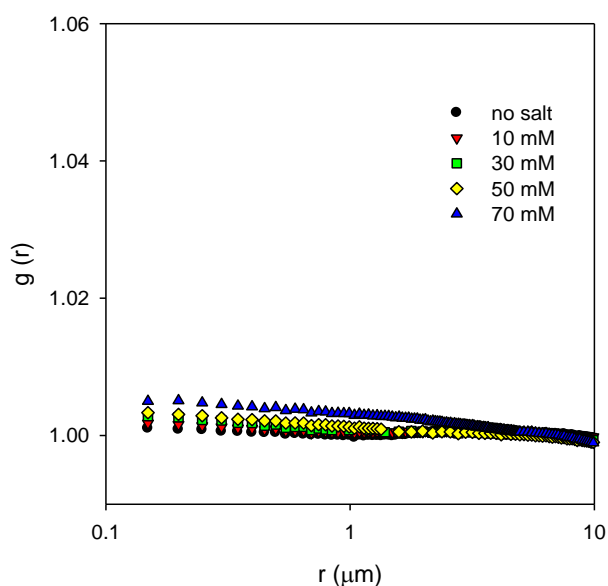
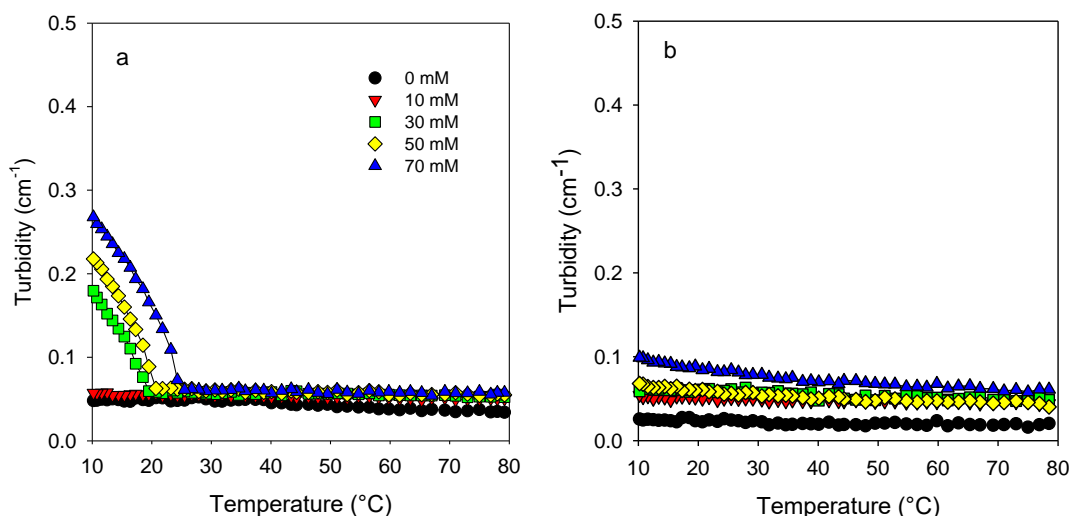


Figure 4.8. Pair correlation functions of the ι -car concentration fluctuations in mixtures containing 10 g/L of each Car and different $[\text{CaCl}_2]$ indicated in the figure.

The rheology results are compatible with microphase separation for the mixed gel, but they also imply that there is no microphase separation in ι -car gel mixed with κ -car coils. CLSM showed that the microstructure of ι -car gels was homogeneous at least on length scales larger than about 100 nm, whereas κ -car gels were heterogeneous on length scales of a few μm . The more heterogeneous microstructure of κ -car gels is consistent with the observed higher turbidity. In the mixed network, the distribution of ι -car was still homogeneous on length scales larger than 100 nm. The implication is that if microphase separation does occur the domains are smaller than 100 nm. Given that the chains in the coil conformation span about 400 nm it is difficult to maintain that distinct ι -car and κ -car domains are formed on length scales smaller than 100 nm. The distribution of κ -car was found to be less heterogeneous in the mixed gel than in the corresponding individual κ -car network, which also argues against microphase separation.

4.2.1.3. Turbidity

Figure 4.9 shows the turbidity as a function of temperature during a cooling ramp at a rate of $1^\circ\text{C}/\text{min}$ for individual Car solutions and mixtures at different $[\text{CaCl}_2]$. The turbidity of κ -car solutions increased sharply below T_c and more so when more CaCl_2 was present. By comparison the turbidity of ι -car gels remained low and increased only weakly with increasing $[\text{CaCl}_2]$. Repeat measurements of the same systems showed the same turbidities within a few percent and upturns at the same temperature with a few degrees.



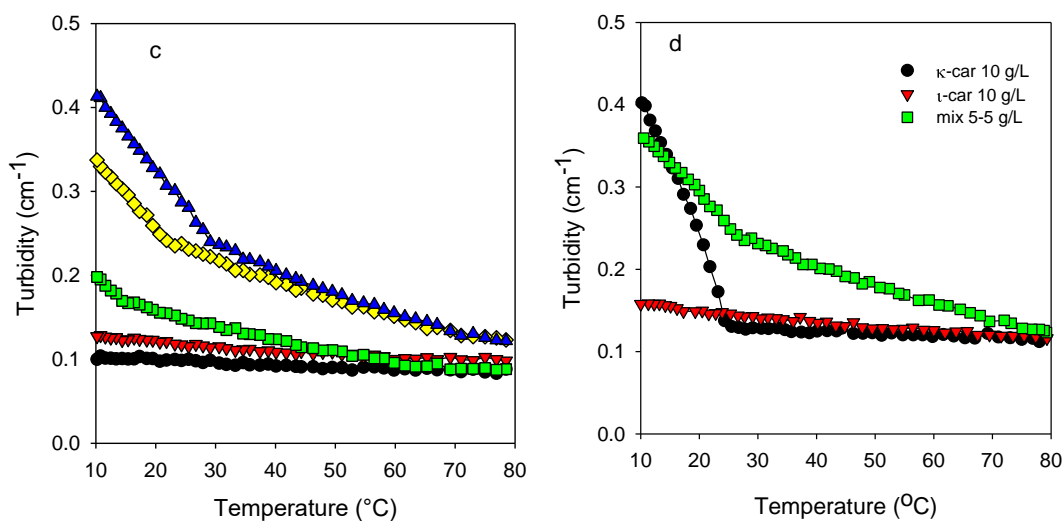


Figure 4.9. Turbidity at 600 nm as a function of temperature for individual κ -car gels (5 g/L) (a), individual ι -car gels (5 g/L) (b) and mixtures (5-5 g/L) (c) at different $[\text{CaCl}_2]$. The comparison between individual and mixed gels is shown in figure 4.9d at $[\text{CaCl}_2] = 50 \text{ mM}$.

The turbidity of the mixtures showed a gradual increase during cooling followed by a sharp increase when κ -car gelled, see Figure 4.9c. The turbidity increased to a greater extent when more $[\text{CaCl}_2]$ was present and implies that gelation of ι -car induced a more heterogeneous distribution of Car in the mixtures. Here we found that the turbidity of the mixtures was higher than that of individual κ -car and ι -car systems at temperatures when only the latter has gelled. Apparently, gelation of ι -car in the presence of κ -car coils induces stronger concentration fluctuations. The same conclusion was drawn by Lundin *et al*¹⁰ for mixtures in the presence of KCl or NaCl. The increased amplitude of the concentration fluctuations is perhaps caused by the presence of κ -car chains that screen electrostatic repulsion between ι -car chains. This would allow the ι -car network to become more heterogeneous, though still on length scales smaller than about 100 nm.

A direct comparison of the turbidity of individual and mixed systems at the same total Car concentration and $[\text{CaCl}_2] = 50 \text{ mM}$ is shown in Figure 4.9d. The comparison shows clearly that gelation of ι -car in the presence of κ -car in the coil conformation led to an increase of the concentration fluctuations compared to individual κ -car solutions or ι -car gels at the same total concentration. However, the increase of the turbidity of the mixture when κ -car gelled was much smaller than for the corresponding individual κ -car systems and as a

consequence the turbidity of the mixed gel was lower than that of the individual κ -car gel even though it was higher at the start of κ -car gelation. The lower turbidity of the mixtures corroborates the more homogeneous distribution of the κ -car chains in the mixed gel that was observed in the CLSM images. It appears that the presence of the ι -car network inhibits coarsening of the κ -car network instead of favoring it as would be expected in the case of microphase separation. It should be realized, however, that the turbidity of car solutions and gels is determined by the overall concentration fluctuations, but not by the relative distribution of κ -car and ι -car chains, because their refractive index increment is practically the same. Therefore microphase separation has no influence on the turbidity if the concentration of each type of Car is the same in each phase. However, as was mentioned above, it seems likely that in a microphase separated mixture the Car concentration of the κ -car phase would be higher than that of the ι -car phase. Microphase separation leading to phases with different Car concentrations would result in large fluctuations of the refractive index and therefore a strong increase of the turbidity that was not observed.

4.2.2. Mixtures of iota and kappa carrageenan in presence of potassium ions

Many studies have been done on the gelation of Car induced by the presence of KCl. Therefore we repeated here some experiments with individual and mixed gels formed in the presence of different KCl concentrations. Figure 4.10 shows G' measured during cooling ramps for solutions of κ -car at concentration 10 g/L (a), ι -car at concentration of 10 g/L (b) and their mixture (10-10 g/L) (c) and [KCl] from 5-70 mM. G' of κ -car solutions increased rapidly at [KCl] > 10 mM and T_c gradually increased with increasing KCl concentration (Figure 4.10a). For ι -car, the gel formed at [KCl] > 10 mM and G' and T_c also increased with increasing KCl concentration, but G' remained much lower than for κ -car. The mixture showed a two step gelation process but the gelation of ι -car in the mixture was less clear compared to that in the mixture in presence of calcium. Figure 4.11 presents G' as a function of time for κ -car (10g/l) and a mixture (10-10 g/l) at different salt concentrations during and after rapid cooling to 5°C. The results show that the G' rapidly increased for all samples, but the syneresis occurred when [KCl] > 30 mM (see Figure 4.11a). Syneresis usually happens with strong κ -car gels in presence of KCl and causes loss of contact between the gel and the plate¹³ and the release of fluid from the gel¹⁴. However, this phenomenon did not occur in the mixed

gel, see Figure 4.11b. These results agree with observations reported in the literature that the presence of ι -car inhibits syneresis in mixed Car gels¹⁵.

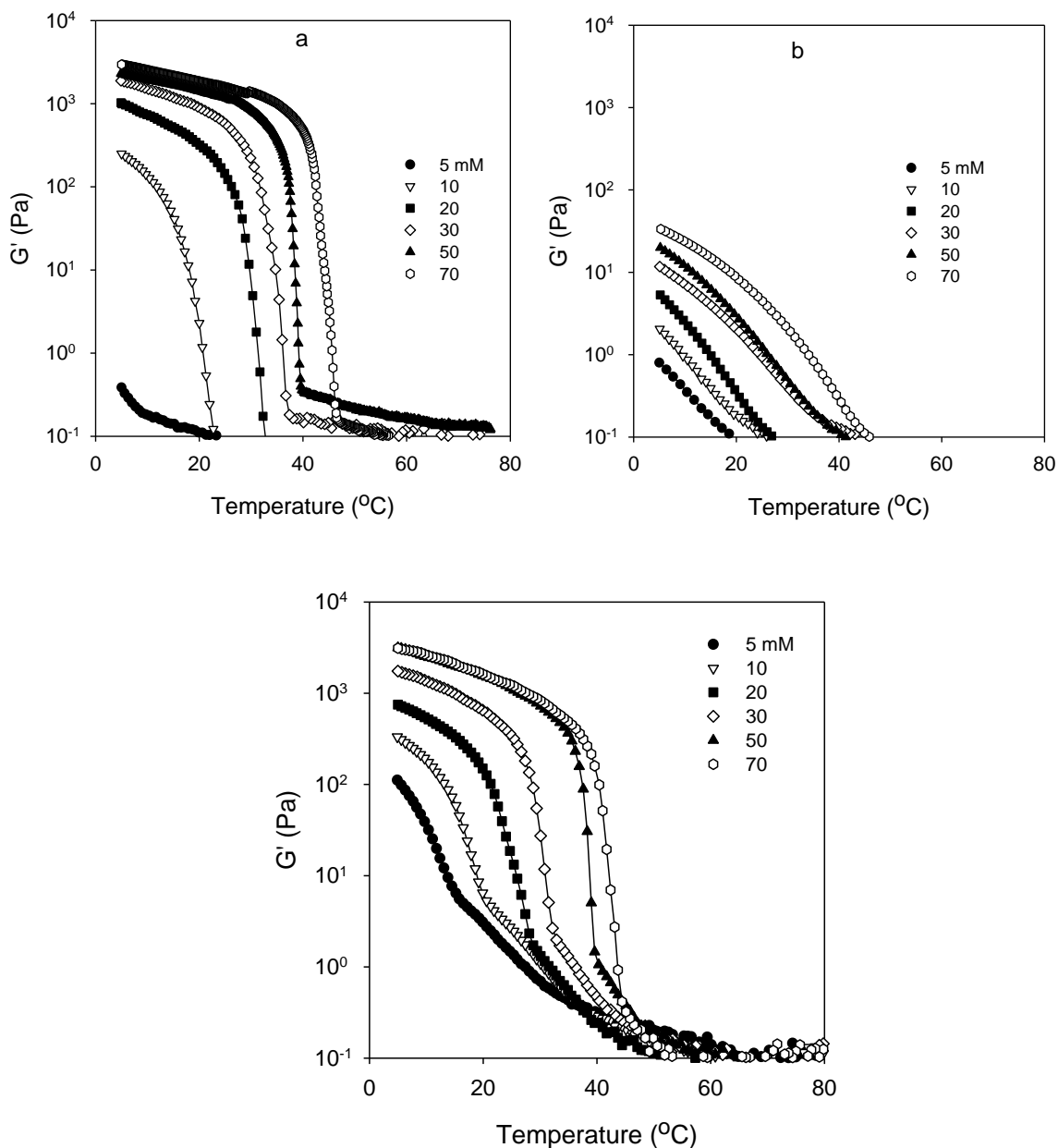


Figure 4.10. Storage moduli measured during cooling ramps at a rate of 2 $^{\circ}\text{C}/\text{min}$ for solutions of 10 g/L of κ -car (a), ι -car (b) and a mixture, 10-10 g/L (c) at different KCl concentrations.

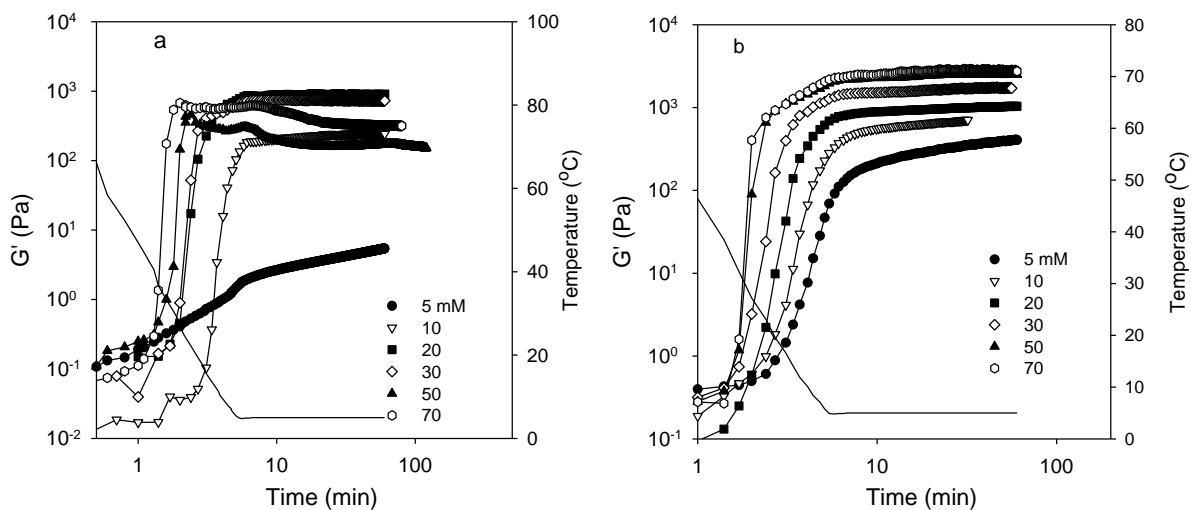


Figure 4.11. Time dependence of G' at 0.1 Hz for κ -car (a) and a mixed gels (b) containing 10 g/L of each Car at different KCl concentrations. The solid line indicates how the temperature decreased to 5°C .

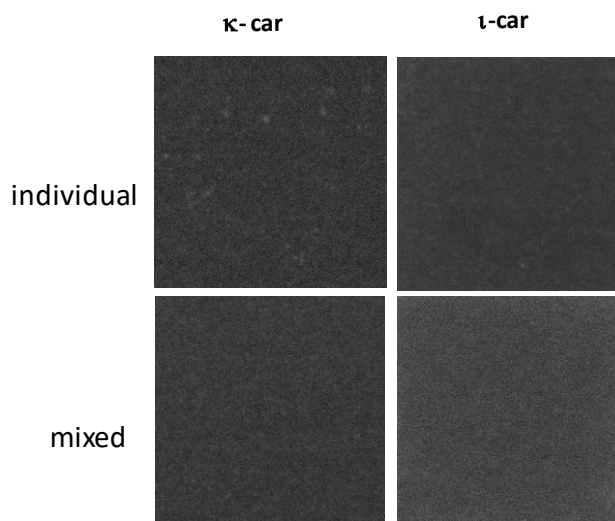


Figure 4.12. CLSM images ($25 \times 25 \mu\text{m}$) of the structure of κ -car and i -car in individual gels at $C = 10 \text{ g/L}$ and in a mixed gel containing 10 g/L of each Car in the presence of 50 mM KCl. The images on the left show the signal from fluorescently labelled κ -car and those on the right show the signal from fluorescently labelled i -car.

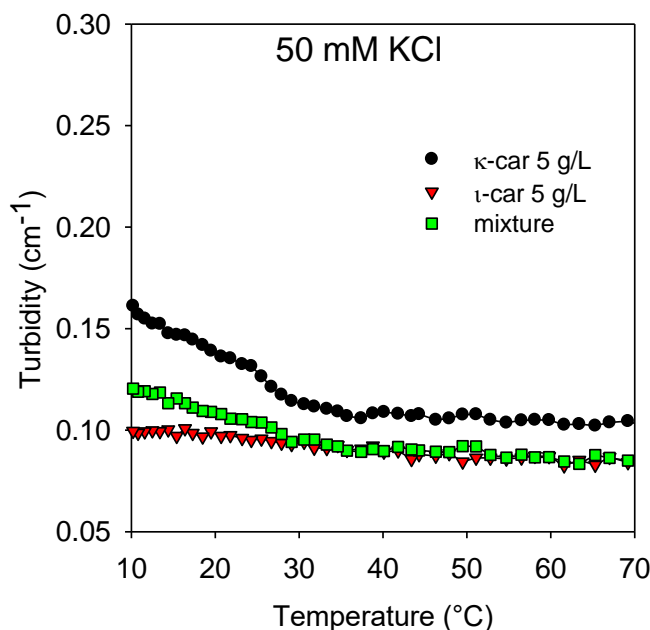


Figure 4.13. Turbidity as a function of temperature for individual κ -car and ι -car solutions at $C = 5$ g/L and mixtures containing 5 g/L of each Car in the presence of 50 mM KCl.

Figure 4.12 shows images of the microstructure of κ -car and ι -car in individual gels at $C = 10$ g/L and in mixed gels containing 10g/L of each Car. The distribution of both types of Car was homogeneous in all systems. This was confirmed by turbidity measurements that showed very low turbidity for mixed and individual gels, see Figure 4.13. The turbidity of the mixed gel was intermediate between that of the individual κ -car and ι -car gels.

The results here render it unlikely that microphase separation had occurred in the mixed gels formed in the presence of KCl. If microphase separation does not occur, the agreement between experimental G_{el} and predictions for microphase separated gels is fortuitous. A different explanation is required for the observation that the stiffness of the mixed gels is much higher than a simple sum of the elastic moduli of the two individual networks. One possibility is that κ -car helices co-aggregate with ι -car helices thereby increasing the crosslink density of the mixed gel. This would also explain why the gel stiffness of ι -car is not modified by κ -car in the coil conformation and why the κ -car chains are distributed more homogeneously in the mixed gel. Another possibility is that the ι -car and κ -car remain independent, but that their structure and stiffness are somehow modified by the interpenetration with the other network. In particular a more homogeneous κ -car network

suggested by the more homogeneous distribution of κ -car in the mixed gel, could be stiffer. In fact, we found that the more homogeneous individual κ -car gels formed with KCl were significantly stiffer than the more heterogeneous gels formed with CaCl_2 .

4.3. Conclusions

50/50 mixtures of ι -car and κ -car gel in two steps during cooling in the presence of CaCl_2 with ι -car gelling at a higher temperature than κ -car. The gel temperatures in the mixtures are the same as for corresponding individual gels indicating independent coil-helix transitions. The gel stiffness of mixed gels is equal to that of the corresponding individual ι -car gel when κ -car is in the coil conformation. However, when both carrageenans have gelled in the mixtures the gel stiffness is much larger than the sum of the corresponding individual gels at the same concentration as in the mixtures. It is in fact between that of individual κ -car and ι -car gels at the same total Car concentration. CLSM images show that ι -car chains are homogeneously distributed in individual and mixed gels, whereas the κ -car network is heterogeneous on length scales of 1-2 μm . However, the κ -car network is more homogeneous in the mixed gels than in the corresponding individual gels. This was confirmed by turbidity measurements that showed that the amplitude of the overall car concentration fluctuations was lower in mixed gels than in individual κ -car gels. Individual κ -car gels and mixed gels formed in the presence of KCl were more homogeneous than gels formed in the presence of CaCl_2 . It is concluded that microphase separation is highly unlikely to occur in mixed gels and it is suggested that the increased gel stiffness is caused by co-aggregation of ι -car and κ -car or changes in the structure of the interpenetrated networks.

References

1. Rochas, C. & Rinaudo, M. Activity coefficients of counterions and conformation in kappa-carrageenan system. *Biopolymers* **19**, 1675–1687 (1980).
2. Norton, I. T., Goodall, D. M., Morris, E. R. & Rees, D. A. Role of cations in the conformation of iota and kappa carrageenan. *J. Chem. Soc. Faraday Trans. 1* **79**, 2475–2488 (1983).
3. Rochas, C., Rinaudo, M. & Landry, S. Relation between the molecular structure and mechanical properties of carrageenan gels. *Carbohydr. Polym.* **10**, 115–127 (1989).
4. Michel, A. S., Mestdagh, M. M. & Axelos, M. A. V. Physico-chemical properties of carrageenan gels in presence of various cations. *International Journal of Biological Macromolecules* **21**, 195–200 (1997).
5. MacArtain, P., Jacquier, J. C. & Dawson, K. A. Physical characteristics of calcium induced κ -carrageenan networks. *Carbohydr. Polym.* **53**, 395–400 (2003).
6. Thrimawithana, T. R., Young, S., Dunstan, D. E. & Alany, R. G. Texture and rheological characterization of kappa and iota carrageenan in the presence of counter ions. *Carbohydr. Polym.* **82**, 69–77 (2010).
7. Nguyen, B. T., Nicolai, T., Benyahia, L. & Chassenieux, C. Synergistic effects of mixed salt on the gelation of κ -carrageenan. *Carbohydr. Polym.* **112**, 10–15 (2014).
8. Robal, M. *et al.* Monocationic salts of carrageenans: Preparation and physico-chemical properties. *Food Hydrocoll.* **63**, 656–667 (2017).
9. Parker, A., Brigand, G., Miniou, C., Trespoey, A. & Vallée, P. Rheology and fracture of mixed ι - and κ -carrageenan gels: Two-step gelation. *Carbohydr. Polym.* **20**, 253–262 (1993).
10. Lundin, L., Odic, K., Foster, T. J., & Norton, I. T. Phase separation in mixed carrageenan systems. In *Supramolecular and colloidal structures in Biomaterials and Biosubstrates* 436–449 (ICP, 2000).
11. Brenner, T., Tuvikene, R., Parker, A., Matsukawa, S. & Nishinari, K. Rheology and structure of mixed kappa-carrageenan/iota-carrageenan gels. *Food Hydrocoll.* **39**, 272–

279 (2014).

12. Du, L., Brenner, T., Xie, J. & Matsukawa, S. A study on phase separation behavior in kappa/iota carrageenan mixtures by micro DSC, rheological measurements and simulating water and cations migration between phases. *Food Hydrocoll.* **55**, 81–88 (2016).
13. Lai, V. M. F., Wong, P. A. L. & Lii, C. Y. Effects of cation properties on sol-gel transition and gel properties of κ -carrageenan. *J. Food Sci.* **65**, 1332–1337 (2000).
14. Ako, K. Influence of elasticity on the syneresis properties of κ -carrageenan gels. *Carbohydr. Polym.* **115**, 408–414 (2015).
15. Mikkelsen, T. R., Scottsdale, A. & Theiler, R. F. Water-based gel with low syneresis field. *United States Patent, US 2013/0157922 A1* 1–6 (2013).

Chapter 5

Mobility of Carrageenan Chains In Iota and Kappa Carrageenan Gels

5.1. Introduction

Car is a gelling polysaccharide with important applications in the areas of cosmetics, drug delivery systems and food ^{1,2}. Understanding the mobility of Car chains within the gel is important for a better understanding of the gel properties. Diffusion of probe molecules in Car gels has been studied in the past and has been related to the structure of the network ³⁻⁷. Zhao et al ⁷ observed with pulsed field gradient NMR (PFG-NMR) that the fraction of κ -car chains with highly mobile segments strongly reduced below the gelation temperature, which they attributed to aggregation of helices. However, they observed that the diffusion coefficient of the residual mobile chains in the gels increased with decreasing temperature. They concluded that the residual mobile chains were made up of the shorter chains within the distribution of chains sizes of the κ -car sample used in their study. The effect of the type of Car on the fraction of mobile chains was not investigated by these authors nor the effect of the types and concentration of added salt. Neither was the mobility related to macroscopic release of Car chains from gels and the gel stiffness. It seems likely that if there is a significant fraction of mobile chains this will influence the gel stiffness and leads to release of Car to the surrounding aqueous phase, which could be important for applications.

In this chapter we will present an investigation of the mobility of Car chains in gels. A systematic study was done of the mobility of sodium κ -car and ι -car chains in gels formed by addition of KCl or CaCl₂ using fluorescence recovery after photon bleaching (FRAP). Using FRAP the mobility of Car chains can be monitored over much longer distances (tens of microns) and much longer times (hours) than by the NMR. The results on the mobility in the gels were compared with their corresponding stiffness determined with oscillatory shear rheology and release of Car chains from macroscopic gel fragments in excess solvent with the same ionic strength.

5.2. Results

5.2.1. Mobility of carrageenan in salt free aqueous solution

FRAP measurements were done for salt free solutions of ι -car and κ -car at different concentrations between $C = 1$ and 20 g/L. For these systems the intensity profile quickly became Gaussian indicating Brownian diffusion of labelled Car, see Figure 5.1. Figure 5.2 shows the normalized recovery of the fluorescence intensity: $F(t) = (I(t) - I_b) / (I_i - I_b)$, where $I(t)$ is the integrated intensity of the bleached area at time t after bleaching, I_i is the intensity before bleaching and I_b is the intensity just after bleaching. The recovery was slower at higher Car concentrations, which is expected because the friction between chains increased. $F(t)$ was plotted on a logarithmic time scale, because full recovery was slow at higher concentrations. For ι -car at $C = 20$ g/L, $F(t)$ stagnated at about 60%. It was found that at this concentration ι -car formed a weak gel at 20°C in salt free water (Figure 5.3). The effect of gelation on $F(t)$ will be discussed in more detail below.

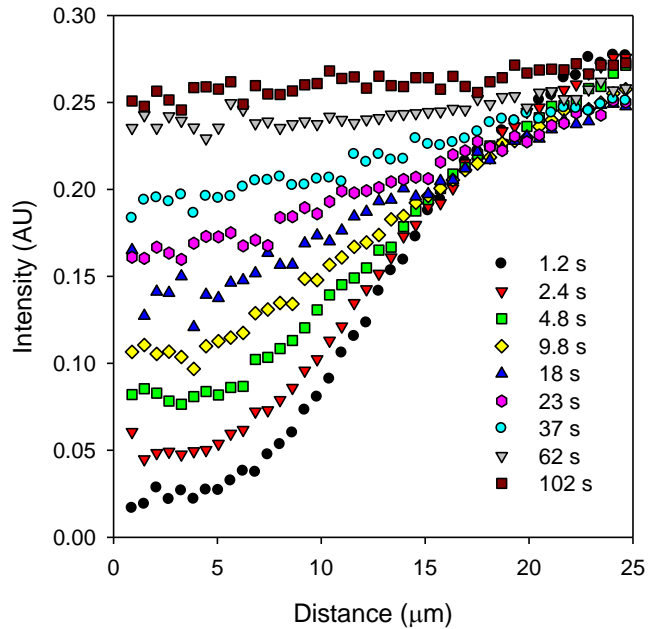


Figure 5.1. Intensity profiles at different times after bleaching for a solution of κ -car in salt free water at $C = 1$ g/L.

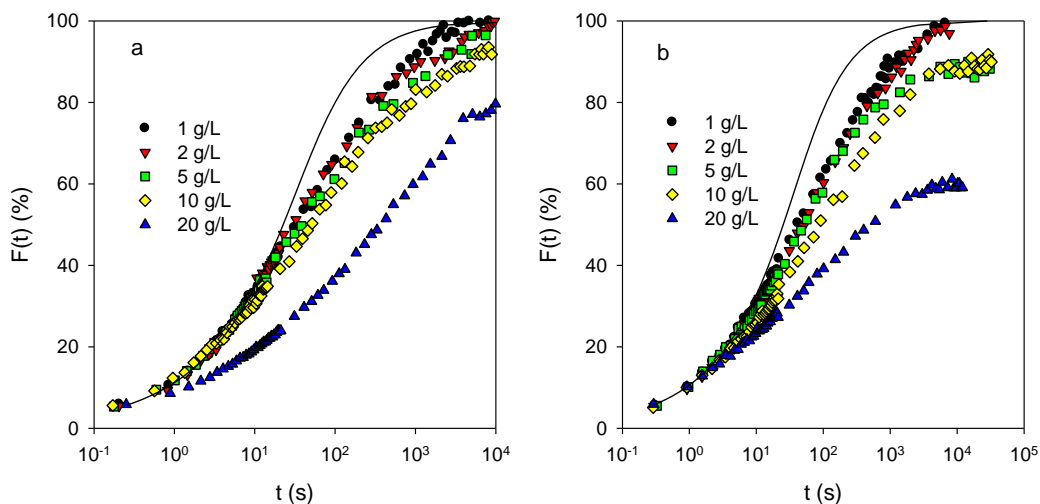


Figure 5.2. Recovery for the fluorescence intensity as a function of time after photobleaching for solutions of κ -car (a) and l -car (b) in salt free water at different concentrations. The solid lines represent the expected behaviour for Brownian diffusion with a single diffusion coefficient.

The solid lines in Figure 5.1 show the predictions of recovery caused by diffusional motion of the labelled chains with a single diffusion coefficient (D): $F(t) = \exp(-2\tau/t) [I_0(2\tau/t) + I_1(2\tau/t)]$, where $\tau = w^2/4D$ is the characteristic time needed to diffuse out of the bleached area with radius w and I_0 and I_1 are Bessel functions⁸. It is clear that $F(t)$ could not be described in terms of a single diffusion coefficient even at the lowest concentrations, which can be explained by the polydispersity of the Car chains. Nevertheless, D was calculated using only images taken during the first 20 s of the recovery. From the value of D extrapolated to $C = 0$, a hydrodynamic radius was calculated using equation $D = kT/6\pi\eta R_h$: $R_h = 43$ nm and 63 nm for κ -car and l -car, respectively. These values are smaller than the z -average R_h obtained from dynamic light scattering 67 nm and 75 nm, respectively. Smaller values are expected, because the Car chains were polydisperse in size and we analyzed the initial recovery of the fluorescence that was dominated by diffusion of the smaller chains.

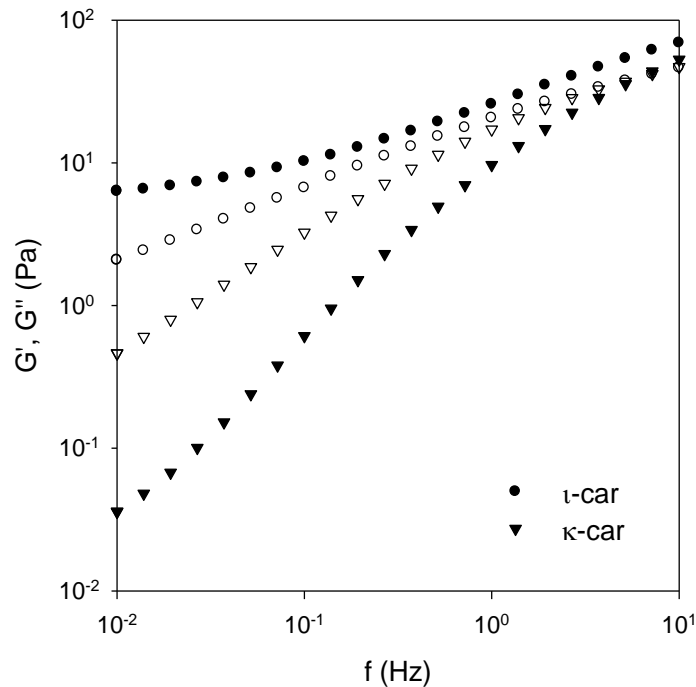


Figure 5.3. Frequency dependence of the storage (filled symbols) and loss (open symbols) modulus of κ -car and ι -car solutions in salt free water at 20 g/L.

5.2.2. Mobility of carrageen in gels

Gelation of Car can be induced by adding salt. Here we have formed gels of κ -car and ι -car by adding CaCl_2 or KCl to aqueous solutions at $C = 10$ g/L. The storage (G') and loss (G'') moduli were measured as a function of the frequency (f) after keeping them for 1 h at 20°C . For gels G' was larger than G'' and independent of f at low frequencies. Examples are shown in Figure 5.4. G' at low frequencies was taken as the elastic modulus (G_{el}) of the gels and is plotted in Figure 5.5 as a function of the salt concentration ($[\text{CaCl}_2]$ or $[\text{KCl}]$). Gels were formed by ι -car at $[\text{CaCl}_2] \geq 2$ mM and $[\text{KCl}] \geq 20$ mM, whereas they were formed by κ -car for $[\text{CaCl}_2] \geq 20$ mM and $[\text{KCl}] \geq 10$ mM. G_{el} increased initially rapidly with increasing salt concentration, but remained constant at higher concentrations at least in range covered here. For ι -car, G_{el} was larger in the presence of CaCl_2 than in the presence of KCl , whereas for κ -car G_{el} was larger in the presence of KCl than in the presence of CaCl_2 . The difference between the gel stiffness in the presence of KCl and in the presence of CaCl_2 was much larger for κ -car than for ι -car.

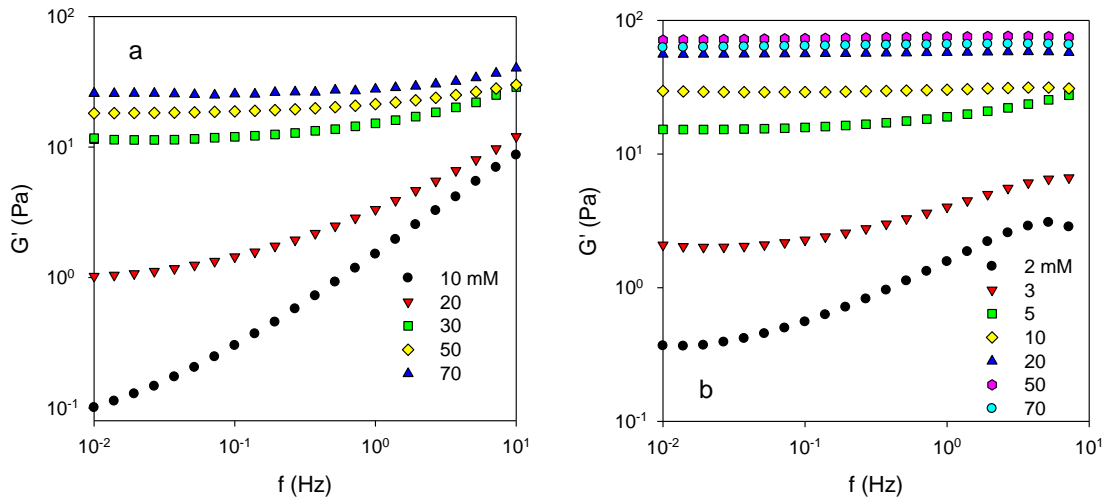


Figure 5.4. Frequency dependence of the storage modulus of *t*-car systems ($C = 10 \text{ g/L}$) at different KCl (a) or CaCl_2 (b) concentrations.

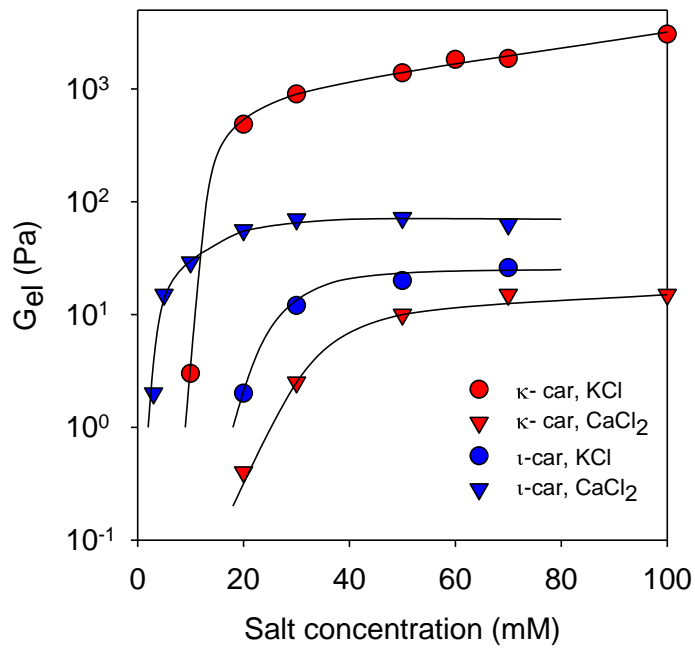


Figure 5.5. Elastic modulus of κ -car and *i*-car gels at $C = 10 \text{ g/L}$ as a function of the KCl or the CaCl_2 concentrations. The solid lines are guides to the eye.

The fluorescence recovery of ι -car and κ -car samples in the presence of different [KCl] or [CaCl₂] is shown in Figure 5.6. The results in Figure 5.6 are shown for freshly prepared samples, but repeat measurements on the same samples after one day showed similar recoveries. After an initial increase of $F(t)$ at short times that was similar for all samples, $F(t)$ was found to stagnate at values (F_{pl}) that decreased with increasing salt concentration and depended on the type of Car and the type of salt. These results show that even though gels were formed, a significant fraction of the Car chains remained mobile. As a consequence the intensity profiles did not become Gaussian, see Figure 5.7. The observation that the recovery up to F_{pl} was similar for all samples shows that residual mobile chains were those that moved fastest also in the solutions. Furthermore it shows that the movement of the mobile chains is not much modified by the immobilization of a fraction of the chains.

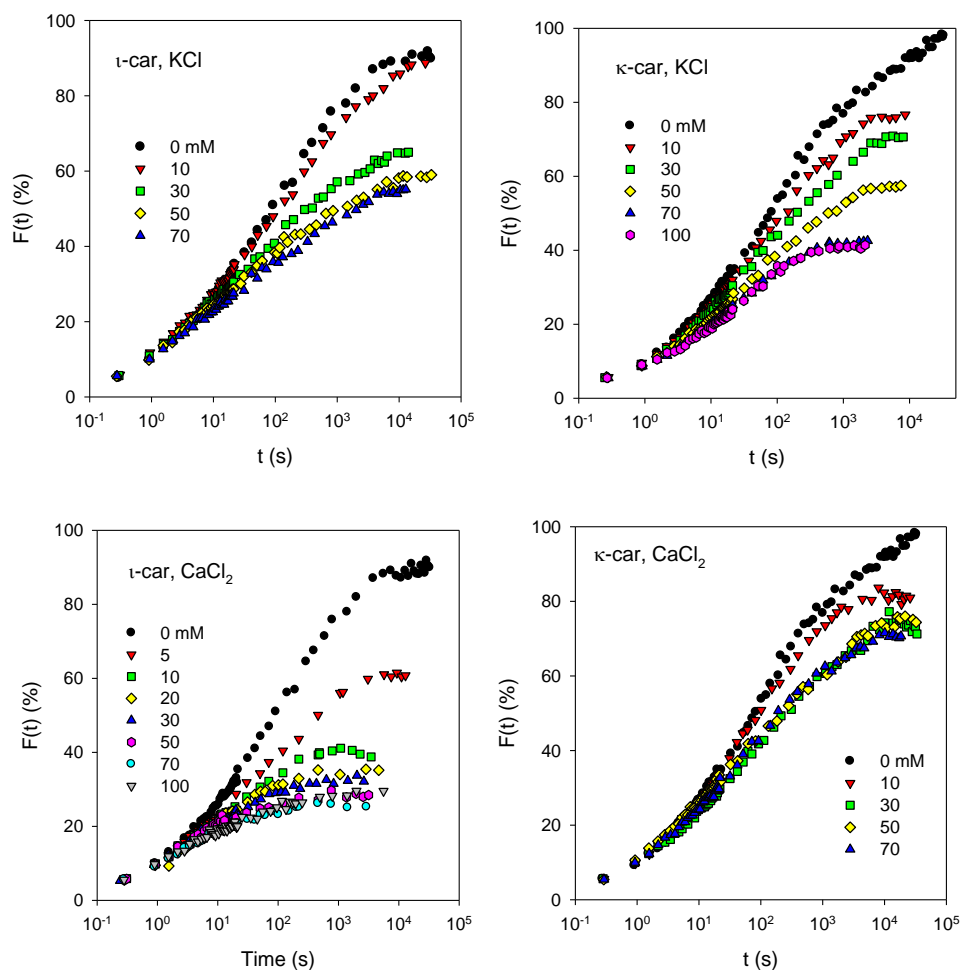


Figure 5.6. Recovery for the fluorescence intensity as a function of time after photobleaching for solutions of κ -car and ι -car at different concentrations of KCl and CaCl₂.

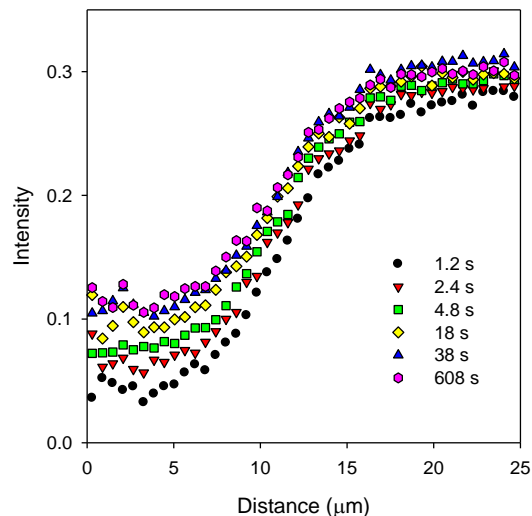


Figure 5.7. Intensity profiles at different times after bleaching for a solution of *t*-car at $C = 10$ g/L at $[CaCl_2] = 50$ mM.

In order to check whether the presence of mobile chains in the gels was particular for our batches of native Car, we did similar measurements with a commercial κ -car sample, see Figure 5.8. The molar mass of the commercial κ -car was smaller leading to faster recovery in salt free solutions. Also for the commercial κ -car we observed that a significant fraction of the chains remained mobile in the gels.

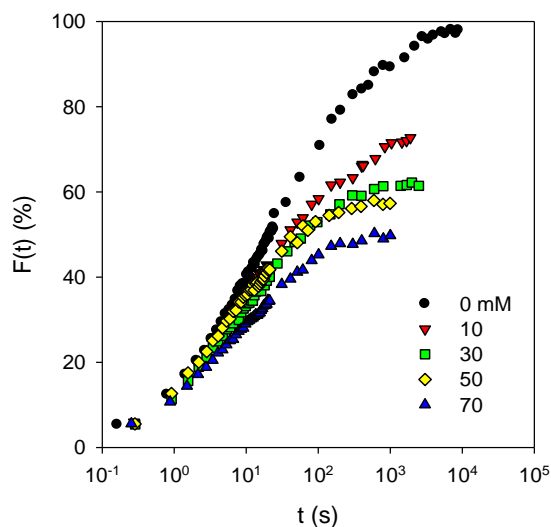


Figure 5.8. Recovery for the fluorescence intensity as a function of time after photobleaching for solutions of commercial κ -car at different KCl concentrations.

The dependence of F_{pl} on the salt concentration is shown in Figure 5.9. $F(t)$ decreased initially rapidly with increasing salt concentration, but the decrease stagnated at higher concentrations. In the presence of CaCl_2 the recovery remained much higher for κ -car (70%) than for ι -car (25%), whereas in the presence of KCl the recovery was similar for the two types of Car (50%). The fraction of mobile chains in gels formed by the commercial κ -car sample had a similar dependence on the KCl concentration as in the gel of the native κ -car sample, but it was smaller in CaCl_2 . Considering that the commercial κ -car chains were smaller, we may conclude that the fraction of mobile chains is not determined by the molar mass of the chains.

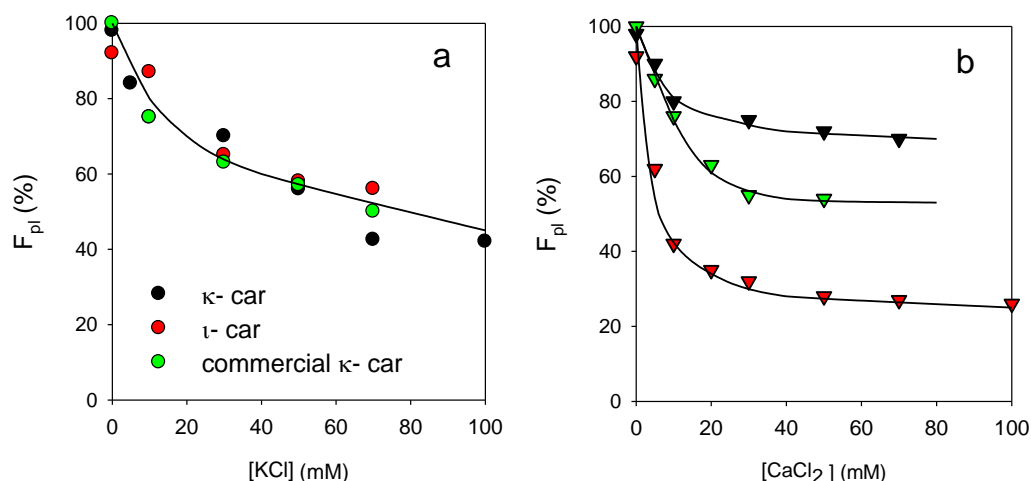


Figure 5.9. Dependence of the fraction of mobile chains in different Car systems as a function of KCl (a) and CaCl_2 (b) concentration. The solid lines are guides to the eye.

One might expect that the fraction of immobile chains is correlated to the gel stiffness. Comparison of Figures 5.5 and 5.6 shows that this is indeed qualitatively the case for gels formed in presence of CaCl_2 . F_{pl} decreased and G_{el} increased with increasing $[\text{CaCl}_2]$ and both values stagnated at higher CaCl_2 concentrations. In addition, the fraction of mobile chains was less in κ -car gels, which were also less stiff. However, in the presence of KCl the fraction of mobile chains was approximately the same for κ -car and ι -car gels, whereas G_{el} was an order of magnitude larger for κ -car gels. G_{el} of the commercial κ -car was much larger both in presence of KCl and CaCl_2 , see Figure 5.10. It is clear that the fraction of mobile chains is not related to the elastic modulus if gels formed by different types of Car or with different types of salt are compared.

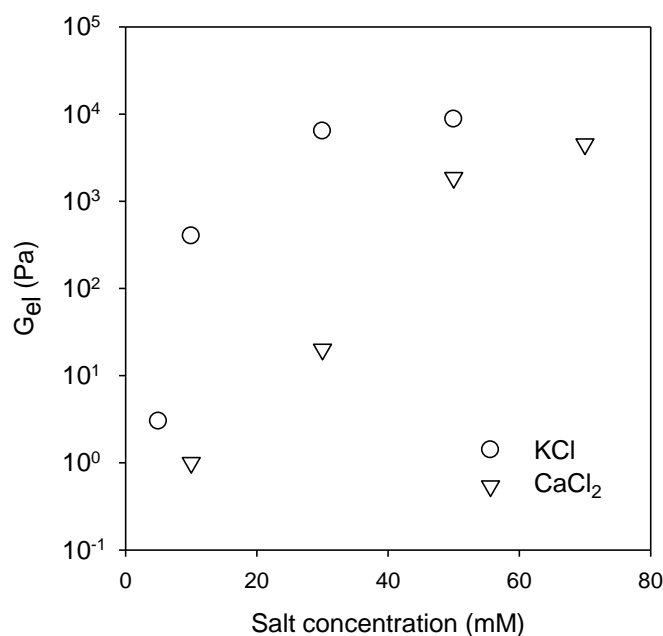


Figure 5.10. Elastic modulus of commercial κ -car gels at $C = 10$ g/L as a function of the salt concentration.

We have also investigated the recovery of either labelled κ -car or labelled ι -car chains in mixtures containing 5 g/L of both types of Car. In Chapter 4 we showed that for gelation of ι -car/ κ -car mixtures in presence of KCl and CaCl₂ the critical temperatures for gelation of ι -car and κ -car in the mixture are the same as for pure samples⁹⁻¹². However, G_{el} of the mixed gels is much larger than the sum of the moduli in pure gels at the same concentration as in the mixture. In fact G_{el} of the mixture was found to be intermediate between G_{el} of the pure gels at the same total Car concentration. F_{pl} as a function of the salt concentration is shown in Figure 5.11 and is compared with that in pure ι -car and κ -car gels at the same total Car concentration. It appears that the fraction of mobile ι -car and κ -car chains in mixed gels is close to that in the corresponding pure gels, which suggests that crosslinking of ι -car is not much perturbed by the presence of κ -car and vice versa.

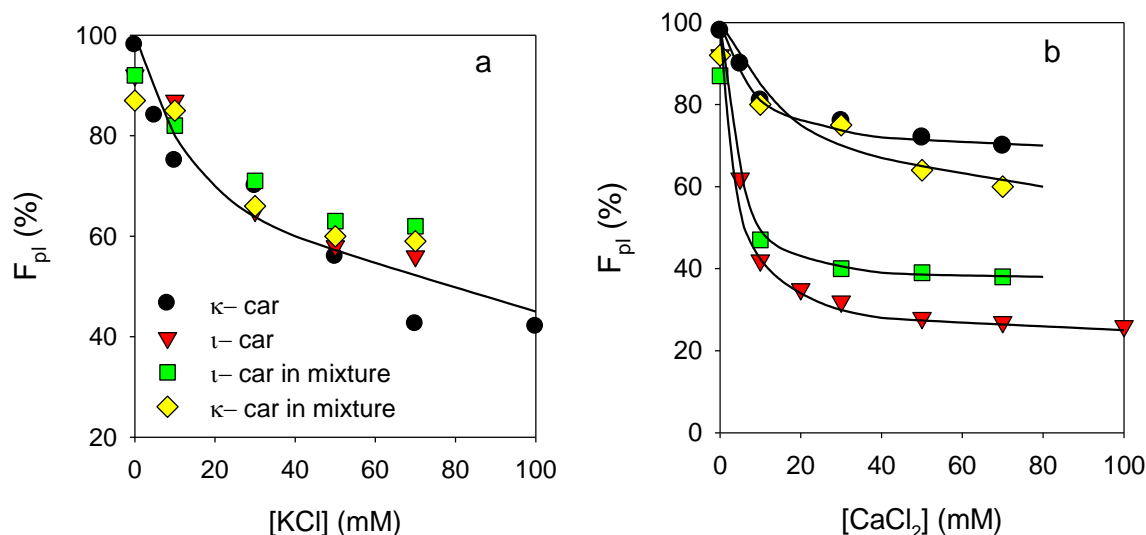


Figure 5.11. Dependence of the fraction of mobile Car chains as a function of the KCl (a) and CaCl₂ (b) concentration in mixtures containing 5 g/L ι-car and 5 g/L κ-car. For comparison of results obtained for individual ι-car and κ-car systems at C = 10 g/L are also shown. The solid lines are guides to the eye.

5.2.3. Release of carrageenan from the gels

If a fraction of Car can diffuse through the gels then it should also be released from macroscopic gels submerged in excess water at the same salt concentration. The release of Car with time was probed for strong ι-car gels at [CaCl₂] = 50 mM and strong κ-car gels at [KCl] = 50 mM by measuring the scattering intensity of the excess water. Notice that the gels for these measurements did not contain labelled Car. The intensity measured at a low scattering angle was found to increase logarithmically with time, see Figure 5.12, but the release was much slower from ι-car gels than from κ-car gels. After 36 hours the immersing liquid and the gel fragments were separated and extensively dialyzed in order to remove all excess salt. It was found that 11% of ι-car was released and 33% of κ-car. Commercial κ-car gels at [KCl] = 50 mM released 16% Car after 36 h. The amount of Car released after 36 h was still significantly less than the mobile fraction determined from FRAP measurements (25% for ι-car, 55% for κ-car and 55% for commercial κ-car). Clearly, 36 h was not enough to remove all the mobile Car from the macroscopic gel fragments.

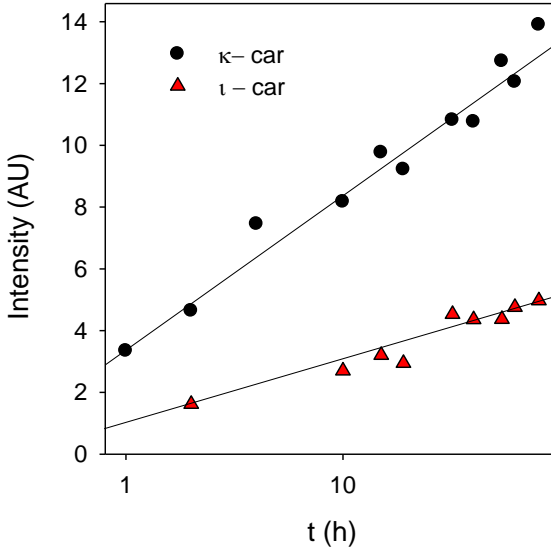


Figure 5.12. Light scattering intensity of the excess salt solution into which pieces of κ -car or ι -car gel were immersed as a function of time. The intensity was measured at a scattering angle of 30° .

The κ -car that was released and the κ -car that was retained in the gel were recovered and their gelation behaviour was studied at $C = 10$ g/L and $[KCl] = 50$ mM. The released κ -car did not form a gel at these conditions, whereas G_{el} of the gel formed by the retained κ -car was higher ($G_{el} = 3.8 \times 10^4$ Pa) than that of the initial κ -car gel ($G_{el} = 1.4 \times 10^4$ Pa), see Figure 5.13. If we consider that the mobile chains do not contribute to G_{el} we should compare the κ -car gel at $C = 10$ g/L with the gel formed by the retained at $C = 6.7$ g/L. For the latter we found $G_{el} = 2.2 \times 10^4$ Pa, which is still larger than G_{el} of the initial gel. It appears that the mobile chains not only did not contribute to the elastic modulus, but rendered the gels less stiff, possible because they inhibited formation of elastic crosslinks.

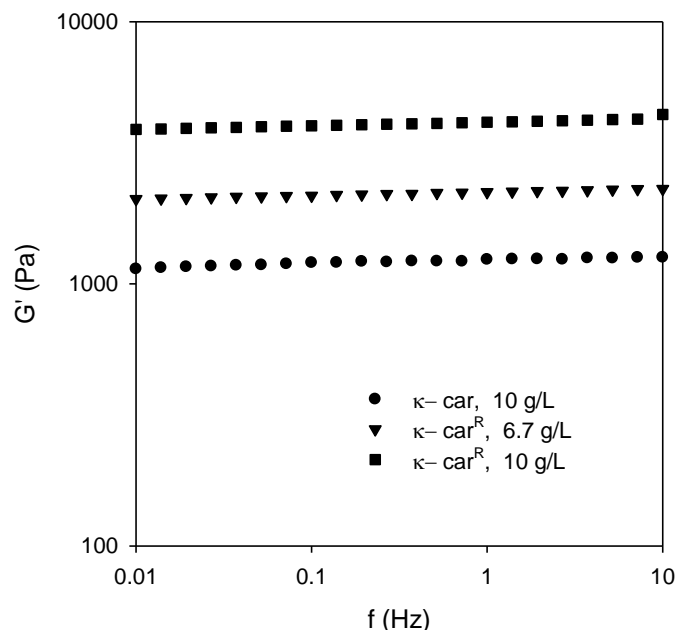


Figure 5.13. Frequency dependence of the storage modulus of Car before release (κ -car) and after release (κ -car^R) systems in presence of 50mM KCl.

We repeated FRAP measurements on a gel formed by κ -car containing 10% labelled chains at $C = 10$ g/L and $[KCl] = 50$ mM after releasing part of the mobile chains (κ -car^R) in the same manner as described above. As expected, the gel showed less recovery than the gel formed with the original κ -car sample at the same conditions, see Figure 5.14. In fact, the reduction of the recovery due to diffusion of labelled κ -car chains from about 60% to about 30% is compatible with the observe release of 33% of the unlabelled κ -car chains. In the FRAP experiments the mobility of labelled Car was determined and since the labelled Car was significantly smaller than the non-labelled Car. These FRAP results show that the fraction of released mobile chains is not much larger for labelled chains than for unlabelled chains.

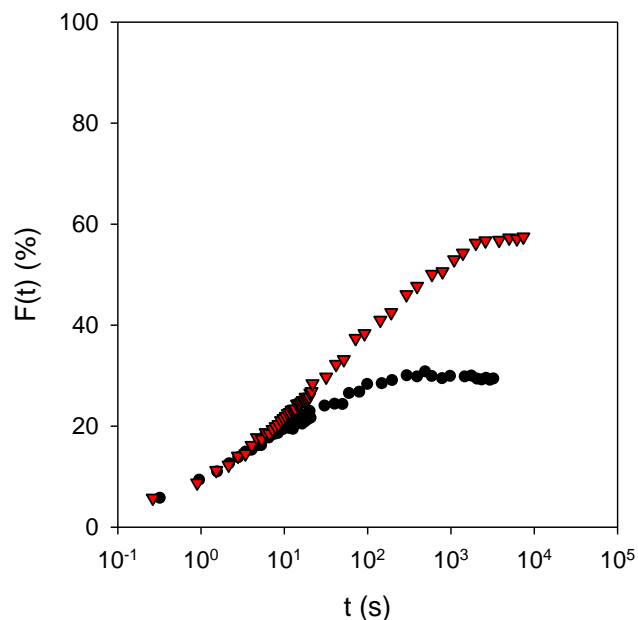


Figure 5.14. Recovery for the fluorescence intensity as a function of time after photobleaching for gels of κ -car at $C = 10$ g/L and $[KCl] = 50$ mM before (red triangles) and after (black circles) release of a fraction of mobile chains.

M_w of the released ι -car (7×10^5 g/mol), κ -car (2.5×10^5 g/mol) and commercial κ -car (1.9×10^5 g/mol) was found to be smaller than the average value found for the initial samples. The difference can be in part explained by the fact that the smaller chains will be released first and in part by the fact that the mobile chains are on average smaller than the immobile chains. As was mentioned in the introduction, Zhao et al.⁷ concluded on the basis of PFG-NMR measurements that the mobile chains in a κ -car gel consisted of the shortest chains in the polydisperse sample. They found that the fraction of mobile chains was only 10%, i.e. substantially less than was found here. The difference cannot be attributed to the effect of labelling as we found significantly more release also for unlabelled chains. However, the polymer concentration was higher (20 g/L) and the salt composition was different containing both KCl and $CaCl_2$ for the system investigated by Zhao et al. The authors did not determine the release from macroscopic gels. Therefore we cannot conclude whether the difference is caused by the difference in the sample or whether with PFG-NMR one does not measure to full amount of mobile chains.

5.3. Conclusion

κ -Car and ι -car gels formed in the presence of KCl or CaCl₂ contain a significant fraction of mobile chains, that diffuse through the gel. The fraction of mobile chains can be determined using FRAP measurements. For a given system the fraction of mobile chains decreased with increasing salt concentration until a plateau value was reached, which mirrored the increase of the elastic shear modulus. However, the fraction of mobile chains at higher salt concentration depended on the Car sample and the type of salt and was not correlated to the gel stiffness. Mobile chains were on average smaller and were slowly released from macroscopic gels submerged in excess solvent with the same salt concentration. Removal of mobile chains led to a decrease of the recovery in FRAP measurements and an increase of the elastic modulus of the κ -car gel.

References

1. Yegappan, R., Selvaprithiviraj, V., Amirthalingam, S. & Jayakumar, R. Carrageenan based hydrogels for drug delivery, tissue engineering and wound healing. *Carbohydr. Polym.***198**, 385–400 (2018).
2. Juteau, A., Doublier, J.-L. & Guichard, E. Flavor release from iota-carrageenan matrices: a kinetic approach. *J. Agric. Food Chem.***52**, 1621–1629 (2004).
3. De Kort, D. W. *et al.* Heterogeneity of network structures and water dynamics in κ -carrageenan gels probed by nanoparticle diffusometry. *Langmuir* **34**, 11110–11120 (2018).
4. Hagman, J., Lorén, N. & Hermansson, A. M. Probe diffusion in κ -carrageenan gels determined by fluorescence recovery after photobleaching. *Food Hydrocoll.***29**, 106–115 (2012).
5. Lorén, N. *et al.* Dendrimer diffusion in κ -carrageenan gel structures. *Biomacromolecules* **10**, 275–284 (2009).
6. Walther, B., Lorén, N., Nydén, M. & Hermansson, A. M. Influence of κ -carrageenan gel structures on the diffusion of probe molecules determined by transmission electron microscopy and NMR diffusometry. *Langmuir* **22**, 8221–8228 (2006).
7. Zhao, Q., Brenner, T. & Matsukawa, S. Molecular mobility and microscopic structure changes in κ -carrageenan solutions studied by gradient NMR. *Carbohydr. Polym.***95**, 458–464 (2013).
8. Soumpasis, D. M. Brief communication theoretical analysis of fluorescence photobleaching recovery experiments. *Biophys. J.***41**, 95–97 (1983).
9. Brenner, T., Tuvikene, R., Fang, Y. & Matsukawa, S. Rheology of highly elastic iota-carrageenan/kappa-carrageenan /xanthan/konjac glucomannan gels. *Food Hydrocoll.***44**, 136–144 (2015).
10. Du, L., Brenner, T., Xie, J. & Matsukawa, S. A study on phase separation behavior in kappa/iota carrageenan mixtures by micro DSC, rheological measurements and simulating water and cations migration between phases. *Food Hydrocoll.***55**, 81–88

(2016).

11. Lundin, L., Odic, K., Foster, T. J., & Norton, I. T. Phase separation in mixed carrageenan systems. In *Supramolecular and colloidal structures in Biomaterials and Biosubstrates*, 436–449 (ICP, 2000)
12. Ridout, M. J., Garza, S., Brownsey, G. J. & Morris, V. J. Mixed iota-kappa carrageenan gels. *Int. J. Biol. Macromol.***18**, 5–8 (1996).

General Conclusion and Outlook

Conclusions

We have determined the structure and rheological properties of Car extracted from three subspecies of *Kappaphycus alvarezii*: *K. alvarezii*, *K. striatum*, and *K. malesianus* and from *Eucheuma denticulatum*. Extracts from Ka, Ks, and Km mainly contained κ -car, whereas the extract from *Ed* contains predominantly ι -car. The yield was higher for the raw extract from *K.alvarezii* (42%) than for the other species (32–37%). The molar mass and the radius of gyration were found to be close for all samples. The zero shear viscosity of κ -car extracted from *K. alvarezii* was found to be systematically larger than the other carrageenan samples. Gelation induced by adding KCl to κ -car from the three subspecies was found to occur at approximately the same temperature leading to gels with approximately the same stiffness. Gel stiffness of Car extracted from Ka and Ed after alkali treatment was larger than for water extracted Car and close to that of commercial ι - and κ -car. Therefore, these types of seaweed from Cam Ranh Bay can be used to produce Car industrially. *K. alvarezii* is the best choice for expanding cultivation areas.

The study of the rheology and microstructure of 50/50 mixtures of ι -car and κ -car gel in the presence of CaCl_2 confirmed that the mixtures showed a two-step gelation process at gelation temperatures (T_c) that coincided with those of the corresponding individual κ -car and ι -car solutions. The stiffness of the mixed gels was much higher than the sum of the corresponding individual gels. Confocal laser scanning microscopy and turbidity measurements showed that the κ -car gel was always more heterogeneous than the ι -car gel, but less in the mixture than in the individual system. In the presence of KCl, individual κ -car gels and mixed gels formed were more homogeneous than gels formed in the presence of CaCl_2 . The results show that microphase separation of ι -car and κ -car in mixed gels is highly unlikely. It is suggested that the increased stiffness of the mixed gels is caused by co-aggregation of κ -car and ι -car or changes in the structure of the interpenetrated networks.

The mobility of Car chains in native κ -car and ι -car gels and commercial κ -car gel was determined by using FRAP measurements. The results showed that there is a significant fraction of the Car chains that remains mobile and diffuses through the gel. The fraction of

mobile chains at higher salt concentrations depended on the type of Car and the type of salt and was not correlated to the gel stiffness. The release of Car from gel fragments into excess solvent at the same salt concentration was probed as a function of time with light scattering. It was found that the released Car chains were on average smaller than in the initial Car sample. Gels made with κ -car from which the mobile chains had been partially removed were significantly stiffer even at the same concentration of immobile chains.

Perspectives

Here we concentrated on Car obtained from mild water extraction and tested only one condition of alkali extraction. However, the quality of Car products from the mentioned seaweeds could be increased by optimizing the alkali treatment. Therefore a more detailed investigation of the influence of alkali treatment on the properties of Car is needed.

The rheological properties and microstructure of mixtures were done on adding KCl or CaCl₂. However, gelation of ι -car and κ -car is favored by different types of salts. Hence it would be interesting to study mixed Car in presence of several types of cations so that gelation of both types is favored within the mixture.

The mobility of Car chains in the gel was determined here only at 20°C after cooling a hot solution. However, Car is applied in various types of products using different processing techniques such as freezing, heating, irradiation etc. Therefore, an investigation of the mobility at different temperatures and after different processing protocols would be useful.

Titre : Structure, propriétés rhéologiques et connectivité de gels de Carraghénanes extraits de différentes espèces d'algues rouges

Mots clés : Carraghénane, Rhéologie, Microstructure, gel

Résumé : Les carraghénanes (Car) sont des polysaccharides linéaires sulfatés extraits de différentes variétés d'algue rouge et sont largement utilisés en tant qu'épaississants, stabilisant et gélifiant dans les industries alimentaire, pharmaceutique et cosmétique. Les rendements d'extraction ainsi que les propriétés physicochimiques de car extraits de différentes espèces cultivées dans la baie de Cam Ranh dans la province de Khanh Hoa au Vietnam ont été déterminés. Les carraghénanes κ -car et ι -car extraits respectivement de *K. alvarezii* et *E. denticulatum* ont été sélectionnés pour l'étude des propriétés rhéologiques et de la microstructure en solution seuls ou en mélange à différentes concentrations en présence de CaCl_2 ou de KCl. Les mélanges présentent un processus de gélification thermique en deux étapes qui correspondent chacune aux températures de gélification du κ -car et ι -car individuellement. Cependant, pour les mélanges, l'élasticité du gel est nettement supérieure à la somme de celle des car seuls. Des mesures en microscopie confocale et de turbidimétrie ont démontré que les

gels obtenus avec le κ -car étaient toujours plus turbides que ceux avec le ι -car mais étaient moins turbides dans les mélanges. Au vu des résultats, un mécanisme de séparation de phase microscopique entre les deux car semble très peu probable pour expliquer cette observation.

Des mesures de FRAP (Recouvrance de Fluorescence Après Photo-blanchiment) ont permis de sonder la mobilité des chaînes de car dans les gels, que ce soit pour les systèmes individuels ou en mélange. Dans tous les cas, une recouvrance a été observée démontrant qu'une fraction des chaînes de Car reste mobile dans les gels. Cette fraction mobile varie de 25% à 75% selon le type de Car et le type/concentration en sel. Cette fraction n'est pas corrélée à la dureté du gel quelles que soient les conditions opératoires. Ces résultats ont été confirmés par des mesures de relargage des chaînes mobiles d'un gel dans un excès de solvant. Il a été démontré que les chaînes relarguées étaient plus petites que la moyenne de l'échantillon initial.

Title : Structure, Rheological Properties and Connectivity of Gels Formed by Carrageenan Extracted from Different Red Algae Species

Keywords : Carrageenan, rheology, microstructure, gel

Abstract: Carrageenan (Car) is a linear sulfated polysaccharide extracted from various species of red algae and is widely used as thickener, stabilizer and gelling agent in food products, pharmaceuticals and cosmetics. The yield and properties of car extracted from different algae species cultured at Cam Ranh Bay in Khanh Hoa province of Vietnam were characterized. κ -car from *K. alvarezii* and ι -car extracted from *E. denticulatum* were selected to study the rheological properties and the microstructure of individual and mixed car solutions at different concentrations in the presence of CaCl_2 and KCl. Mixtures showed a two-step gelation process with gelation temperatures that coincided with those of corresponding individual κ -car and ι -Car solutions. However, the stiffness of the mixed gels was much higher than the sum of the corresponding individual gels. Confocal laser scanning microscopy and turbidity measurements showed that the κ -car gel was always more

heterogeneous than the ι -car gel, but less in the mixture than in the individual system. The results show that microphase separation of ι -car and κ -car in mixed gels is highly unlikely.

The mobility of car chains in individual gels of κ -Car, ι -car and their mixtures was determined using fluorescence recovery after photobleaching. Slow recovery of the fluorescence was observed for the gels showing that a fraction of the Car chains remained mobile. The fraction of mobile chains in the gels varied between 25% and 75% depending on the type of Car and the type and concentration of salt. The fraction of mobile chains in gels of different Car or indifferent types of salt was not correlated to the gel stiffness. These results were confirmed by the release of Car from gel fragments into excess solvent. It was found that released Car chains were smaller than the average size of the initial Car sample.